UNIVERSITY OF LJUBLJANA
SCHOOL OF ECONOMICS AND BUSINESS

MASTER'S THESIS

ELECTRICITY MARKET UNCERTAINTY AND TIME-VARYING VOLATILITY ESTIMATION

Ljubljana, March 2019

BLAŽ KOVAČ

AUTHORSHIP STATEMENT

The undersigned Blaž Kovač, a student at the University of Ljubljana, School of Economics and Business, (hereinafter: SEB LU), author of this written final work of studies with the title Electricity Market Uncertainty and Time-varying Volatility Estimation, prepared under supervision of Professor, Igor Masten PhD.

DECLARE

1. this written final work of studies to be based on the results of my own research;
2. the printed form of this written final work of studies to be identical to its electronic form;
3. the text of this written final work of studies to be language-edited and technically in adherence with the FELU's Technical Guidelines for Written Works, which means that I cited and / or quoted works and opinions of other authors in this written final work of studies in accordance with the FELU's Technical Guidelines for Written Works;
4. to be aware of the fact that plagiarism (in written or graphical form) is a criminal offence and can be prosecuted in accordance with the Criminal Code of the Republic of Slovenia;
5. to be aware of the consequences a proven plagiarism charge based on the this written final work could have for my status at the FELU in accordance with the relevant FELU Rules;
6. to have obtained all the necessary permits to use the data and works of other authors which are (in written or graphical form) referred to in this written final work of studies and to have clearly marked them;
7. to have acted in accordance with ethical principles during the preparation of this written final work of studies and to have, where necessary, obtained permission of the Ethics Committee;
8. my consent to use the electronic form of this written final work of studies for the detection of content similarity with other written works, using similarity detection software that is connected with the FELU Study Information System;
9. to transfer to the University of Ljubljana free of charge, non-exclusively, geographically and time-wise unlimited the right of saving this written final work of studies in the electronic form, the right of its reproduction, as well as the right of making this written final work of studies available to the public on the World Wide Web via the Repository of the University of Ljubljana;
10. my consent to publication of my personal data that are included in this written final work of studies and in this declaration, when this written final work of studies is published.

Ljubljana, March 20th 2019 Author's signature: ___________________

TABLE OF CONTENTS

LIST OF TABLES

LIST OF FIGURES

LIST OF APPENDICES

LIST OF ABBREVIATIONS

ACER	Agency for the Cooperation of Energy Regulators
ADF	Augmented Diceky-Fuller
AI	Artificial Inteligence
AIC	Akaike Information Criterion
APX	Amsterdam Power Exchange
ARCH	Autoregressive Conditional Heteroscedasticity
ARDL	Autoregressive Distributed Lag
ARIMA	Autoregressive Integrated Moving-Average
ARMA	Autoregressive Moving-Average
ARMAX	Autoregressive Moving-Average with Exogenous Inputs
ASIS	Ancillarity-Sufficient Interweaving Strategy
ASN	Autorité de sûreté nucléaire (en. Nuclear Safety Authority)
AWOL	All Without a Loop'
BACE	Bayesian Averageing of Classical Estimates
BRP	Balance Responsible Party
C	Centered Parametrization
CL	Closed-Lag
DI	Diffusion Index
DM	Diebold-Mariano
EEX	European Energy Exchange
EPEX	European Power Exchange
EU	Eurpean Union
EU ETS	European Union Emissions Trading Scheme
EUA	EU Emission Allowances
FAVAR	Factor-Augmented Vector Autoregression
GARCH	Generalised Autoregressive Conditional Heteroscedasticity

HLN	Harvey, Leybourne, and Newbold
ICE	Intercontinental Exchange
JB	Jarqe-Berra
LHS	Left-Hand Side
LRM	Long Run Multiplier
MAE	Mean Absolute Error
MCMC	Markov chain Monte Carlo
mDCC	Multiplicative Dynamic Conditional Correlation
MGARCH	Multivariate GARCH
MH	Metropolis-Hastings
MH	Metropolis-Hastings
NC	Non-Centered Parametrization
OLS	Ordinary Least Squares
OL	Open-Lag
OOS	Out-Of-Sample
OTC	Over-the-Counter
PCA	Principal Component Analysis
PCHIP	Piecewise Cubic Hermite Interpolating Polynomial
PV	Photovoltaics
QML	Quasi-Maximum Likelihood
RES	Renewable Energy Sources
RHS	Right-Hand Side
RMPSE	Root Mean Squared Percentage Error
RMSE	Root Mean Squared Error
SV	Stochastic Volatility
TSO	Transmission System Operator
VAR	Vector Autoregression
VARMA	Vector Autoregression Moving-Average
WFA	Walk Forward Analysis

INTRODUCTION

Electricity markets have been subject to growing attention amid their transformation process over the last twenty to thirty years. Until the nineties, electricity was produced, sold and transported mainly by vertically integrated state-owned companies, which were operating in monopoly markets. Additionally, these companies often had full responsibility of guaranteeing sufficient supply of electricity to all market participants on the demand side. However, multiple successful liberalizations of some other vertically integrated markets like railway and telecommunications led to believe that electricity markets could also benefit from similar market transformation which then started in the mid-nineties.

This notion of belief was also supported by politics and already known “free market” ideology with the main arguments focusing on the positive effects of competition, which would be introduced to the market. This transformed market structure was assumed to stimulate better allocation of resources, boost technological innovation and improve the efficiency on the supply side, where all was made possible by technological progress in transmission and generation of electricity (Weron, 2006).

The European energy market is one of those that experienced a significant transformation, where all EU members have liberalized their electricity markets with the exception of Malta and Bulgaria. The main goals of liberalization were lower prices, efficiency, and market transparency, with a final objective to create an EU-wide integrated single energy market. In order to achieve market integration, differences between member states had to be removed. This involved a European level competition between suppliers, common sets of rules, transparent and aligned prices with common environmental objectives.

To support that notion, the EU adopted multiple legislation packages. Their aim was to support the liberalization and integration of the members’ markets, opening this sector for competition. First directive[1] concerned with common rules for internal markets was adopted in 1996 and 1998 for electricity and gas respectively. The second directive[2] setting up the legal framework for the liberalized market came in 2003. Further opening of the markets and an establishment of the Agency for the Cooperation of Energy Regulators (hereinafter: ACER) was adopted with the third directive in 2009.[3]

Liberalization of the electricity market has also created a need for organized markets at the wholesale level where power exchanges have emerged across Europe to facilitate electricity trading. Due to specific electricity market characteristics resulting in volatile spot prices,

[1] Directive 96/92/EC of the European Parliament and of the Council of 19 December 1996 concerning common rules for the internal market in electricity.

[2] Directive 2003/54/EC of the European Parliament and of the Council of 26 June 2003 concerning common rules for the internal market in electricity.

[3] Directive 2009/72/EC of the European Parliament and of the Council of 13 July 2009 concerning common rules for the internal market in electricity.

trading has become vital for market participants and electricity companies trying to mitigate the risk of unexpected price movements. This has translated into a growing demand for derivative products primarily used for hedging, which has become a standard practice of managing commodity price risk. Many different instruments have therefore been introduced to the market through the years ranging from forward and future contracts to options on delivery or consumption of electrical energy.

In general, the main objective of power exchanges is to ensure a transparent and reliable wholesale price formation mechanism on the electricity market by matching supply and demand at a fair price and ensure that the trades done at the exchange are finally delivered and paid.

Exposure to the market price related risk that is not controlled for, can cause overwhelming problems with costly consequences for market participants in the electricity industry. History and experience in financial markets suggest that properly utilized and well understood financial derivatives prove to be valuable for controlling the risks through well-structured hedging strategies (Deng & Oren, 2006). In order to be able to efficiently and appropriately utilize these hedging strategies, market participants are faced with the valuation of financial derivatives. One of the key parameters for derivatives valuation is also volatility, which measures the degree of variation of a price from its mean. Two main types of volatility are (actual) historical, focusing on past evolutions of the price, and implied, which is more forward-looking and derived from an option price. A wide range of research has also been devoted to estimating, modelling and forecasting the volatility of financial returns.

The main goal of this thesis is to construct estimates of uncertainty for electricity and energy commodity futures market by using data-rich environment to encompass multiple possible sources of uncertainty. For this, I adopt the approach of Jurado, Ludvigson, and Ng (2015) and their econometric formalization of uncertainty. Individual uncertainty forecasts are estimated for daily electricity and energy prices defined as continuous first-nearby futures prices with monthly (quarterly/yearly) delivery. A measure or index of electricity market uncertainty is then constructed by aggregating individual uncertainties. I also compare the aggregated uncertainty estimates with aggregated historical volatilities and with conditional volatilities estimated using a GARCH (p,q) model.

Moreover, as I try to construct a comprehensive measure of electricity market uncertainty I hypothesize that these uncertainty estimates significantly differ from a conditional volatility estimates obtained by employing a GARCH model. I also analyze the out-of-sample predictive accuracy of the two approaches where I argue that by considering a wide array of exogenous predictors should result in better multi-period ahead predictions of uncertainty for electricity and commodity prices. Furthermore, I hypothesize that predictors' dynamics significantly contributes to the uncertainty estimates.

The thesis is structured as follows. First, unique electricity market characteristics are described with their relation to volatility and uncertainty. Next, a short review of existing empirical literature on volatility modelling is presented. The third section depicts the econometric framework used in this analysis. The data used for the analysis is described in section four which is followed by a presentation of key results and concluding remarks.

1 ELECTRICITY MARKET CHARACTERISTICS

In order to provide a better understanding of price movements in electricity markets, the market structure and the price-setting process of the wholesale market will be first briefly described. This process includes the bidding mechanism, different market types and the time dimension of the market design.

Electricity can be traded on different types of wholesale markets (KU Leuven Energy Institute, 2015):

- In a power exchange or multilateral trading platform, market participants submit generation and demand bids. The market is cleared once per predefined time period and a single market price is determined.[1]
- In bilateral over-the-counter (hereinafter: OTC) trading, a generator and consumer agree on a trade contract by directly interacting with each other. OTC trading can take the market price published by the power exchange as a reference price.
- In organized OTC trading, market participants submit generation and demand bids to a market platform which is cleared continuously; one market player can bilaterally accept the bid of another market player, resulting in different prices for each trade.

1.1 The time dimension of the electricity market design

Electricity as a tradable good has a special property, which is a physical constraint of storage. The only exception from this is the conversion of electric energy into hydro potential energy using hydro pumps. However, those facilities are not common. The main consequence of this limitation is the fact that generation must equal consumption of electricity (plus grid losses) at all times. If this is violated, the grid frequency starts deviating from its reference value. This can result in a collapse of the system. For this reason one of the main roles of transmission system operators (hereinafter: TSO) is ensuring the balance of supply and demand, which occurs in a separate market (balancing market).

Different types of electricity markets can be described in sequential order. They start years before the actual delivery of energy and end after the actual delivery. Figure 1 gives an overview of the temporal ordering of the different electricity markets. Next, I provide a

[1] Common “market clearing" refers to the situation when the curve made up of generation bids intersects with the curve of demand bids, which then determines the quantity to be generated (and consumed) and the corresponding price.

Figure 1: Timeline of consecutive electricity markets

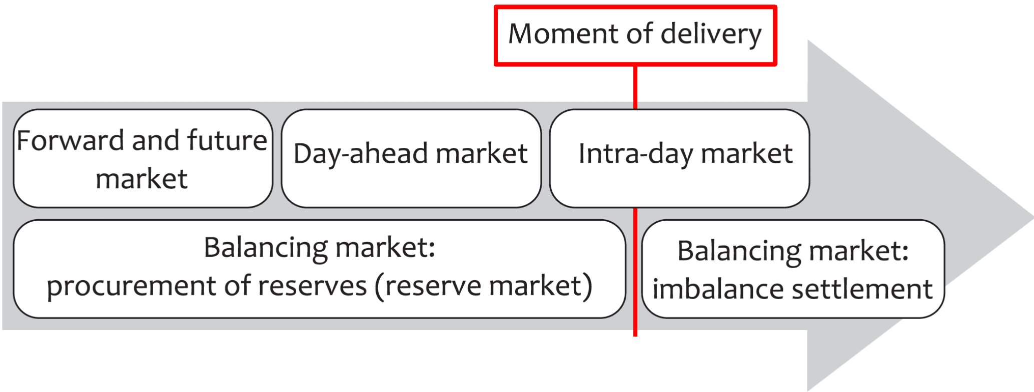

Source: KU Leuven Energy Institute (2015).

brief description of the time dimension of electricity market structure presented in Figure 1, to better depict the role of forward and future markets.

In general, commodities are traded on future/forward markets for delivery in the future. Strictly speaking, day-ahead markets, intra-day markets, and reserve markets are forward/future markets as they deal with electricity and reserves for future use. However, the term forward/future market is principally used in the context of electricity markets to denote markets that take place before the day-ahead market (KU Leuven Energy Institute, 2015).

1.1.1 Forward and future market

Forward and future markets start years before delivery and end a day before delivery. Forwards and futures are contracts to consume or deliver a certain amount of electric energy. Similarly to financial markets, futures are standardized and can be traded on power exchanges, whereas non-standardized forwards are mainly traded bilaterally giving more flexibility to the participants.

Typical market participants mainly use those derivatives for hedging. Producers sell electrical energy on forward and futures markets in order to lock their prices of future sales. On the other hand, large electricity consumers or retailers can buy electrical energy on these markets to secure their consumption at known costs. Since in forward and futures markets, electrical energy can be traded between countries/market zones, where a market zone mostly coincides with a member country, market participants also trade with transmission capacity. This means that market participants first buy the right to use the transmission capacity before buying or selling electrical energy in another country/market zone (KU Leuven Energy Institute, 2015).

1.1.2 Day-ahead market

In the day-ahead market, electricity is traded one day before the actual delivery. The main importance of the day-ahead market is to ensure the balance of the market zone at the end of the day. This means that scheduled generation in the market zone must equal forecasted demand in the market zone and net exports to other zones, where the forecasts of demand are commonly provided by local TSOs. Electricity can be traded day-ahead bilaterally (over-the-counter trading) or on the day-ahead power exchange. The final stage of the day-ahead market is the submission of balanced portfolios by Balance Responsible Parties[2] (hereinafter: BRPs) to the TSO, which is called nomination. These nominations then constitute the planned generation or consumption for every unit of BRP (KU Leuven Energy Institute, 2015).

1.1.3 Intra-day market

In the intra-day market, electricity is traded on the delivery day and the day before after 12 p.m. up to 30 minutes before delivery (which is an example in Germany). This market allows the market players to adjust for the shifts in their day-ahead nominations due to changed weather conditions (wind, precipitation), unexpected power plant outages, etc. in order to ensure the balance between supply and demand. Any imbalances after the intra-day market in the BRP's portfolio are further dealt with in the balancing market (KU Leuven Energy Institute, 2015).

1.1.4 Balancing market

Individual BRPs can face imbalances, which are net differences in 15-minute blocks between the BRP's total supply and total offtake. The TSO is in charge of maintaining the system balance by activating reserves or regulation. There are three types of reserves/regulation: Primary regulation is activated first to stabilize the frequency within the time frame; Secondary regulation is activated in range of seconds up to 15 minutes and is used to stabilize the imbalance; Tertiary regulation is activated in case of major imbalances, when the first two are unable to stabilize the system. The regulation can be positive, which means an increase in production or decrease in off-take, or negative, where production needs to be decreased or demand boosted. TSO also imposes a tariff to BRPs with imbalanced portfolios. This imbalance settlement takes place after the actual delivery (KU Leuven Energy Institute, 2015).

[2] The final responsibility for maintaining the instantaneous generation-consumption balance lies with a TSO, i.e., ELES in Slovenia. Before the actual delivery, the balance responsibility is passed on to Balance Responsible Parties (hereinafter: BRP). A BRP is a private legal entity that takes up the responsibility to compose a balanced portfolio. The portfolio of a BRP may consist of own generation, own consumption, and/or electricity traded with other BRPs.

Figure 2: EEX: Total Derivatives Volumes

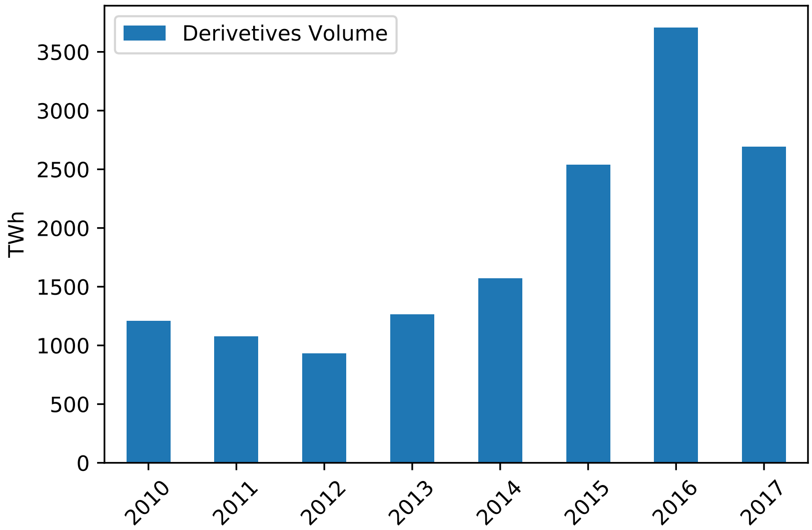

Source: Own work.

1.2 Electricity markets in Europe

Liberalization of electricity markets resulted in significant growth of trading with electrical energy where but a few energy exchanges were established across Europe. The main markets or exchanges are Nordpool, the Intercontinental Exchange (hereinafter: ICE), Amsterdam Power Exchange (hereinafter: APX), European Power Exchange (hereinafter: EPEX) and European Energy Exchange (hereinafter: EEX). While EPEX provides a multilateral trading platform on spot market (day-ahead, intraday), derivative contracts as futures and options are traded on EEX.

Mostly traded contracts on EEX are futures. They are offered for different periods of delivery, such as monthly, quarterly, yearly and delivery for a calendar year. They contain the financial balancing of payments, which would occur from the sale or purchase of a constant volume of electricity during the period of validity, e.g. one month in the case of monthly futures (Keles, 2014).

Power derivatives trading volume on EEX exchange has been on an upward trend in the last years reaching record levels in 2016 as presented in Figures 2 and 3. In their annual report for the year 2016 EEX states that this was mainly due to temporarily very high rates of volatility combined with a growing market share.

1.3 Electricity price and uncertainty

I now turn to a brief description of some of the main characteristics of electricity prices with a short depiction of the main sources of uncertainty. With this, I try to provide some insight

Figure 3: EEX: Options Volumes

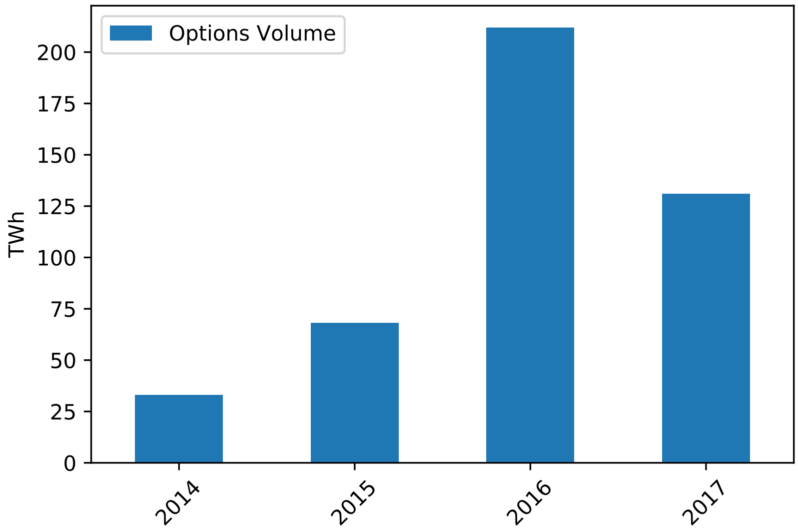

Source: Own work.

into how these different sources of uncertainty could translate into the electricity prices in the future markets.

1.3.1 Electricity price characteristics

Electricity wholesale prices have become very volatile since the establishment of trading on electricity exchanges. This especially holds for spot market prices, where electricity is traded with hourly or block products. Hourly trade leads to large variations between different hours of the day since each hour of electricity is a separate and different product with the main driver of the price being the actual consumption or system load.[3] Another reason for hourly variability of prices is the non-storability constraint. Moreover, the prices result from the highest marginal costs of production units (merit order), which is driven by the supply and demand situation (Keles, 2014).

It is not obvious if hourly price variation on the spot market directly translates to the future market. However, it gives a good indication about the main drivers behind it that do. As Weron (2006) describes it, load characteristics are directly displayed in electricity prices on the spot market. That means that prices reach their peaks when the load is the largest (high prices in the morning or in the evening, and low prices at night).[4] Analogously, electricity prices display weakly pattern, caused by lower demand on weekends, and annual seasonality, similarly caused by shifts in demand between different seasons.

[3]An end-use device or customer that receives power from the electric system (NERC Glossary).
[4]As a consequence of hourly seasonality, the most common hour blocks traded are baseload and peak.

1.3.2 Commodity prices

According to the Eurostat, almost half (48.7 %) of the net electricity generated in the EU-28 in 2016 came from fossil fuels (such as natural gas, coal, and oil), which is shown in Figure 4. Consequently, their uncertain price movements translate into uncertainty on electricity markets. It was shown by Bencivenga, Sargenti and D'Ecclesia (2010) that gas, oil, and electricity markets are integrated. Similarly, Frydenberg, Onochie, Westgaard, Midtsund and Ueland (2014) have found cointegration between UK electricity prices, Coal and Gas, and between Nordic electricity prices and Coal. They have also analyzed the stationarity of spreads between German electricity prices, Gas, Oil, and Coal prices.

Figure 4: Net electricity generation, EU-28, 2016

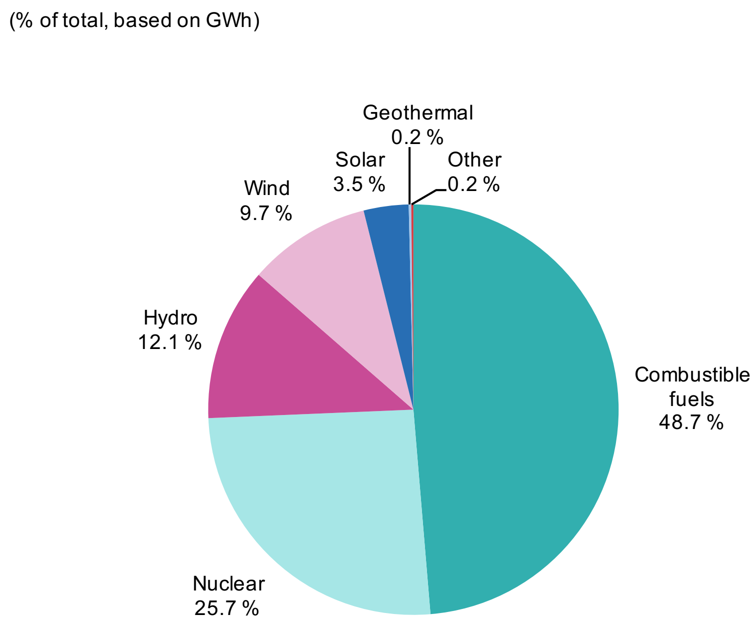

Source: Eurostat (2018).

As was noted by Frydenberg, Onochie, Westgaard, Midtsund and Ueland (2014), the relationship between fossil fuels and electricity prices is also market/country dependent. The main reason for that is country specific generation mix. For example, 46.5 % of net electricity generation in Germany came from hard coal and lignite in 2016, indicating a strong relationship with the coal market. On the other hand, almost 40 % of electrical energy is produced from gas-fuelled power plants in Italy which links electricity prices to the gas market.

Another important source of uncertainty is price dynamics of EU Emission Allowances (hereinafter: EUA) or carbon credits used in the European Union Emissions Trading

Scheme[5] (hereinafter: EU ETS). They present an influential part of generation costs, especially in fossil fuel concentrated markets, like Germany. However, determination or estimation of EUA price uncertainty is very challenging, since prices are not only market driven, but also strongly dependant on political and regulatory environments.

1.3.3 Uncertain power generation

The supply side of the electricity market has become more volatile due to the expansion of electricity generation from renewable energy sources (hereinafter: RES). One of the main types of RES are wind power, photovoltaics (hereinafter: PV) or solar, and hydropower. Fluctuations of energy generation from RES complicate the dispatch of conventional power plants delivering the residual load, which is the difference between system load and fed-in RES electricity, as was already noted by Schill (2014). The volatility of generation mix required for the residual load is hence increasing due to volatile feed-in from RES resources. This, together with non-storability constraint, results in uncertain electricity prices as described in paragraph 1.3.1.

1.3.4 Other sources of uncertainty

Power plants' availability is another source of uncertainty on the supply side of the electricity market. It is true, that planned revisions and scheduled maintenance periods should not be seen as an uncertain reduction of power plant availability. However, there is a significant amount of unpredictable outages causing a deficit on the supply side and contributing to the uncertainty. Power plants most commonly affected by the latter are the ones powered by fossil fuels like coal, lignite and oil (Keles, 2014).

Power plant outages can be regarded as a short-term source of uncertainty, which mainly affects the supply of energy and spot market trading. On the other hand, there are also long-term uncertainties, which in general have an impact on the structural development of the sector. Those are mainly technological developments, political and regulatory changes, and the long-term demand outlook (Keles, 2014).

2 RELATED EMPIRICAL LITERATURE

With liberalization and deregulation of electricity markets, there has been an exponential growth for the need of models, that could give an efficient insight into the new patterns that have emerged with electricity derivatives market. The main goal was to improve the decision making for all market participants (Fanelli, Maddalena & Musti, 2016). In this section I provide a brief overview of related literature, where I try to focus on the work applicable to derivatives markets and volatility modelling.

[5] Operators of power generating installations are required to surrender enough allowances to cover all its CO_2 emissions or heavy fines are imposed. The EUA Futures contracts are available on different exchanges like ICE and EEX.

As it has been noted by Bauwens, Hafner and Pierret (2013), the main focus of research on electricity markets has been analyzing and modelling the spot price behaviour. Weron (2014) has provided a comprehensive overview of the empirical literature on electricity price forecasting with the focus on spot market.

Despite the growing popularity of electricity price forecasting in the research community, there is only small number of books on this topic, indicating that this research area is not yet mature. The three books that appear to be addressing the question of electricity price forecasting are (Weron, 2014):

- Shahidehpour et al. (2002, Chapter 3, pp. 57–113) discussing the electricity price forecasting and shedding some light on neural networks.
- Weron (2006, Chapter 4, pp. 101–155) gives an overview of modelling approaches with focus on practical application of different statistical methods such as ARMA ann GARCH-type models and turns to stochastic models for derivatives pricing.
- Zareipour (2008, Chapters 3–4) reviews linear time series models (ARIMA, ARMAX) and nonlinear models (regression splines, neural networks).

Weron (2014) also provides a thorough review of survey articles. He starts in early 2000s, when Bunn (2000) presented his main conclusion of mutual connection between load and price forecasting. From that time, a variety of methods and ideas have been tested for electricity price forecasting. They range from equilibrium (multi-agent) models such as Nash-Cournot framework used for strategic bidding behaviour in electricity markets (Ventosa, Baıllo, Ramos & Rivier, 2005), to time series models like ARIMA or seasonal ARIMA (García-Martos & Conejo, 2001), and AI methods that were reviewed by Hong (2014) with their applicability for new smart grid markets. There have also been many classifications of approaches provided by the same group of researches. As a brief overview I present the classification of Werion (2014) with five groups of models:

- Multi-agent (multi-agent simulation, equilibrium, game theoretic) models, which simulate the operation of a system of heterogeneous agents (generating units, companies) interacting with each other, and build the price process by matching the demand and supply in the market.
- Fundamental (structural) methods, which describe the price dynamics by modelling the impacts of important physical and economic factors on the price of electricity.
- Reduced-form (quantitative, stochastic) models, which characterize the statistical properties of electricity prices over time, with the ultimate objective of derivatives evaluation and risk management.
- Statistical (econometric, technical analysis) approaches, which are either direct applications of the statistical techniques of load forecasting or power market implementations of econometric models.

- Computational intelligence (artificial intelligence-based, non-parametric, non-linear statistical) techniques, which combine elements of learning, evolution and fuzziness to create approaches that are capable of adapting to complex dynamic systems, and may be regarded as "intelligent" in this sense.

As presented, relatively large array of different modelling approaches have been developed for spot market which Weron (2014) classified into five groups. However, when it comes to derivatives market and its pricing, the most widely applied approaches are reduced form and statistical - econometric.

Reduced form models or financial mathematical models are dominating the derivatives valuation field (Möst & Keles, 2010). Majority of pricing models are expressed as one or two factor models focused on stochastic behaviour of underlying commodity price with derivation of future price dynamics by using arbitrage price theory (Biagini, Bregman & Meyer-Brandis, 2015; Carmona, Coulon & Schwarz, 2013; Mahringer & Prokopczuk, 2015). Some typical types of processes of these factors are mean-reversion (Brownian Motion), regime switching (Markov models) or jump-diffusion (The Poisson process). Additionaly, Biagini, Bergman and Meyer-Brandis (2015) have replaced Brownian Motion with more general Lévy process, also taking into account the occurrence of spikes. The latter has allowed them to employ well established and known techniques from interest rate term structure modelling. A new modelling framework has also been proposed by Barndorff-Nielsen, Benth and Veraart (2014), who showed that the concept of stochastic tempo-spatial or ambit fields can be used to develop a general framework for electricity futures. They also show that ambit fields easily incorporate leptokurtic behaviour in price increments, stochastic volatility and leverage effects, and the observed Samuelson effect in the volatility.

These models are mainly used for short term forecasts of spot and futures prices and for financial derivatives pricing (Islyaev & Date, 2015). Some part of the research community has been using these type of models focusing on seasonality in volatility (Fanelli, Maddalena & Musti, 2016; Arismendi, Back, Prokopczuk, Paschke & Rudolf, 2016) as it is one of the main parameters in derivatives valuation. Additionally, due to particular specification of electricity market (non-storability), it has been shown that including electricity demand and capacity forecasts can be beneficial in electricity derivatives pricing, thus confirming the importance of forward-looking information in electricity markets (Füss, Mahringer & Prokopczuk, 2015).

In contrast, econometric time-series models relate electricity prices to the impact of explanatory factors as weather, other commodities, etc. This approach is often applied to electricity demand forecasting. These models are also similar to financial models, as they apply statistical methods to historical time series. However, their focus is on the impact of explanatory variables on electricity price, where stochastic processes are not considered in the same way as in reduced-form models (Möst & Keles, 2010). As already described, empirical literature so far has been considering econometric and time-series models mainly to model spot prices in relation with supply-demand situation with additional explanatory factors. However, econometric models have also been considered in derivatives electricity markets where futures price series or volatility dynamics were analysed.

Panel data methods and cointegration analysis have been applied to analyze cointegration relationships among electricity and fossil fuel prices (Madaleno, Moutinho & Mota, 2015). Daily settlement prices of monthly futures contracts were modelled as a function of time-to-maturity using a linear regression model in order to test for Samuelson effect (Jaeck & Lautier, 2014). They have also implemented VAR framework with different maturities of the same futures contracts to test for directional volatility spillovers by employing the method developed by Diebold & Yilmaz (2012). Price returns and volatility spillovers between electricity and fuel price markets have been investigated also by combining MGARCH models with VAR and VARMA models, which show for volatility short and long-run persistence effects (Wei, 2016). Volatility of electricity futures has also been analysed by Bauwens, Hafner and Pierret (2013), where they propose a new multivariate volatility model where long-run and short-run components are separated using Multiplicative Dynamic Conditional Correlation (hereinafter: mDCC) model and for the short-run dynamics, the Multivariate GARCH model is adopted.

The intention of this thesis is to contribute to the econometric part of empirical research, where time series of electricity futures are analysed with respect to their past evolutions and a wide array of exogenous factors. The main goal is to construct an econometric estimate of conditional volatility and electricity market uncertainty. For that, I adopt the approach of Jurado, Ludvigson and Ng (2015) and their econometric formalization of uncertainty. The main forecasting model is represented as a Factor-Augmented Vector Autoregression (hereinafter: FAVAR) with time-varying variances following some latent stochastic process and modelled with Stochastic Volatility (hereinafter: SV) model. Main volatility estimates are also compared to widely used GARCH (p,q) conditional volatility forecasts.

3 ECONOMETRIC FRAMEWORK

This thesis provides an adoption of a recently developed measure of uncertainty proposed by Jurado, Ludvigson and Ng (2015), which allows for a relation to a wide array of exogenous factors and sources of uncertainty, as described in section 1.3. Moreover, the main idea is to provide a comprehensive econometric estimate of uncertainty in the electricity market relaxed of specific theoretical model structures and restrictive one-factor dependencies. Additionally, the notion of uncertainty here is not concerned with the variability of particular economic series (price), but whether the market has become more or less predictable as it is also described by Jurado, Ludvigson and Ng (2015).

Jurado, Ludvigson and Ng (2015) emphasize two features of this definition. First, uncertainty has to be distinguished from conditional volatility in a series y_t, which requires removing the forecastable component from $E[y_{jt+h}|I_t]$. If this condition is not met, forecastable variations can be wrongly categorized as "uncertain". Second, they also provide a distinction between market uncertainty and uncertainty in a single series y_t. The former is defined as a measure of common variation in uncertainty across multiple series.

3.1 Uncertainty

The h-period ahead individual uncertainty in variable $y_{jt} \in Y_t = (y_{1t}, ..., y_{jt})'$ denoted by $\mathscr{U}^y_{jt}(h)$ is defined as the conditional volatility of purely unforcestable component of the future value of the series. Specifically,

$$\mathscr{U}^y_{jt}(h) \equiv \sqrt{E\left[(y_{jt+h} - E[y_{jt+h}|I_t])^2|I_t\right]}, \tag{1}$$

where $E[\cdot|I_t]$ is the expectation formed with respect to information I_t available at time t. Conditional expectations about the squared errors in y_{jt+h} forecasts are hence directly translated into uncertainty, where higher expected squared errors mean higher uncertainty. By aggregating individual uncertainties at each t, an index of market uncertainty is constructed. This is done using the following formula:

$$\mathscr{U}^y_t(h) \equiv plim_{N_y \to \infty} \sum_{j=1}^{N_y} w_j \mathscr{U}^y_{jt}(h) \equiv E_w\left[\mathscr{U}^y_{jt}(h)\right], \tag{2}$$

where w_j are aggregation weights.

The main objective of this thesis is therefore to obtain the estimates of (1) and (2) for the German electricity market. This is done in three key steps. In the first step, an estimate of the $E[y_{jt+h}|I_t]$ is required. Since I have a large set of predictors $\{X_{it}\}$, $i = 1, 2, ..., N$ with N equal to 312, I employ the diffusion index forecast to approximate $E[y_{jt+h}|I_t]$, which is ideal for data-rich environments (Stock & Watson, 1998, 2002b; Jurado, Ludvigson & Ng, 2015). Next, the h - step forecast error is defined as $V^y_{jt+h} \equiv y_{jt+h} - E[y_{jt+h}|I_t]$, where an estimate of conditional volatility of this error is required, namely $E[(V^y_{jt+h})^2|I_t]$. For this, a parametric stochastic volatility model is specified for one-step prediction errors in both, dependent variables y_{jt} and factors. The latter are assumed to follow an AR (p) process. These volatility estimates are then used to recursively compute the values of $E[(V^y_{jt+h})^2|I_t]$ for $h > 1$. As was shown by Jurado, Ludvigson and Ng (2015), an important property of forecasts for $h > 1$ is that time-varying volatility in the errors of the predictor set also contributes to the uncertainty in y_{jt+h}. Finally, an estimate of market uncertainty $\mathscr{U}^y_t(h)$ is constructed from individual uncertainties $\mathscr{U}^y_{jt}(h)$, where in the base case, this is done by using a simple equally-weighted average. I now turn to a more detailed description of the methodology.

3.2 Forecast errors

An important first step in the analysis is to obtain the basis for my (individual) uncertainty measure. For this, I need to substitute the conditional expectations in (1) with a forecast from which forecast errors are constructed. An important assumption here is that the model forecast errors represent only the unforecastable component, hence a true forecast error. In order to achieve this, the model has to take into account multiple sources of variability and uncertainty. Moreover, it was noted by Jurado, Ludvigson and Ng (2015) that an omitted information bias may occur if relevant information is not used in forming forecasts. This could lead to spurious estimates of uncertainty and its dynamics, hence a large array of predictors was constructed and used.

Stock and Watson (2002b) have shown that forecasting with a large number of predictors which are summarized with a small number of indexes outperform univariate autoregressions, small vector autoregressions, and leading indicator models. The diffusion index forecasting introduced by Stock and Watson (1998) is hence employed in this exercise where in the first step a relatively small number of factors is estimated from a large set of predictors.

3.2.1 Approximate factor model

Let $\mathbf{X}_t = (X_{1t},...,X_{Nt})'$ denote the full set of predictors used in this analysis where $\mathbf{X}_t$ has been transformed to ensure stationarity. Jurado, Ludvigson and Ng (2015) assume that X_{it} has a factor structure represented as

$$X_{it} = \Lambda_i^{F'}\mathbf{F}_t + e_{it}^X, \tag{3}$$

for $i = 1,...,N$, where e_{it}^X is a vector of idiosyncratic errors, $\mathbf{F}_t$ is an $r_F \times 1$ vector of latent common factors and $\Lambda_i^{F'}$is a corresponding $r_F \times 1$ vector of latent factor loadings. An important assumption for this analysis is the allowance of some cross-sectional correlation in idiosyncratic errors e_t, which sets up the model to have an Approximate Factor Structure.

The approximate factor structure in the sense of Chamberlain and Rotshild (1982) requires the largest egienvalue of the $N \times N$ covariance matrix $E(e_t e_t')$ to be bounded. Common factors are estimated by a method of Asymptotic Principal Components as presented by Bai and Ng (2002). This allows for estimation of $min\{T,N\}$ number of factors, which is larger than permitted by state-space models. Estimates of Λ_i^F and $\mathbf{F}_t$ are obtained by solving the optimization problem

$$\min_{\Lambda,\mathbf{F}}(NT)^{-1}\sum_{i=1}^{N}\sum_{t=1}^{T}(X_{it} - \Lambda_i^{F'}\mathbf{F}_t)^2 \tag{4}$$

subject to normalization of $\Lambda^{F'}\Lambda^F/N = I$, where $\hat{\Lambda}^F$ is constructed as $\sqrt{N}$ multiplied with eigenvectors corresponding to the r_F largest eigenvalues of the $N \times N$ matrix $X'X$. The normalization that $\hat{\Lambda}^{F'}\hat{\Lambda}^F/N = I$ implies $\hat{\mathbf{F}} = X\hat{\Lambda}^F/N$. The number of common factors considered r_F and hence the dimensions of $\hat{\mathbf{F}}$ and $\hat{\Lambda}^F$ are determined by information criteria proposed by Bai and Ng (2002), where the penalty for overfitting is a function of both N and T.

3.2.2 Diffusion index forecasts

In the next step, the focus turns to the h-step-ahead forecast. Stock and Watson (2002b) present two possible approaches for the multi-step forecast. One option is the development of VAR model, but they note that this entails an estimation of a large number of parameters, that could erode forecasting performance. Another approach is to recognize the linear relationship between contemporaneous and lagged values of F_t, y_t and the multi-step forecasts, which is employed in Jurado, Ludvigsona and Ng (2015), as is here.

Let y_{jt} denote the individual series in which I wish to compute uncertainty. The h-step forecast for $h \geq 1$ is estimated from factor-augmented forecasting model

$$y_{jt+1} = \phi_j^y(L)y_{jt} + \gamma_j^F(L)\hat{\mathbf{F}}_t + \gamma_j^W(L)\mathbf{W}_t + v_{jt+1}^y, \tag{5}$$

where $\phi_j^y(L)$, $\gamma_j^F(L)$ and $\gamma_j^W(L)$ represent finite-order polynomials in the lag operator L of orders p_y, p_F and p_W respectively. $\hat{\mathbf{F}}_t = (\hat{F}_{1t}, ...\hat{F}_{r_F t})$ is a vector of common factors from (3). In addition, I also include $\mathbf{W}_t$, which is an $r_W \times 1$ vector consisting of quadratic terms which are used to capture possible nonlinearities and effects of conditional volatilities. Specifically, the main components of $\mathbf{W}_t$ are the squares of the first component of $\hat{\mathbf{F}}_t$ and additional factors in X_{jt}^2 collected into the $N_G \times 1$ vector $\hat{\mathbf{G}}_t$. Jurado, Ludvigson and Ng (2015) also stipulate an important feature of this method. Namely, the one-step-ahead forecast errors in y_{jt+1} and all predictor series $F_{k,t+1}$ and $W_{\ell,t+1}$ are permitted to have time-varying volatilities σ_{jt+1}^y, σ_{kt+1}^F and $\sigma_{\ell t+1}^W$ respectively, which generates time-varying uncertainty in series y_{jt}.

Another representation of (5) would also be in the form of the most general diffusion index (hereinafter: DI) forecasting function, which has an autoregressive distributed lag (hereinafter: ARDL) model structure

$$y_{jt+1} = \alpha + \phi_1^y y_{jt} + \cdots + \phi_{p_y}^y y_{jt-p_y} + \sum_{k=1}^{k_i} (\gamma_1^k \hat{\mathbf{Z}}_t^k + \cdots + \gamma_q^k \hat{\mathbf{Z}}_{t-q}^k) + v_{jt+1}^y, \tag{6}$$

where $\mathbf{Z}_t = (\hat{\mathbf{F}}_t, \mathbf{W}_t)'$. In order to obtain parameter estimates of α, ϕ^y andγ^k I use two different approaches.

First, I employ the approach already used by Jurado, Ludvigson and Ng (2015), where the final predictor set is selected using a conservative threshold rule. Specifically, the idea is to only include those predictors that have a significant incremental predictive power. I start with full set of candidate predictors in $\mathbf{Z}_t$, which results in $k_i = r_F + r_W$ in (6). In the next step, a subset of predictors is chosen by first running a regression of y_{jt+1} on a constant, p_y of its own lags $(y_{jt-1}, ..., y_{jt-p_y})$ and full set of $\mathbf{Z}_t$ entering with q number of lags. Next, I only retain the regressors that have marginal t-statistic greater than 1.96. The model is then re-estimated with only the final set of predictors. Since one of the main assumptions in the analysis is the allowance of time-varying volatility in y_{jt+1} and $\mathbf{Z}_t$, the fourth assumption[1]

[1]Homoscedasticity and non-autocorrelation: $E[\varepsilon_i^2|X] = \sigma^2$ and $E[\varepsilon_i\varepsilon_j|X] = 0$ for $i \neq j$.

of the Classical Linear Regression Model is relaxed. For this reason, the Newey-West robust estimator of the covariance matrix is applied.

Next, I employ the Bayesian Averaging of Classical Estimates (hereinafter: BACE) as presented by Doppelhofer, Miller and Sala-i-Martin (2004). The main idea of BACE approach is an operation with a wide range of equations/models per dependent variable, where each model is assigned a weight reflecting its relative predictive performance. Weighting the coefficients from all admissible models results in a posterior model. Again, I start with (6), although, $k_i = r_F + r_W$ does not hold in this case. The array of individual models is constructed by considering all possible combinations of k_i predictors out of $r_F + r_W$ set of all possible predictors in $\mathbf{Z}_t$, where $k_i << r_F + r_W$. Next, for each specific model i with its k_i predetermined subset of predictors, an optimal lag structure is chosen for autoregressive and exogenous terms p_y and q respectively. This is done by estimating all possible lag combinations (up to a certain limit set by maximum values of p_y and q) for each specific model i, where an optimal model is chosen based on the Akaike Information Criterion (AIC) and additional model specification tests for multicollinearity, model stability and unit roots. Finally, the posterior model is obtained first by calculating the posterior probabilities of each admissible (statistically well-specified) model i using

$$P(M_i|y) = \frac{P(M_i)T^{k_i/2}SSE_j^{-T/2}}{\sum_{i=1}^{I} P(M_i)T^{-k_i/2}SSE_i^{-T/2}}. \quad (7)$$

Note that in the numerator I use prior probability $P(M_i)$, where I assign an equal prior to each model. Additional factors appearing in (7) are $T^{k_i/2}$, which can be thought as a penalty for model complexity and $SSE_i^{-T/2}$, which represents a model performance factor. Hence, a posterior probability of model i is a function of its performance with a penalty for its complexity. Finally, when the model weights are calculated, the posterior means of parameter estimates can be obtained with

$$E(\Theta|y) = \sum_{i=1}^{I} P(M_i|y)\hat{\Theta}_i \quad (8)$$

where $\Theta = (\phi, \gamma)'$ and $\hat{\Theta}_i = E(\Theta|y, M_i)$ is the Ordinary Least Squares (hereinafter: OLS) estimate[2] for Θ with the predictor set defining model i (Doppelhofer, Miller & Sala-i-Martin (2004)).

Another non-trivial difference between the two approaches considered is that with BACE I force a closed-lag (hereinafter: CL) model structure, meaning that lags of all variables on the RHS of (6) enter without gaps, as opposed to the open-lag (hereinafter: OL) structure in the first approach. Consequently, this results in a richer model with a greater number of estimated parameters.

[2] Θ_i is the posterior mean conditional on model i.

3.2.3 Forecast uncertainty

Since the factors have an autoregressive dynamics, I use a more compact representation of (5). As in Jurado, Ludvigson and Ng (2015), the model can be expressed as a Factor-Augmented Vector Autoregression (hereinafter: FAVAR). First, I define $\mathbf{Z}_t \equiv (\hat{\mathbf{F}}_t, \mathbf{W}_t)'$ as a $r = r_F + r_W$ vector of r_F estimated factors and r_W additional predictors and let $\mathscr{Z}_t \equiv (\mathbf{Z}'_t, ...\mathbf{Z}'_{t-q+1})$. Next, I also let $Y_t = (y_{jt}, y_{jt-1}, ..., y_{jt-q+1})'$. Finally, the forecast for any $h > 1$ can be obtained from the FAVAR system, stacked in the first-order companion form

$$\underbrace{\begin{pmatrix} Z_t \\ Y_{jt} \end{pmatrix}}_{(r+1)q\times 1} = \begin{pmatrix} \underbrace{\Phi^Z}_{qr\times qr} & \underbrace{0}_{qr\times q} \\ \underbrace{\Lambda'_j}_{q\times qr} & \underbrace{\Phi^Y_j}_{q\times q} \end{pmatrix} \begin{pmatrix} \mathscr{Z}_{t-1} \\ Y_{jt-1} \end{pmatrix} + \begin{pmatrix} \mathscr{V}^{\mathscr{Z}}_t \\ \mathscr{V}^Y_{jt} \end{pmatrix} \tag{9}$$

$$\mathscr{Y}_{jt} = \Phi^{\mathscr{Y}}_j \mathscr{Y}_{jt-1} + \mathscr{V}^{\mathscr{Y}}_{jt}, \tag{10}$$

with Λ'_j and Φ^Y_j being functions of the coefficients in the lag polynomials in (5) and $\Phi^{\mathscr{Z}}$ representing stacked autoregressive coefficients of the predictors in $\mathscr{Z}_t$. It is worth noting that the above specification assumes that the coefficients are time-invariant.

Assuming stationarity, where the largest eigenvalue of $\Phi^{\mathscr{Y}}_j$ is less than one, the h-period ahead forecast can be expressed as the conditional mean

$$E_t \mathscr{Y}_{jt+h} = (\Phi^{\mathscr{Y}}_j)^h \mathscr{Y}_{jt}. \tag{11}$$

The forecast variance at time t is defined as

$$\Omega^{\mathscr{Y}}_{jt}(h) = E_t[(\mathscr{Y}_{jt+h} - E\mathscr{Y}_{jt+h})(\mathscr{Y}_{jt+h} - E\mathscr{Y}_{jt+h})']. \tag{12}$$

According to Jurado, Ludvigson and Ng (2015) the source of time variation in squared forecast error are time-varying variances of shocks in both y_{jt} and the predictors $\mathbf{Z}_T$. This has the following implications.

Note first that for $h = 1$, the forecast error variance has the form

$$\Omega^{\mathscr{Y}}_{jt}(1) = E_t(\mathscr{V}^{\mathscr{Y}}_{jt+1} \mathscr{V}^{\mathscr{Y}'}_{jt+1}). \tag{13}$$

When forecasting for more than one period in the future, meaning for $h > 1$, the forecast error variance of $\mathscr{Y}_{jt+h}$ evolves according to

$$\Omega^{\mathscr{Y}}_{jt}(h) = \Phi^{\mathscr{Y}}_j \Omega^{\mathscr{Y}}_{jt}(h-1) \Phi^{\mathscr{Y}'}_j + E_t(\mathscr{V}^{\mathscr{Y}}_{jt+h} \mathscr{V}^{\mathscr{Y}'}_{jt+h}). \tag{14}$$

As $h \to \infty$, the forecast converges towards the unconditional mean and the forecast variance towards the unconditional variance of $\mathscr{Y}_{jt}$, which implies lower variability of $\Omega^{\mathscr{Y}}_{jt}(h)$ with higher h (Jurado, Ludvigson & Ng 2015).

What I am interested in here is the expected uncertainty of a single series y_{jt+h} conditional on the available information in t, denoted as $\mathscr{U}_{jt}^{\mathscr{Y}}(h)$. This is obtained by choosing an appropriate entry of the forecast error variance $\Omega_{jt}^{\mathscr{Y}}(h)$ and calculating the square root,

$$\mathscr{U}_{jt}^{\mathscr{Y}}(h) = \sqrt{1_j' \Omega_{jt}^{\mathscr{Y}}(h) 1_j}, \tag{15}$$

where 1_j is a selection vector. An estimate of market uncertainty is then constructed as a weighted average of individual uncertainty estimates as

$$\sum_{j=1}^{N_y} w_j \mathscr{U}_{jt}^{\mathscr{Y}}(h). \tag{16}$$

A simple weighting approach is implemented here, where each individual uncertainty series is given an equal weight of $w_j = 1/N_y$. More complex weighting schemes were also considered by Jurado, Ludvigson and Ng (2015), but this is not the scope of this thesis, so only equal weighting is implemented.

3.3 Time-varying volatility

The intention of this section is to show how time-varying volatility in the predictor set $\mathbf{Z}$ and in series y_j contributes to the corresponding multi-step ahead forecast of uncertainty. As is stipulated by Jurado, Ludvigson and Ng (2015), the choice of the stochastic volatility model is important for one main reason. It allows for the construction of an exogenous shock to the second moment which is independent of innovations to y_t itself. They also note that this is consistent with the vast majority of the theoretical literature on uncertainty presuming the existence of an uncertainty shock that independently affects real activity. In contrast, this is not reflected in GARCH-type models, which instead have a shock that is not independent from innovations to y_t (Jurado, Ludvigson & Ng 2015).

Let us first consider the predictor set $\mathbf{F}_t$ (the same holds for $\mathbf{W}_t$). Assuming that elements of $\mathbf{F}_t$ are serially correlated and well described by a first-order univariate autoregressive process AR (1):

$$\mathbf{F}_t = \Phi^F \mathbf{F}_{t-1} + \mathbf{v}_t^F, \tag{17}$$

where subscripts are momentarily omitted for simplicity. If v_t^F was zero-difference with constant variance $(\sigma^F)^2$, the forecast error variance described in (14) would be $\Omega^F(h) = \Omega^F(h-1) + (\Phi^F)^{2(h-1)}(\sigma^F)^2$. This means that the variance would increase with h but remain the same for all t. I on the other hand allow the shocks to $\mathbf{F}$ to exhibit time-varying stochastic volatility as

$$v_t^F = \sigma_t^F \varepsilon_t^F, \qquad \varepsilon_t^F \overset{iid}{\sim} N(0,1), \tag{18}$$

with σ_t^F representing the latent volatility at time t. Following Jurado, Ludvigson and Ng (2015), the log volatility is assumed to have an autoregressive structure

$$\log(\sigma_t^F)^2 = \alpha^F + \beta^F \log(\sigma_{t-1}^F)^2 + \tau^F \eta_t^F, \tag{19}$$

with $\eta_t^F \overset{iid}{\sim} \mathcal{N}(0,1)$. The log volatility $\log(\sigma_t^F)^2$ is assumed to follow a stationary process so that $|\beta^F| < 1$. Moreover, the parameters $\alpha^F, \beta^F \tau^F$ represent the level of the log-variance α^F, the persistence of the log-variance β^F and the volatility of the log-variance τ^F (Kastner, 2016).

Equations (18) and (19) form a stochastic volatility model as presented in Kim, Shephard and Chib (1998), where the variance is specified to follow some latent stochastic process, in contrast to a function of the squares of previous observations and past variances which are represented in ARCH and GARCH type models (Kim, Shephard & Chib, 1998).

Again, an important feature of the stochastic volatility model is also that it allows for a shock to the second moment that is independent of the first moment (Jurado, Ludvigson & Ng 2015). The model implies

$$E_t(\sigma_{t+h}^F)^2 = \exp\left[\alpha^F \sum_{s=0}^{h-1} (\beta^F)^s + \frac{(\tau^F)^2}{2} \sum_{s=0}^{h-1} (\beta^F)^{2(s)} + (\beta^F)^h \log(\sigma_t^F)^2\right], \tag{20}$$

and since I assume $\varepsilon_t^F \overset{iid}{\sim} \mathcal{N}(0,1)$, it holds that $E_t(\nu_{t+h}^F)^2 = E_t(\sigma_{t+h}^F)^2$. This allows me the derivation of the $h > 1$ forecast error variance for F using the recursion

$$\Omega_t^F(h) = \Phi^F \Omega_t^F(h-1)\Phi^{F'} + E_t(\nu_{t+h}^F \nu_{t+h}^{F'}), \tag{21}$$

where for $h = 1$ holds that $\Omega_t^F(1) = E_t(\nu_{t+1}^F)^2$. The h period ahead predictor uncertainty at time t is then calculated as the square root of the h-step forecast error variance of the predictor

$$\mathcal{U}_t^F(h) = \sqrt{1_F' \Omega_t^F(h) 1_F}, \tag{22}$$

where 1_F is again an appropriate selection vector.

To efficiently represent how uncertainty in the predictors effects uncertainty in the individual variable of interest y_j, Jurado, Ludvigson and Ng (2015) assume that the forecasting model for y_j only has a single predictor $\hat{F}$. The model is given by

$$y_{jt+1} = \phi_j^y y_{jt} + \gamma_j^F \hat{F}_t + \nu_{jt+1}^y, \tag{23}$$

where analogously $\nu_{jt+1}^y = \sigma_{jt+1}^y \varepsilon_{jt+1}^y$ with $\varepsilon_{jt+1}^y \overset{iid}{\sim} \mathcal{N}(0,1)$ and

$$\log(\sigma_{jt+1}^y)^2 = \alpha_j^y + \beta_j^y \log(\sigma_{jt}^y)^2 + \tau_j^y \eta_{jt+1}^y, \qquad \eta_{jt+1}^y \overset{iid}{\sim} \mathcal{N}(0,1). \tag{24}$$

At $h=1$, the forecast error V^y_{jt+1} equals v^y_{jt+1} and is uncorrelated with the one-period ahead forecast error variance of the predictor $\hat{F}_{t+1}$, given by $V^F_{t+1} = v^F_{t+1}$. In the next step, for $h=2$, the forecast error in the predictor equals $V^2_{t+1} = \Phi^F V^F_{t+1} + v^F_{t+2}$. On the other side, the forecast error for y_{jt+2} is

$$V^y_{jt+2} = v^y_{jt+2} + \phi^y_j V^y_{jt+1} + \gamma^F_j V^F_{t+1}, \tag{25}$$

where the dependence on the one-period-ahead forecast error is obvious. However, V^y_{jt+1} and V^F_{t+1} are uncorrelated. When we continue to $h=3$, the forecast error evolves to

$$V^y_{jt+3} = v^y_{jt+3} + \phi^y_j V^y_{jt+2} + \gamma^F_j V^F_{t+2}, \tag{26}$$

which again depends on forecasting errors made for the preceding period made at time t, namely V^y_{jt+2} and V^F_{t+2}. However, unlike in the previous step ($h=2$) these two components are now correlated because they are both dependent on V^F_{t+1}.

Returning to the general case with the full predictor set $\mathbf{Z}_t = (\mathbf{F}', \mathbf{W}')'$ and its distributed lags, the h-step ahead forecasting error variance for Y_{jt+h} decomposes according to

$$\Omega^Y_{jt}(h) = \Phi^Y_j \Omega^Y_{jt}(h-1)\Phi^Y_j + \Omega^{\mathscr{Z}}_{jt}(h-1) + E_t(\mathscr{V}^Y_{jt+h}\mathscr{V}^{Y'}_{jt+h}) + 2\Phi^Y_j \Omega^{Y\mathbf{Z}}_{jt}(h-1), \tag{27}$$

where $\Omega^{Y\mathbf{Z}}_{jt}(h) = Cov(\mathscr{V}^Y_{jt+h}\mathscr{V}^{\mathscr{Z}}_{jt+h})$. The terms in $E_t(\mathscr{V}^Y_{jt+h}\mathscr{V}^{Y'}_{jt+h})$ are calculated assuming that $E_t(v^y_{jt+h})^2 = E_t(\sigma^y_{jt+h})^2$, $E_t(v^F_{t+h})^2 = E_t(\sigma^F_{t+h})^2$ and $E_t(v^W_{t+h})^2 = E_t(\sigma^W_{t+h})^2$.

Breaking down the RHS of (27), it can be observed that the time variation in uncertainty can be mathematically decomposed into four sources. $\Phi^Y_j \Omega^Y_{jt}(h-1)\Phi^Y_j$ represents the autoregresive component, common predictors are effecting the uncertainty through $\Omega^{\mathscr{Z}}_{jt}(h-1)$, $E_t(\mathscr{V}^Y_{jt+h}\mathscr{V}^{Y'}_{jt+h})$ is the source of stochastic volatility with the covariance term $2\Phi^Y_j \Omega^{Y\mathbf{Z}}_{jt}(h-1)$ at the end (Jurado, Ludvigson & Ng, 2015).

The uncertainty representation in (27), which is equivalent to (1) for subvector $\mathbf{Y}_t$, shows the importance of the predictor uncertainty through the second term $\Omega^{\mathscr{Z}}_{jt}(h-1)$. Due to the assumption of stochastic volatility in the innovations of individual factors, it provides time-variation to the uncertainty. Stochastic volatility in the series y_j comes through the third term with the covariance between the series and the predictor set at the end. Moreover, computation of the LHS of (27) requires stochastic volatility estimates in the forecast errors of every series y_j and of every factor in the predictor set $\mathbf{Z}$.

3.4 Stochastic volatility model

Kastner (2016) notes that the main feature of the stochastic volatility (hereinafter: SV) model is that each observation (in this case v^y_{t+1} and v^F_{t+1}) is assumed to have its "own" contemporaneous variance (σ^y_{t+1} and σ^F_{t+1} respectively). However, the variance is not allowed to vary unrestrictedly with time, otherwise, the estimation feasibility would be an issue. For that reason, the logarithm is assumed to follow an autoregressive process of the first order, as in (19) and (24). It is worth noting that this is fundamentally different from GARCH-type models with deterministic evolution of the time-varying volatility. Now, I first turn to a brief overview of the SV parametrization methods leading to the Markov chain Monte Carlo (hereinafter: MCMC) estimation presented by Kastner and Frühwirth-Schnatter (2014) and applied in this analysis.

The standard SV model presented in Kim, Shephard and Chib (1998) and first introduced by Taylor (1982) is specified as

$$
\begin{aligned}
y_t &= \beta e^{h_t/2}\varepsilon_t, \qquad t \geqq 1, \\
h_{t+1} &= \mu + \phi(h_t - \mu) + \sigma_\eta \eta_t, \\
h_0 &\sim \mathcal{N}\left(\mu, \frac{\sigma^2}{1-\phi^2}\right),
\end{aligned}
\tag{28}
$$

where y_t is the log return, h_t is the log volatility with the initial state h_0 drawn from the stationary distribution. Note that y_t and h_t in this generalized representation are equivalent to the one-step forecasting error ν_t and time-varying volatility σ_t in my analysis respectively.

Hautsch and Ou (2008) note that the main difficulty of SV framework, compared to the widely used GARCH-type models, is the availability of the likelihood of the SV model. Moreover, because the likelihood cannot be computed in closed form, the estimation becomes all but straightforward. Let $\theta = (\mu, \phi, \sigma_\eta^2)$ denote the set of model parameters in (28). The corresponding likelihood is defined by

$$
p(y|\theta) = \int_h p(y|h,\theta)p(h|\theta)dh, \tag{29}
$$

which is an intractable integral with respect to the unknown volatilities h. Harvey, Ruiz and Shephard (1994) have proposed a Quasi-Maximum Likelihood (hereinafter: QML) estimation with the state-space representation of the model in (28). This together with the linear transformation of the model and assumption of normality for the disturbances allowed them to employ the Kalman filter.[3] However, it has been noted that, even though this QML estimator is consistent and asymptotically normally distributed, it is suboptimal in finite samples. This is because the logarithm of the disturbance ε_t in (28) is poorly approximated by the normal distribution. Consequently, the QML estimator under the assumption of normality of $\log \varepsilon_t$ has poor small sample properties (Kim, Shephard & Chib, 1998).

Kim, Shephard and Chib (1998) provide the first complete MCMC simulation-based analysis of the SV model. The idea behind it is to produce variates from a given

[3]Kalman filter is an algorithm with prediction and correction mechanism. The algorithm predicts a new state based on a previous estimation and a correction term to the prediction error. Since it rests on the assumption of normality of the initial state vector and the disturbances of the system, the likelihood function can be recursively evaluated with the prediction errors generated from the filter (Jalles, 2009).

multivariate density. This is done with repeated sampling of a Markov chain, whose invariant distribution is the density of interest.

The goal is a direct analysis of the posterior density $\pi(\theta|y)$ by MCMC method. They also note that the key issue precluding this is that the likelihood function $f(y|\theta) = \int f(y|h,\theta)f(h|\theta)$ is intractable as already mentioned. However, they present an approach which overcomes this problem. Instead of analysing $\pi(\theta|y)$ density function, they focus on the density $\pi(\theta,h|y)$, where $h = (h_1,...,h_n)$ is the vector of latent volatilities. They show that this density can be sampled without computation of the likelihood function $f(y|\theta)$, by developing an MCMC procedure. The posterior moments and marginal densities are then estimated by averaging the relevant function of interest over the sampled variates.

Kim, Shephard and Chib (1998) start with the Gibbs sampler where they employ a rejection procedure for obtaining the latent volatility samples from $f(h_t|\mathbf{h}_{-t},y_t,\theta)$. One of the main drawbacks of this sampling algorithm is the slow convergence towards stationary distribution, which can be explained by high correlation in the components of $h|y,\theta$. Specifically, the sample draws in Gibbs sampler are not independent, which adds to high inefficiency of the sampler. This has prompted them to improve their MCMC algorithm with a linear approximation in the form of an offset mixture time series model with normal densities, which allows for the representation in a conditionally Gaussian state space model also analyzed by Carter and Kohn (1996) and leads to more efficient sampling. An important improvement of the sampler was that it allowed joint draws of h and μ. Additionally, draws of ϕ and σ_η^2 were obtained with the Metropolis-Hastings (hereinafter: MH) sampling algorithm. Kim, Shephard and Chib (1998) also show that it is possible to correct for the minor approximation error.

Kastner and Frühwirth-Schnatter (2014) note that simulation efficiency in state-space models can be improved with model reparametrization. The same was observed by Kim, Shephard and Chib (1998) with their offset mixture representation. In general, the model presented in (28) is considered a SV model in its centered parametrization (hereinafter: C). With shifting the level μ of h_t from state equation to observation equation by setting $\bar{h}_t = h_t - \mu$, one applies a partially non-centered parametrization. As already noted by Kim, Shephard and Chib (1998), the latter suffers from high inefficiency when sampling μ. However, the centered parametrization has several disadvantages as well (Kastner & Frühwirth-Schnatter, 2014).

The fully non-centered paramterization (hereinafter: NC) presented by Kastner and Frühwirth-Schnatter (2014) is expressed as

$$y_t \sim \mathcal{N}\left(0, \omega e^{\sigma \tilde{h}_t}\right), \tag{30}$$

$$\tilde{h}_t = \phi \tilde{h}_{t-1} + \eta_t, \qquad \eta_t \sim \mathcal{N}(0,1), \tag{31}$$

where $\omega = e^{\mu}$ and $\tilde{h}_t = (h_t - \mu)/\sigma$. Note that the initial value of $\tilde{h}_0|\phi$ is again drawn from stationary distribution of the latent process, namely $\tilde{h}_0|\phi \sim \mathcal{N}(0, 1/(1-\phi^2))$. It has been noted in the literature, that MCMC sampling and estimation improve when considering the non-centering or non-centered version of state-space model.

By analyzing the impact of alternative parameterizations, Kastner and Frühwirth-Schnatter (2014) observe that simulation efficiency depends on the true parameter values. They conclude that no single "best" parameterization can be identified. For that reason, they provide a strategy to overcome this deficiency. Moreover, they employ both C and NC by applying an ancillarity-sufficient interweaving strategy (hereinafter: ASIS) introduced by Yu and Meng (2011). This results in an efficient and robust sampler that always outperforms the more efficient parameterization considering all parameters at a small cost of design and computation.

Regardless of the parametrization method chosen, Kastner and Frühwirth-Schnatter (2014) note that the likelihood in the SV model still has an intractable form. Hence, Bayesian inference usually relies on sampling the latent states $\mathbf{h}$ and by treating these as known updating the parameters $\theta = (\mu, \phi, \sigma)$. Several sampling methods have been proposed in the literature (some of which were already mentioned). Kastner and Frühwirth-Schnatter (2014) adopted the sampling method by Rue (2001). They propose sampling latent volatilities through Cholesky factorization of the precision matrix within a more general Gaussian state-space framework by exploiting its band-diagonal structure. This is possible since the states (conditional distribution of states h given observed variable y) in Gaussian linear state-space models are recognized as a special case of Gaussian Markov random fields (McCausland, Miller & Pelletier, 2011). The latent volatilities are sampled "all without a loop" (hereinafter: AWOL). I now turn to a detailed description of this sampling algorithm, which is used in this analysis.

3.5 Bayesian inference: Markov Chain Monte Carlo (MCMC)

In this section, the MCMC sampling method presented by Kastner and Frühwirth-Schnatter (2014), will be described in more detail. The method is employed in this thesis to sample the latent volatilities of (18) and estimate parameters in (19) and (24).

3.5.1 Prior distributions

To complete the SV model presented in (19) and (24) and be able to perform the Bayesian inference, a set of prior distributions for parameters[4] $\boldsymbol{\theta} = (\mu, \beta, \tau)$ needs to be specified. Following Kim, Shephard and Chib (1998), the components for each parameter in $\boldsymbol{\theta}$ are independent, i.e., $p(\boldsymbol{\theta}) = p(\mu)p(\beta)p(\tau)$.

[4] I avoid using superscripts for generalization, since same applies to both SV models for $(\sigma^F)^2$ and $(\sigma^y)^2$ and for corresponding sets of parameters $\boldsymbol{\theta}^F = (\mu^F, \beta^F, \tau^F)'$ and $\boldsymbol{\theta}^y = (\mu^y, \beta^y, \tau^y)'$.

The level parameter $\mu \in \mathbb{R}$ is assigned with the usual normal prior $\mu \sim \mathcal{N}(b_\mu, B_\mu)$. In practice, this prior is usually uninformative through setting $b_\mu = 0$ and $B_\mu \geq 100$. It is noted by Kastner (2016) that this choice is not very influential.

For the persistence parameter $\beta \in (-1, 1)$, Kastner amd Frühwirth-Schnatter (2014) follow Kim, Shephard and Chib (1998) by choosing $(\beta+1)/2 \sim \mathscr{B}(a_0, b_0)$, which implies

$$p(\beta) = \frac{1}{2B(a_0,b_0)} \left(\frac{1+\beta}{2}\right)^{a_0-1} \left(\frac{1+\beta}{2}\right)^{b_0-1}, \tag{32}$$

with a_0 and b_0 being positive hyperparamters and $B(x,y) = \int_0^1 t^{x-1}(1-t)^{y-1}dt$ denotes the beta function. The support for this distribution is the interval (-1,1), which ensures the stationarity of the autoregressive volatility process.

For the volatility of log-volatility $\tau \in \mathbb{R}^+$, Kastner and Frühwirth-Schnatter choose

$$\tau^2 \sim B_\tau \times \chi_1^2 = \mathscr{G}\left(\frac{1}{2}, \frac{1}{2B_\tau}\right), \tag{33}$$

which is motivated by Frühwirth-Schnatter and Wagner (2010), so the prior for $\pm\sqrt{\tau^2}$ follows a centered normal distribution, i.e. $\pm\sqrt{\tau^2} \sim \mathcal{N}(0, B_\tau)$. This specification differs from usually assumed conjugate Inverse-Gamma prior used in Kim, Shephard and Chib (1998).

3.5.2 MCMC Methodology

First step in applying the MCMC sampling methodology as Kastner and Frühwirth-Schnatter (2014) is rewriting my SV model in state-space form with transformation of observation equation (18) into logarithms as[5]

$$\tilde{v}_t = \tilde{\sigma}_t^2 + \log \varepsilon_t^2, \qquad \varepsilon_t \sim \mathcal{N}(0,1), \tag{34}$$

where $\tilde{v}_t = \log v_t$ and $\tilde{\sigma}_t^2 = \log \sigma_t^2$. Equation (34) now takes the form of non-Gaussian linear state space model. However, following Kim, Shephard and Chib (1988) and Omori, Chib, Shephard and Nakajama (2007), the distribution of $\log \varepsilon_t^2$ can be approximated by a mixture of normal distributions, i.e.

$$\log \varepsilon_t^2 | s_t = i \sim \mathcal{N}(m_i, v_i^2), \tag{35}$$

$$P(s_t = i) = q_i, \tag{36}$$

where $s_t \in \{1, ..., 10\}$ defines the mixture component indicator[6] at time t, and $\mathcal{N}(m_i, v_i^2)$ denotes the density function of a normal distribution with mean m_i and variance v_i^2 of the

[5]The same logic applies to latent time-varying volatility $(\sigma^F)^2$ and $(\sigma^y)^2$ with corresponding parameter vectors $\boldsymbol{\theta}^F$ and $\boldsymbol{\theta}^y$.

[6]Kim, Shephard and Chib (1998) were using $K = 7$ components whereas Omori, Chib, Shephard and Nakajama (2007) have shown that a move to $K = 10$ components leads to a better approximation.

s_t-th mixture component as shown in Omori, Chib, Shephard and Nakajama (2007). This allows rewriting (34) with corresponding state equation (19) in a form of a linear and conditionally Gaussian state space model,

$$\tilde{v}_t = m_i + \tilde{\sigma}_t^2 + z_t, \tag{37}$$

$$\tilde{\sigma}_t^2 = \alpha + \beta \tilde{\sigma}_{t-1}^2 + \tau \eta_t, \tag{38}$$

where $z_t \sim \mathcal{N}(0, v_{s_t}^2)$, η_t is assumed to be standard normal, $\alpha = (1-\beta)\mu$ and initial value $\tilde{\sigma}_0^2|\mu, \beta, \tau$ is drawn from stationary distribution $\mathcal{N} \sim \Big(\mu, \tau^2/(1-\beta^2)\Big)$. Equations (37) and (38) represent the C parametrization of the SV model.

Additional NC parametrization of the system above is

$$\tilde{v}_t \sim \mathcal{N}(0, \omega e^{\tau \bar{\sigma}_t^2}) \tag{39}$$

$$\bar{\sigma}_t^2 = \beta \bar{\sigma}_{t-1}^2 + \eta_t, \tag{40}$$

where $\omega = e^{\mu}$, $\bar{\sigma}_t^2 = (\tilde{\sigma}_t^2 - \mu)/\tau$ and the initial value $\bar{\sigma}_0^2|\beta$ is again drawn from stationary distribution $\mathcal{N} \sim \Big(0, 1/(1-\beta^2)\Big)$. With this, MCMC AWOL sampling as in Kastner and Frühwirth-Schnatter (2014) becomes possible by repeating the following three steps:

[Step - 1] Sample latent volatilities AWOL by drawing from $\tilde{\boldsymbol{\sigma}}_{[-0]}^2|\tilde{\boldsymbol{\nu}}, \mathbf{s}, \mu, \beta, \tau^2$ or $\bar{\boldsymbol{\sigma}}_{[-0]}^2|\tilde{\boldsymbol{\nu}}, \mathbf{s}, \mu, \beta, \tau^2$ respectively, where the initial value is drawn from $\tilde{\sigma}_0^2|\tilde{\sigma}_1^2, \mu, \beta, \tau^2$ or from $\bar{\sigma}_0^2|\bar{\sigma}_1^2, \beta$.

[Step - 2] Sample μ, β, τ^2 via Bayesian regression.

- For C, a 2-block sampler is employed where τ^2 is drawn from $\tau^2|\tilde{\boldsymbol{\sigma}}^2, \mu, \beta$ while μ and β are jointly drawn from $\mu, \beta|\tilde{\boldsymbol{\sigma}}^2, \tau^2$.
- In NC, MH is needed only for updating β by drawing from $\beta|\bar{\boldsymbol{\sigma}}^2$, while μ and τ^2 are Gibbs-updated jointly from $\mu, \tau^2|\tilde{\boldsymbol{\nu}}, \bar{\boldsymbol{\sigma}}^2, \mathbf{s}$.

[Step - 3] Update the indicators $\mathbf{s}$ from $\mathbf{s}|\tilde{\boldsymbol{\nu}}, \tilde{\boldsymbol{\sigma}}^2$ in C or $\mathbf{s}|\tilde{\boldsymbol{\nu}}, \bar{\boldsymbol{\sigma}}^2, \mu, \tau^2$ in NC by employing inverse transform sampling.

The choice of prior hyperparameters of the parameter vector $\boldsymbol{\theta} = (\alpha, \beta, \tau)'$ is required before the first step. These are set as presented by Kastner (2016). Additionally, the indicators $\mathbf{s} = (s_1, ..., s_T)'$ and corresponding constants $\{q_i, m_i, v_i^2\}$ are set to best approximate the exact density of $\log \varepsilon_t^2$. Next, the three sampling steps are described in more detail.

3.5.2.1 Step - 1: Sampling the latent volatilities AWOL

Kastner and Frühwirth-Schnatter (2014) note that the joint density for $\tilde{\boldsymbol{\sigma}}^2$ (or $\bar{\boldsymbol{\sigma}}^2$) conditional on all other variables is multivariate normal. Since the latent volatility process is assumed to be well described with an autoregressive process of the first order, this distribution can be represented in terms of a tridiagonal precision matrix (inverse covariance matrix) $\boldsymbol{\Omega}$ with corresponding co-vector $\boldsymbol{c}$, which allows the use AWOL sampling.[7] This method presented in Rue (2001) and McCausland, Miller and Pelletier (2011) is computationally efficient and convenient as it requires no complex loops in its implementation.

In the case of centered parametrization (C), latent volatilities $\tilde{\boldsymbol{\sigma}}^2$ are drawn from $\tilde{\boldsymbol{\sigma}}^2_{[-0]}|\tilde{\boldsymbol{\nu}},\mathbf{s},\mu,\beta,\tau^2 \sim \mathcal{N}_T(\boldsymbol{\Omega}^{-1}\boldsymbol{c},\boldsymbol{\Omega}^{-1})$ where

$$\boldsymbol{\Omega} = \begin{bmatrix} \frac{1}{v^2_{s_1}}+\frac{1}{\tau^2} & \frac{-\beta}{\tau^2} & 0 & \cdots & 0 \\ \frac{-\beta}{\tau^2} & \frac{1}{v^2_{s_2}}+\frac{1+\beta^2}{\tau^2} & \frac{-\beta}{\tau^2} & \ddots & \vdots \\ 0 & \frac{-\beta}{\tau^2} & \ddots & \ddots & 0 \\ \vdots & \ddots & \ddots & \frac{1}{v^2_{s_{T-1}}}+\frac{1+\beta^2}{\tau^2} & \frac{-\beta}{\tau^2} \\ 0 & \cdots & 0 & \frac{-\beta}{\tau^2} & \frac{1}{v^2_{s_T}}+\frac{1+\beta^2}{\tau^2} \end{bmatrix} \tag{41}$$

and

$$\boldsymbol{c} = \begin{bmatrix} \frac{1}{v^2_{s_1}}(\tilde{\nu}_1 - m_{s_1}) + \frac{\mu(1-\beta)}{\tau^2} \\ \frac{1}{v^2_{s_2}}(\tilde{\nu}_2 - m_{s_2}) + \frac{\mu(1-\beta)}{\tau^2} \\ \vdots \\ \frac{1}{v^2_{s_{T-1}}}(\tilde{\nu}_{T-1} - m_{s_{T-1}}) + \frac{\mu(1-\beta)}{\tau^2} \\ \frac{1}{v^2_{s_T}}(\tilde{\nu}_T - m_{s_T}) + \frac{\mu(1-\beta)}{\tau^2} \end{bmatrix}. \tag{42}$$

For the noncentered parametrization, the latent volatilities are analogously drawn from $\bar{\boldsymbol{\sigma}}^2_{[-0]}|\tilde{\boldsymbol{\nu}},\mathbf{s},\mu,\beta,\tau^2 \sim \mathcal{N}_T(\boldsymbol{\Omega}^{-1}\boldsymbol{c},\boldsymbol{\Omega}^{-1})$ with

$$\boldsymbol{\Omega} = \begin{bmatrix} \frac{\tau^2}{v^2_{s_1}}+1 & -\beta & 0 & \cdots & 0 \\ -\beta & \frac{\tau^2}{v^2_{s_2}}+1+\beta^2 & -\beta & \ddots & \vdots \\ 0 & -\beta & \ddots & \ddots & 0 \\ \vdots & \ddots & \ddots & \frac{\tau^2}{v^2_{s_{T-1}}}+1+\beta^2 & -\beta \\ 0 & \cdots & 0 & -\beta & \frac{\tau^2}{v^2_{s_T}}+1+\beta^2 \end{bmatrix} \tag{43}$$

and

[7] Detailed derivation of both $\boldsymbol{\Omega}$ and $\boldsymbol{c}$ is described in Rue (2001) and McCausland, Miller and Pelletier (2011).

$$
\boldsymbol{c} = \begin{bmatrix} \frac{\tau}{v_{s_1}^2}(\tilde{v}_1 - m_{s_1} - \alpha) \\ \frac{\tau}{v_{s_2}^2}(\tilde{v}_2 - m_{s_2} - \alpha) \\ \vdots \\ \frac{\tau}{v_{s_{T-1}}^2}(\tilde{v}_{T-1} - m_{s_{T-1}} - \alpha) \\ \frac{\tau}{v_{s_T}^2}(\tilde{v}_T - m_{s_T} - \alpha) \end{bmatrix}. \tag{44}
$$

In both cases, C and NC, the precondition is a computation of the Cholesky decomposition $\boldsymbol{\Omega} = \boldsymbol{L}\boldsymbol{L}'$ using an algorithm that exploits the band-diagonal structure of $\boldsymbol{\Omega}$. It is worth noting that $\boldsymbol{L}$ also has a tridiagonal structure. To draw the latent volatilities, the algorithm first draws $\boldsymbol{\epsilon} \sim \mathscr{N}_T(\mathbf{0}, \boldsymbol{I}_T)$. Then $\boldsymbol{L}\boldsymbol{a} = \boldsymbol{c}$ is efficiently solved for $\boldsymbol{a}$ which then allows for computation of $\boldsymbol{h} = (\boldsymbol{L}')^{-1}\boldsymbol{L}^{-1}\boldsymbol{c} + \boldsymbol{\epsilon}$ using band back-substitution. Finally, the initial values can be sampled from $\tilde{\sigma}_0^2|\tilde{\sigma}_1^2, \mu, \beta, \tau \sim \mathscr{N}(\mu + \beta(\tilde{\sigma}_1^2 - \mu), \tau^2)$ for C and from $\bar{\sigma}_0^2|\bar{\sigma}_1^2, \beta \sim \mathscr{N}(\bar{\sigma}_1^2\beta^2, 1)$ in NC.

3.5.2.2 *Step - 2 (C): Sampling parameters α, β and τ*

Next step is sampling $\boldsymbol{\theta} = (\mu, \beta, \tau^2)$, for which a conditional AR (1) representation of (19) is exploited, namely[8]

$$
\tilde{\sigma}_t^2 = \alpha + \beta\tilde{\sigma}_{t-1}^2 + \eta_t, \qquad \eta_t \sim \mathscr{N}\left(0, \tau^2\right), \tag{45}
$$

where $\alpha = (1-\beta)\mu$. It is important to note that implied conditional prior $p(\alpha|\beta)$ is normal with mean $b_\mu(1-\beta)$ and variance $B_\mu(1-\beta)^2$.

In the two-block sampler employed here, the first block is sampled from the full conditional distribution $\alpha, \beta|\tilde{\boldsymbol{\sigma}}^2, \tau^2 \sim \mathscr{N}_2(\boldsymbol{b}_T, \tau^2\boldsymbol{B}_T)$ where $\boldsymbol{B}_T = (\boldsymbol{X}'\boldsymbol{X} + \boldsymbol{B}_0^{-1})$ and $\boldsymbol{b}_T = \boldsymbol{B}_T\boldsymbol{X}'\tilde{\boldsymbol{\sigma}}_{[-0]}^2$, with $\boldsymbol{X}$ being a $T \times 2$ design matrix $[\mathbf{1}, \tilde{\boldsymbol{\sigma}}_{[-T]}^2]$ (Kastner & Frühwirth-Schnatter, 2014). The acceptance probability for MH is given by $\min(1, R)$, where

$$
R = \frac{p(\tilde{\sigma}_0^2|\alpha_{\text{new}}, \beta_{\text{new}})p(\alpha_{\text{new}}|\beta_{\text{new}})p(\beta_{\text{new}})}{p(\tilde{\sigma}_0^2|\alpha_{\text{old}}, \beta_{\text{old}})p(\alpha_{\text{old}}|\beta_{\text{old}})p(\beta_{\text{old}})} \times \frac{p_{aux}(\beta_{\text{old}}, \alpha_{\text{old}})}{p_{aux}(\beta_{\text{new}}, \alpha_{\text{new}})}. \tag{46}
$$

Next, τ^2 is drawn from suitable proposal for the full conditional density $p(\tau^2|\tilde{\boldsymbol{\sigma}}^2, \mu, \beta)$, for which an auxiliary conjugate prior $p_{\text{aux}}(\tau^2) \propto \tau^{-1}$, under which Kastner and Frühwirth-Schnatter (2014) obtain

$$
\tau^2|\tilde{\boldsymbol{\sigma}}^2, \mu, \beta \sim \mathscr{G}^{-1}(c_T, C_T), \tag{47}
$$

[8] Analogoulsy, the same applies to the model in (24).

where $c_T = T/2$ and $C_T = \frac{1}{2}\left(\sum_{t=1}^{T}((\tilde{\sigma}_t^2 - \mu) - \beta(\tilde{\sigma}_{t-1}^2 - \mu))^2 + (\tilde{\sigma}_t^2 - \mu)^2(1-\beta^2)\right)$. The acceptance probability is simplified to $\min(1, R)$ where

$$R = \frac{p(\tau_{\text{new}}^2)}{p(\tau_{\text{old}}^2)} \times \frac{p_{\text{aux}}(\tau_{\text{old}}^2)}{p_{\text{aux}}(\tau_{\text{new}}^2)} = \exp\left\{\frac{\tau_{\text{old}}^2 - \tau_{\text{new}}^2}{2B_\tau}\right\}. \tag{48}$$

3.5.2.3 Step - 2 (NC): Sampling parameters α, β and τ

For the non-centered case, the state equation is only left with one parameter β, which is sampled from a flat auxiliary prior $p_{\text{aux}}(\beta) \propto c$. This yields in the proposal distribution

$$\beta|\bar{\boldsymbol{\sigma}}^2 \sim \mathcal{N}\left(\frac{\sum_{t=0}^{T-1}\bar{\sigma}_t^2\bar{\sigma}_{t+1}^2}{\sum_{t=0}^{T-1}(\bar{\sigma}_t^2)^2}, \frac{1}{\sum_{t=0}^{T-1}(\bar{\sigma}_t^2)^2}\right), \tag{49}$$

with an acceptance probability of $\min(1, R)$, where

$$R = \frac{p(\bar{\sigma}_0^2|\beta_{\text{new}})p(\beta_{\text{new}})}{p(\bar{\sigma}_0^2|\beta_{\text{old}})p(\beta_{\text{old}})}. \tag{50}$$

For sampling μ and τ, Kastner and Frühwirth-Schnatter (2014) rewrite the conditional observation equation (37) as a regression model with homoscedastic errors

$$\check{\boldsymbol{\nu}} = \boldsymbol{X}\begin{bmatrix}\mu \\ \tau\end{bmatrix} + \boldsymbol{z}, \tag{51}$$

where $\boldsymbol{z} \sim \mathcal{N}_K(\boldsymbol{0}, \boldsymbol{I}_K)$, and

$$\check{\boldsymbol{\nu}} = \begin{bmatrix}(\tilde{v}_1 - m_{s_1})/v_{s_1} \\ \vdots \\ (\tilde{v}_T - m_{s_T})/v_{s_T}\end{bmatrix}, \boldsymbol{X} = \begin{bmatrix}(\bar{\sigma}_1/v_{s_1})^2 & 1/v_{s_1} \\ \vdots & \vdots \\ (\bar{\sigma}_T/v_{s_T}^2 & 1/v_{s_T}\end{bmatrix}. \tag{52}$$

The joint posterior distribution is bivariate Gaussian with the variance-covariance matrix $\boldsymbol{B}_T = (\boldsymbol{B}_0^{-1} + \boldsymbol{X}'\boldsymbol{X})^{-1}$ and mean $\boldsymbol{b}_T = \boldsymbol{B}_T(\boldsymbol{B}_0^{-1}\boldsymbol{b}_0 + \boldsymbol{X}'\check{\boldsymbol{\nu}})$, with $\boldsymbol{b}_0 = (b_\mu, 0)'$ and $\boldsymbol{B}_0 = \text{diag}(B_\mu, B_\tau)$ denoting the mean and variance of the joint prior density $p(\mu, \tau)$, respectively (Kastner & Frühwirth-Schnatter, 2014).

3.5.2.4 Step - 3: Sampling the indicators s

Following Omori, Chib, Shephard and Nakajama (2007), the next step involves sampling the indicators s. Kastner and Frühwirth-Schnatter (2014) note that by rearranging the equation (37) as

$$\tilde{v}_t = m_i + \tilde{\sigma}_t^2 + z_t^*, \qquad z_t^* \sim \mathcal{N}(m_{s_t}, v_{s_t}^2) \tag{53}$$

the posterior probabilities $P(s_t = i|\cdot)$ for $i \in \{1,...,10\}$ and $t \in \{1,...,T\}$ can be obtained according to

$$P(s_t = i|\cdot) \propto P(s_t = i)\frac{1}{v_i}\exp\left\{-\frac{(z_t^* - m_i)^2}{2v_i^2}\right\} \tag{54}$$

where $P(s_t = i)$ denotes the mixture weights of the i-th component.

3.5.2.5 Interweaving C and NC by ASIS

Each parametrization, centered and non-centered, exhibits some sampling inefficiencies regarding the draws of particular parameters. Moreover, Kastner and Frühwirth-Schnatter (2014) note that the efficiency of each parametrization depends on the value of β. If $\beta = 0$, the state equation (38) reduces to $\tilde{\sigma}_t^2 \sim \mathcal{N}(\mu, \tau^2)$. Consequently, $\tilde{\sigma}_t^2$ becomes informative for draws μ if the variance τ^2 approaches 0, which results in C being inefficient. However, if β approaches 1, $\tilde{\sigma}_t^2$ would be less informative about μ meaning that little information is lost with $\tilde{\sigma}_t^2$ as a latent process. On the other hand, β approaching zero poises no trouble for NC, since state equation (40) reduces to $\bar{\sigma}_t^2 \sim \mathcal{N}(0,1)$, which is independent of τ.

Following Yu and Meng (2011), Kastner and Frühwirth-Schnatter (2014) note that the latent process $\tilde{\boldsymbol{\sigma}}^2$ forms a sufficient statistic for μ and τ, whereas the transformed version $\bar{\boldsymbol{\sigma}}$ in NC forms a ancillary statistic for the same set of parameters. Yu and Meng (2011) observe that if one parameterization leads to fast convergence, then the other is usualy slow and propose an ASIS. They also show, that this algorithm in certain situations converges geometrically when C and/or NC do not, and even outperforms both. Yu and Meng (2011) relate this result to Basu's theorem on the independence of complete sufficient and ancillary statistics, and show that the convergence rate of the interwoven sampler is in general driven by individual rates of convergence and posterior correlation. This implies the possibility of ancillary-sufficiency pairs of latent variables reducing sampling inefficiency.

The algorithm itself is simply based on sampling the parameters μ, β and τ twice. In this analysis the latent volatilities and indicators are drawn once with centered parameterization, while μ, β and τ are sampled once with each parameterization within each iteration. Morover, the algorithm starts with choice of appropriate starting values, then it repeats the following steps:

[Step - 1] Sample latent volatilities $\tilde{\boldsymbol{\sigma}}$ (C).

[Step - 2] Draw μ, β, τ (C).

- [Step - 2.1] Move to NC with deterministic transformation $\bar{sigma}_t = \frac{\tilde{\sigma}_t - \mu}{\tau}$ for all t.
- [Step - 2.2] Redraw μ, β, τ (NC).
- [Step - 2.3] Move back to C by calculationg $\tilde{\sigma}_t = \mu + \tau \bar{sigma}_t$ for all t.

[Step - 3] Sample the indicators $\boldsymbol{s}$ (C).

It is worth noting that the implementation of individual sampling steps follows the description in section 3.5.2.

4 DATA

For this empirical analysis, a large dataset with focus on German electricity market was created, which is comprised of 312 variables and 550 daily observations that range from February 2015 to April 2017 (see Appendix B). The size of the original dataset was initially 678 observations of 330 variables, which was later adjusted due to the missing data issue. First, the data set was truncated, which resulted in significant improvement in terms of missing observations, where some variables were also omitted due to the same reason. Next, Piecewise Cubic Hermite Interpolating Polynomial (hereinafter: PCHIP) interpolation was applied to fill in the rest of the missing observations. Finally, all variables have been appropriately transformed to ensure stationarity. This was tested by employing the Augmented Dickey-Fuller (hereinafter: ADF) test. In addition, when forming forecasting factors, the data was also standardized before performing Principal Component Analysis (hereinafter: PCA).

Table 1: Variable overview

Vartype	Data type	# of variables	Transformation	Adjustment
1	Futures contract	12	Δ	Contract jumps adjustment
2	Electricity Day-ahead price	9	Δ	Day-type weighted standardization
3	Exchange rate	3	Δ	
4	Temperature	1	Δ	
5	Electricity Consumption	8	Δ	
6	Electricity Generation	21	Δ	
7	Net Scheduled Commercial exchange of electricity	8	Δ	
8	Stock price (DAX)	28	Δln	
9	49 Industry Portfolios - Returns (FF)	49		
10	ETF Price (Energy)	173	Δln	

Source: Own work.

All 312 variables have been split into 10 groups based on their common characteristics (e.g. source, type), where the summary of all groups is presented in Table 1. The first group is selected to represent the derivatives market for electricity with commodities derivatives relevant for German electricity market, which are API2 Rotterdam Coal, European Emission Allowances, German NCG Gas and Brent Oil. These variables also constitute the set of dependent variables for which the conditional volatilities are estimated. and further aggregated to represent a market level electricity futures market uncertainty indicator. The dependent variables are also standardized prior model estimation. A graphical analysis is presented in Appendix C, where standard deviations are calculated for 20 days rolling window and plotted on the right hand side of Figures 16, 17 and 18. Growing volatilities in 2016 with record highs in the last two quarters of the same year can be observed for electricity prices. This was also noted by EEX in their 2016 Annual

Report, where historically high volatility in the second half of 2016 was explained by unscheduled production downtime at around one-third of French nuclear power plants.

Table 2 provides some descriptive statistics for the set of dependent variables (post-adjustment described below), where deviations from normality can be observed. Specifically, the dependent series, in general, appear to be slightly skewed with significant excess kurtosis which already sheds some light on possible tail events and their persistence. Graphical representation of empirical distributions for the dependent variables is reported in Figure 19 of the Appendix C. I also conducted a Jarqe-Berra (hereinafter: JB) test for normality, where I reject the null for all series with a significance level of 0,001. It is worth noting that JB test statistic is asymptotically Chi-squared distributed with two degrees of freedom. However, an approximation of this distribution tends to be overly sensitive for small sample sizes and often rejecting the null. That is why I use the MATLAB implementation of the test, which uses a table of critical values computed using Monte Carlo simulation for small sample sizes (Deb & Sefton, 1996).

Table 2: Descriptive statistics of dependent variables

Statistic	BREM1	AP2M1	NCGM1	EUAY1	BASEY1	BASEQ1	BASEM1	BASEM2	BASEM3	BASEM4	BASEM5
nObs	550	550	550	550	550	550	550	550	550	550	550
Mean	-0,043	0,077	-0,005	-0,021	0,000	0,003	0,029	0,005	0,002	0,007	0,002
Std	1,207	0,987	0,165	0,323	0,444	0,373	0,650	0,507	0,478	0,430	0,449
Min	-4,59	-4,00	-0,70	-1,34	-2,04	-1,28	-2,89	-2,41	-2,38	-1,65	-2,36
Max	4,42	7,80	0,72	1,03	2,42	1,41	3,44	2,11	2,18	2,56	2,53
Skew	0,164	1,002	0,012	0,017	0,323	0,271	0,286	0,187	0,059	0,492	0,071
Kurt	3,825	11,209	5,412	4,257	7,673	4,773	7,808	7,033	8,429	6,147	7,061
JB	18,0	1636,4	133,4	36,3	509,9	78,8	537,2	375,9	675,8	249,2	378,3
P-Value	0,002	0,001	0,001	0,001	0,001	0,001	0,001	0,001	0,001	0,001	0,001

Source: Own work.

The second group of predictors represents the electricity spot market for Germany and all neighboring and otherwise relevant markets. Temperature is represented in the third group as a weather indicator related to RES production. Exchange rates are captured in group four representing possible exchange rate risks. Electricity consumption, generation and commercial exchange have been represented in groups 5, 6 and 7. The last three groups represent the financial market with emphasis on German real sector and international energy sector. First difference transformation (Δ) has been applied to all electricity-related variables, whereas financial variables are transformed using logarithmic returns (Δln). Due to some characteristics specific for electricity spot and futures markets, additional adjustments noted in the last column of Table 1 have been employed and are described below.

4.1 Contract jumps adjustment

Futures contract prices represent the set of dependent variables used for uncertainty estimation in this thesis. In order to be able to properly model these prices, continuous futures contracts were constructed. That was achieved by concatenating several sequential futures contracts with the same delivery period. Front-month is the most common continuous futures price representation, where prices are comprised of the contracts for the month with the nearest expiration date. However, this is often times not straightforward, which especially holds for electricity prices.

Figure 5: Contract shift adjustment for DE M+1 (Front Month)

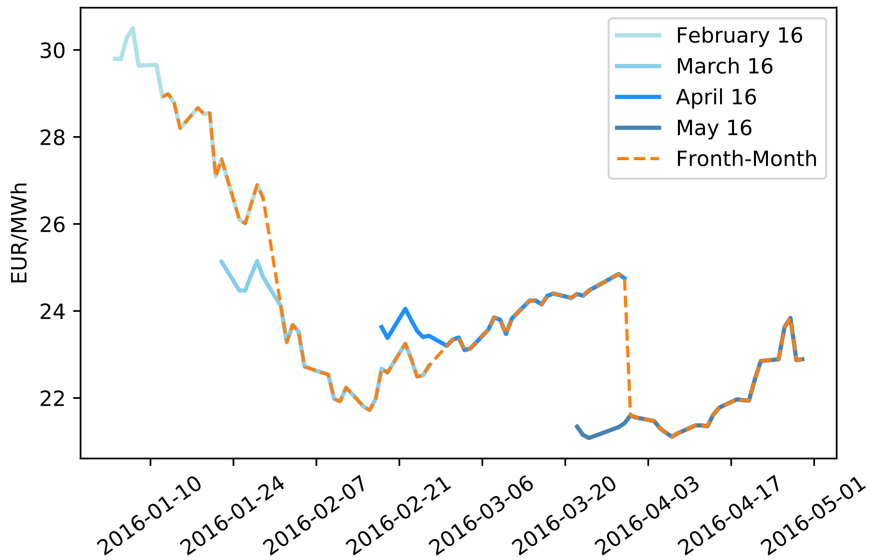

Source: Own work.

Usually, an adjustment is involved with the concatenation to control for the gaps between different contracts, which are presented in Figure 5. These gaps have some common reasons across different markets such as the time premium for example. However, as already emphasised, seasonality is a very important factor in electricity market. Delivery for a particular period is effectively a different product with the price driven by its seasonal load profile. This results in different prices for different months (quarters/years) reflective of the seasonal demand expectations.

Using the front-month price series as depicted with the orange dotted line in Figure 5, would result in artificial breaks in price and spikes in historical volatility. Since I transform the underlying price series into first differences, I want to avoid modeling these spikes and drops. A simple solution would be to exclude observations where prices jumps from one contract to another occur. However, this would cause a significant reduction in the number of observations. For that reason, I adopted a different adjustment. As is presented in Figure 5, the difference between April and May contracts would result in a large drop on 31st of March. However, this drop is replaced with the difference calculated on the same day, where as the reference price $(t-1)$, the price for the same (May) contract is used. The same logic is applied to all products and all delivery periods. This results in a smooth price series without breaks between contracts which is especially well depicted with historical volatility on the right-hand side of Figure 6.

Figure 6: Adjusted price and historical volatility for DE M+1 (Front Month)

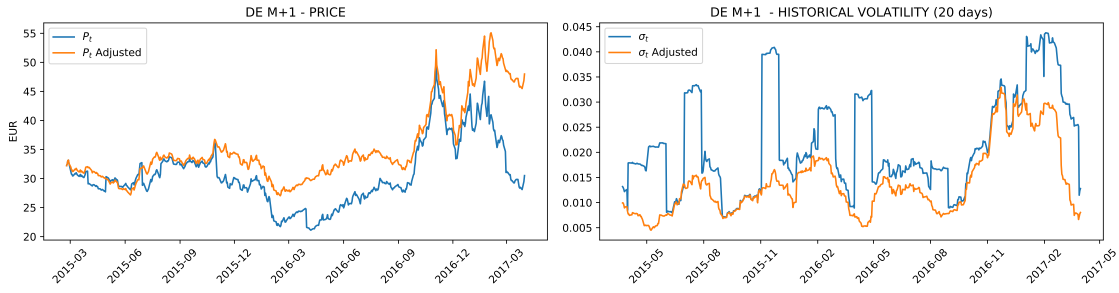

Source: Own work.

4.2 Day-type standardization

One of the key specific characteristics of electricity spot prices is the seasonal pattern at the daily, weekly and annual level, which is driven by seasonality in demand with the non-storability constraint (Weron, 2014; Bessec, Fouquau & Meritet, 2016; Haldrup, Knapik & Proietti, 2016; Misiorek, Trueck & Weron, 2006). In order to control for daily seasonality, some researchers have adopted a dummy variable approach in adjusting the time series models (Haldrup & Nielsen, 2006; Misiorek, Trueck & Weron 2006; deJong & Huisman, 2002). On the other hand, I have controlled for daily seasonality of spot prices by day-type standardization. With this, I controlled for differences in means and variances of different days on the spot market. The adjusted daily price at time t for weekday i $P_{t,i}^{adj}$ was calculated using

$$P_{t,i}^{adj} = \frac{P_{t,i} - \bar{P}_i}{\sigma_i}, \tag{55}$$

where $P_{t,i}$ is price at time t on weekday i, $\bar{P}_i$ the mean of daily prices for weekday i and σ_i the variance of daily prices for weekday i.

5 ESTIMATION AND EMPIRICAL RESULTS

This analysis is centered around the estimation of uncertainty for electricity and commodity derivatives market. Forecasts are formed for each individual contract, which are at the end aggregated into an electricity futures market uncertainty indicator. Moreover, formation of historically accurate volatility estimates is not the main goal of this analysis, but to provide reliable and accurate multi-period forecasts. The aggregated level of uncertainty is calculated for German electricity futures market.

For this analysis, a large dataset $\boldsymbol{X}$ was formed with which I try to account for all possible sources of uncertainty as described in section 1.3. The dataset can be mainly split in two parts. The first part contains 90 variables directly related to German electricity market or German real sector performance. The second part represents the global financial market for different industries, where the focus is on the energy and energy related sectors and commodities in particular. Detailed list of all the variables is presented in Appendix B.

5.1 Estimates of individual volatilities and market uncertainty

Using the full dataset $\boldsymbol{X}$, I estimate individual uncertainties for the set of dependent variables $\boldsymbol{y}$ presented in the first 12 rows of Table 12 of Appendix B. This is done by forming a set of forecast errors representing only the unforecastable component. Forecasting errors are formed by employing the diffusion index forecasting, where relatively small set of diffusion indexes or underlying factors $\boldsymbol{F}_t$ is first estimated for the full dataset $\boldsymbol{X}$.

5.1.1 Common Factors

The factors used in forming the forecast errors are estimated using a Principal Components Analysis (hereinafter: PCA). Specifically, the common factors are estimated using an asymptotic PCA where the number of the factors r_F is determined by the information criteria by Bai and Ng (2002). Using the full $\boldsymbol{X}$ dataset, this criterion suggests $r_F = 11$ factors $\hat{\boldsymbol{F}}_t$. With this dimensionality reduction, the full set of common factors $\hat{\boldsymbol{F}}_t$ explains about 57 percent of variation observed in $\boldsymbol{X}$, where the first three factors account for 28, 8 and 5 percent respectively. The factor structure and description of $\hat{\boldsymbol{F}}_t$ is presented in Table 3.

The first factor loads mainly on the Energy ETF Returns, while the second and third factors represent price movements on the precious metals markets (e.g. gold, silver). The fourth factor represents the German real sector with DAX returns, while the fifth factor loads mainly on electricity spot prices. The next two factors load heavily on electricity derivatives price. Finally, the last four factors mainly load on the energy and commodity financial market returns with the exception of tenth factor, which mainly captures the electricity consumption and generation. Detailed representation of the factor structure for $\boldsymbol{F}_t$ is provided in Table 18 in the Appendix D.

The common factors $\hat{\boldsymbol{F}}_t = (\hat{F}_{1,t}, ..., \hat{F}_{r_F,t})$ constitute the first subset of potential predictors used in forecasting models for each y_{jt}. Following Jurado, Ludvigson and Ng (2015), I also consider an additional subset of predictors $\boldsymbol{W}_t$. Specifically, $\boldsymbol{W}_t$ consists of two additional factors. One is calculated as squares of the first common factor of $\hat{\boldsymbol{F}}_t$, while for the second is the factor with the largest eigenvalue from $X_{i,t}^2$ which were collected into a $N_G \times 1$ vector $\hat{\boldsymbol{G}}_t$. The main purpose of the quadratic terms in $\boldsymbol{W}_t$ is to capture possible nonliniarities or possible additional effects of conditional volatility on the conditional mean function.

The final set of all possible predictors is at the end summarized with a small number of indexes $\hat{\boldsymbol{F}}_t$ and $\boldsymbol{W}_t$ (and corresponding distributed lags). In the next step, the empirical

Table 3: $\hat{\boldsymbol{F}}_t$ factor structure and description

Factor	Share of explained variance	Description
1	27,6%	Energy, Oil and Gas
2	8,2%	Gold
3	4,5%	Gold, Silver and other precious metals
4	3,4%	German real sector (DAX)
5	2,6%	Electricity spot prices
6	2,3%	Electricity futures prices
7	2,0%	Electricity, coal and gas futures prices
8	1,9%	Energy infrastructure
9	1,8%	Natural gas market
10	1,6%	Electricity consumption and production
11	1,4%	Copper, industrial metals, other

Source: Own work.

analysis focuses on the h-step-ahead forecasts to obtain the forecasting error. This is done by employing the diffusion index forecasting. I now turn to these results.

5.1.2 Diffusion index forecasting

Following Jurado, Ludvigson and Ng (2015), the predictors which were ultimately used in the forecasting model were chosen based on their incremental predictive power or their significance. This was done by employing two different methods. The first method is motivated by Jurado, Ludvigson and Ng (2015), while in the second I employ the Bayesian averaging of Doppelhofer, Miller and Sala-i-Martin (2004).

5.1.2.1 Open-Lag (OL) models

As Jurado, Ludvigson and Ng (2015), I start with a full set of possible predictors. This includes all the estimated factors in X_{it}, the first estimated factor in X_{it}^2 and the square of the first estimated factor of X_{it}. These constitute my predictor vectors $\hat{\boldsymbol{F}}_t$ and $\boldsymbol{W}_t = (\hat{G}_{1,t}^2, \hat{F}_{1,t}^2)$ respectively.

The ultimate set of predictors using this method is chosen by estimating the model in (6) for each dependent variable y_{jt+1}. The models are structured by using a constant, five lags of dependent variable and five distributed lags of predictors in $\hat{\boldsymbol{F}}_t$ and $\boldsymbol{W}_t$. Next a two-step procedure is employed. The first step involves estimating the model parameters using Least-squares Regression and a full set of predictors. Since one of the key assumptions is that the forecast errors exhibit time-varying volatility, the Newey-West estimator of the covariance matrix is used. In the second step, a threshold rule is employed, where only the predictors with t-statistic greater than 1.96 are kept. After excluding all the insignificant predictors, the models are re-estimated for which an overview of results is presented in Table 4.

Table 4: DI Model estimation results with OL models

Model	Predictor ($\boldsymbol{k}$)												
y_{jt+1}	$\hat{F}_1$	$\hat{F}_2$	$\hat{F}_3$	$\hat{F}_4$	$\hat{F}_5$	$\hat{F}_6$	$\hat{F}_7$	$\hat{F}_8$	$\hat{F}_9$	$\hat{F}_{10}$	$\hat{F}_{11}$	W_1	W_2
BREM1	(1)	(1)	(1)	(1)							(1)		
AP2M1		(2)				(1)	(1,2)	(1)				(4)	(4)
EUAY1	(1,3)	(2)		(3)	(2)			(3)					
NCGM1		(2)		(3)	(2)		(1,2)	(1,3)				(2,4)	(2,4)
BASEQ1	(5)	(2)						(3)				(4)	(2,4)
BASEY1	(4)	(2)			(2)			(3)			(3)	(2,4)	(2,4)
BASEM1	(2)							(3)					
BASEM2	(2,4,5)	(2,5)					(5)	(3)				(5)	(5)
BASEM3	(5)	(2)	(3)		(4)		(4)	(3,5)				(2,5)	(2)
BASEM4	(1,5)	(2)		(1,3)	(2,5)	(1,5)	(1,3,5)	(3,5)					(4)
BASEM5	(1)			(1)	(4)	(1)	(1,5)						
BASEM6		(2)	(2)	(1,5)		(1)	(1)	(1,3)			(3)		

Notes: The numbers in the brackets represent the vector of lags $\boldsymbol{k} \in (1, ..., 5)$ with which the predictors listed in the columns enter (if they enter) particular model summarised in each row.

Source: Own work.

It can be observed that the predictor most frequently selected is the second factor $\hat{F}_2$ describing the gold price movements, followed by the first and eight factors $\hat{F}_1$ and $\hat{F}_8$ mostly correlated with Energy, Oil and Gas related ETF returns and Energy infrastructure ETF returns respectively. Next, the similarities in terms of lag structure can be observed, where some of the factors are entering multiple models with the same lags. The second factor $\hat{F}_2$ representing the movements in gold prices is consistently appearing in the models with second lag. Same holds for the fourth and eighth factors, which are mainly represented with the the first and the third lag. It is also important to note that all models include a constant and five lags of the dependent variable, which were all statistically significant in each model.

Due to its design, the method described above and used in Jurado, Ludvigson and Ng (2015) allows for open lag structure which is evident from Table 4. Secondly, in determining the relevant predictors for each model it solely focuses on their statistical significance, which alone may not be a good basis for variable selection, especially when used in forecasting model. This leads me to employ the second model build and variable selection method.

5.1.2.2 Closed-Lag (CL) models

I again start with all possible predictors in $\hat{\boldsymbol{F}}_t$ and $\boldsymbol{W}_t$. Employing the bayesian averaging methodology, I next construct an array of individual models. This is done by first considering all possible combinations of k_i regressors for model i out of r_F and r_W total predictors. With $k_i = 2$ and $r_F + r_W = 13$ this results in 91 distinct models. Next, for each model i an optimal lag structure is chosen. For this, I consider all possible lag combinations with up to 5 autoregressive terms and 5 distributed lags and forcing a closed lag structure. All models are then estimated using an OLS estimator and screened for statistical validity. Finally only the best model i is chosen based on the Akaike (hereinafter: AIC) information criterion.

With this method, I obtain 91 statistically well-specified ARDL models for each dependent variable y_{jt}. Next, posterior probabilities are calculated for the set of final models as shown in (7). Averaged across the 12 sets of models for each dependent variable, the first 15 models account for almost 88 % cumulative posterior probability, which can be deduced from Figure (7). Moreover, it is consistent across the set of dependent variables that 10 to 15 models trump the rest in terms of fit statistic and are hence assigned higher posterior probabilities. Additionally, around 10 models on average share similar and relatively high level of posterior probability, which results in a rich set of predictors per model.

Figure 7: Ranked average posterior probabilities of well specified ARDL models

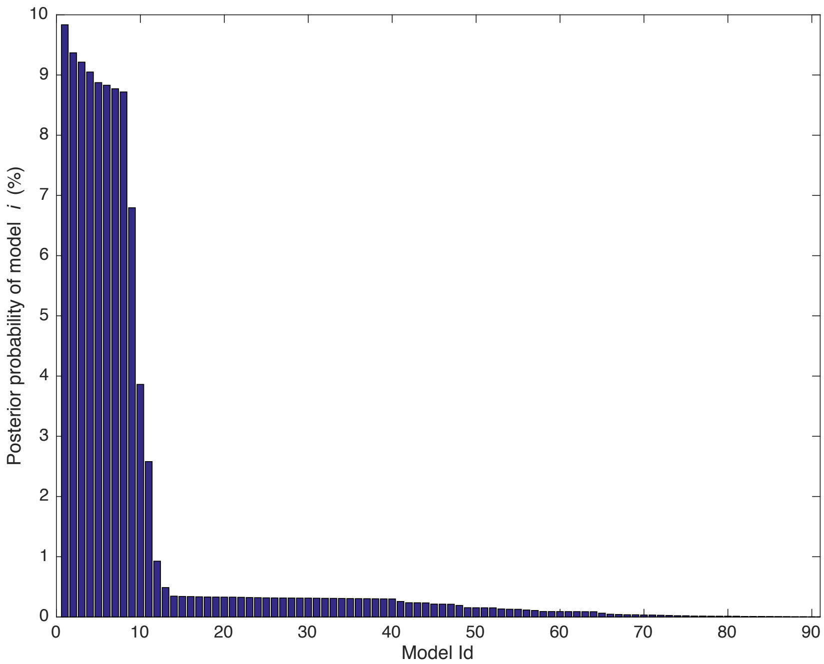

Source: Own work.

Finally, with obtained posterior probabilities, the posterior mean parameters are calculated as shown in (8). With this, I obtain one posterior model equation for each dependent variable y_{jt+1} which has a closed lag structure and is richer in terms of predictors. The closed lag structure also allows me to describe the models in terms of Long-Run Multipliers (hereinafter: LRM) with respect to the predictor Z_t^k. The LRM for each predictor Z_t^k is calculated using

$$\sum_{l=0}^{\infty} \frac{\partial E(y_{jt+l})}{\partial Z_t^k} = (\gamma_1^k + \cdots + \gamma_q^k)/(1 - \sum_{i=1}^{p_y} \phi_{p_y}^y) \equiv \Theta^k. \tag{56}$$

Furthermore, summarising the model coefficient estimates on contemporaneous and distributed lags of a predictor on a multiplier basis enables a comprehensive and concise interpretation of possibly complex models. Additionally, I also calculate normalised LRMs or LRMs based on normalized model coefficients. The latter is computed by multiplying the initial model coefficients by the ratio of the standard deviation of the predictor variable and the standard deviation of the dependent variable. The resulting coefficients, and hence the normalized LRMs, are thereby scale-free and comparable in magnitudes across predictors within each model, which is especially useful if the predictor variables come with an interpretability constraint. The model results in terms of LRMs are presented in Table (5).

Table 5: DI Model estimation results with CL models

Model	Predictor												
y_{jt+1}	$\hat{F}_1$	$\hat{F}_2$	$\hat{F}_3$	$\hat{F}_4$	$\hat{F}_5$	$\hat{F}_6$	$\hat{F}_7$	$\hat{F}_8$	$\hat{F}_9$	$\hat{F}_{10}$	$\hat{F}_{11}$	W_1	W_2
BREM1	-9,76	0,60	-5,53	-1,13	4,06	-0,18	4,12	2,46	-1,38	2,62	0,01	4,78	-6,51
	(10,2%)	(2,1%)	(10,5%)	(10,1%)	(10,3%)	(10,0%)	(10,1%)	(10,1%)	(10,1%)	(10,1%)	(0,0%)	(10,2%)	(10,4%)
AP2M1	2,68	2,70	3,13	2,30	-3,55	18,70	3,64	8,24	3,20	0,41	-2,99	-7,57	8,09
	(10,0%)	(2,1%)	(10,3%)	(10,3%)	(10,4%)	(13,0%)	(3,3%)	(10,4%)	(10,1%)	(2,3%)	(10,3%)	(10,6%)	(10,7%)
EUAY1	-0,38	3,21	3,29	-3,30	5,20	-0,40	6,36	0,42	4,68	-1,85	11,49	-12,91	15,52
	(0,5%)	(2,5%)	(11,4%)	(11,4%)	(11,3%)	(11,3%)	(11,7%)	(0,5%)	(11,2%)	(2,3%)	(12,6%)	(12,9%)	(13,3%)
NCGM1	4,84	3,38	1,69	-3,36	-2,37	5,24	0,62	2,17	-0,66	-0,76	4,77	-3,66	6,88
	(12,6%)	(2,9%)	(12,3%)	(12,5%)	(2,7%)	(12,6%)	(2,9%)	(0,8%)	(12,3%)	(2,6%)	(12,6%)	(12,2%)	(12,6%)
BASEQ1	0,00	4,37	6,97	0,77	-1,98	-8,22	5,94	0,94	6,68	-1,96	6,52	-7,82	12,05
	(0,0%)	(2,5%)	(12,0%)	(11,6%)	(2,3%)	(12,0%)	(11,8%)	(0,5%)	(12,0%)	(11,7%)	(11,9%)	(11,8%)	(12,3%)
BASEY1	-0,39	3,94	8,38	3,38	-2,04	-3,20	13,19	1,23	4,78	-1,85	1,16	-12,23	15,36
	(0,5%)	(2,9%)	(13,1%)	(12,6%)	(2,7%)	(12,6%)	(13,5%)	(0,6%)	(12,7%)	(12,5%)	(0,5%)	(13,3%)	(13,9%)
BASEM1	-0,10	3,25	8,11	2,19	-1,89	4,90	9,84	0,98	2,19	-3,35	2,80	-7,45	11,95
	(0,1%)	(2,4%)	(12,1%)	(11,6%)	(2,3%)	(11,8%)	(12,1%)	(0,5%)	(11,6%)	(11,7%)	(11,7%)	(12,1%)	(12,6%)
BASEM2	-0,06	2,78	5,74	1,50	-11,51	7,42	-0,76	1,44	4,40	0,31	6,85	-6,51	11,92
	(0,1%)	(2,2%)	(10,9%)	(10,6%)	(11,9%)	(12,1%)	(10,6%)	(0,6%)	(10,8%)	(10,6%)	(10,9%)	(11,0%)	(12,6%)
BASEM3	-4,15	3,66	6,61	0,42	1,41	3,64	3,63	0,96	8,98	0,89	5,44	-6,96	9,00
	(10,2%)	(2,2%)	(9,9%)	(10,0%)	(10,0%)	(10,1%)	(9,9%)	(0,4%)	(10,7%)	(10,0%)	(10,3%)	(10,2%)	(10,2%)
BASEM4	-8,04	3,28	6,33	0,79	-2,03	0,93	20,61	0,67	4,72	2,37	2,97	-9,44	13,39
	(11,7%)	(2,5%)	(11,5%)	(1,4%)	(2,3%)	(11,2%)	(13,8%)	(0,5%)	(11,4%)	(11,2%)	(11,3%)	(12,3%)	(12,8%)
BASEM5	-9,31	1,95	6,80	6,84	-1,02	16,55	12,16	0,21	2,92	-1,39	0,68	-6,23	8,71
	(11,3%)	(2,3%)	(11,8%)	(11,8%)	(0,8%)	(13,5%)	(12,7%)	(0,1%)	(11,7%)	(11,6%)	(0,4%)	(11,7%)	(11,8%)
BASEM6	-3,89	4,70	-0,91	1,31	-0,88	13,10	0,76	10,52	0,94	1,00	0,44	-8,19	3,97
	(12,6%)	(2,9%)	(12,4%)	(12,5%)	(0,5%)	(13,6%)	(2,7%)	(13,3%)	(12,5%)	(12,5%)	(0,5%)	(12,9%)	(2,7%)
Avg. Inclusion Probability	(6,7%)	(2,5%)	(11,5%)	(10,5%)	(5,6%)	(12,0%)	(9,6%)	(3,2%)	(11,4%)	(9,1%)	(7,8%)	(11,8%)	(11,3%)

Notes: Each model is summarised in two rows. The top number represents the normalized LRM multiplied by a factor 10^3 for easier representation. The bottom number (in the brackets) represents the probability of inclusion, which can be thought of as the probability that the predictor enters the final model equation.

Source: Own work.

In line with expectations, the main distinction between the two methodologies is the model size. By comparing models depicted in Tables 4 and 5, it can be observed that the models in the second table are richer in structure since all models are taking into account all possible predictors in contrast to the models in Table 4. It is also important to note that each model contains a constant and up to 5 lags of dependent variable.

Next, it can be observed from Table 5 that models are relatively well balanced in terms of key predictors for each of the dependent variables, meaning that there are no single factors dominating the models. This observation is based on inclusion probabilities[1] for predictors across the set of models. Averaging across the models, more than 65% of the predictors have probability of inclusion greater than 10%. However, there are some slight distinctions between different sets of models. In general, both factors in $\boldsymbol{W}_t$ appear to be one of the most significant predictors present in all models indicating the relevance of possible nonlinearities and additional effects of conditional volatility. Additionally, factors $\hat{F}_6$ and $\hat{F}_9$ representing the electricity futures market and financial returns related to the natural gas market respectively resemble this notion. However, some differentiation can be observed in relation to the first factor $\hat{F}_1$ describing Energy, Oil, and Gas ETF Price movements and the eight factor $\hat{F}_8$ loaded on the energy infrastructure returns. Specifically, these two factors appear to be more relevant for energy futures prices such as oil, gas, and coal according to higher inclusion probabilities while in general insignificant for electricity futures prices. Interestingly, the second factor $\hat{F}_2$ appears to be consistently negligible having a low probability of inclusion and low normalized LRM. In contrast to being the most frequently selected factor by using OL models motivated by Jurado, Ludvigson and Ng (2015), gold price appears to be insignificant once imposing the closed lag structure. To a lesser extent, similar contrast can be observed for the $\hat{F}_8$ factor.

5.1.3 Individual uncertainty estimates

In this section I present the individual uncertainty estimates $\hat{\mathscr{U}}_{jt}^{\mathscr{Y}}$ for the 12 dependent variables listed in Table (12). Using the models presented in the section above allows me to replace the conditional expectation in (1) by constructing a forecast error which is the basis for my individual uncertainty measure. An important next step is the estimation of stochastic and time-varying volatility of the forecast errors and the estimation of the stochastic volatility parameters[2] α^F, β^F and τ^F. For the estimation of the SV model, Markov Chain Monte Carlo (MCMC) method as presented by Kastner and Frühwirth-Schnatter (2014) is employed. Using the MCMC methodology first requires the specification of the prior distributions.

For this analysis, the following prior hyperparameters for the parameter vector[3] $\boldsymbol{\theta} = (\mu, \beta, \tau)$ are used. For the level parameter μ a rather uninformative prior with (b_μ, B_μ) = (0,100) is set as proposed by Kastner (2016) for daily log-returns. For the persistence parameter β the hyperparameters a_0 and b_0 in (32) must be specified. For these the values proposed by Kastner (2016) are again used, where $a_0 = 5$ and $b_0 = 1.5$ imply a prior mean of 0.54 and

[1] Inclusion probability for predictor Z^k can also be described as the share of final models used in Bayesian averaging containing that predictor Z^k.

[2] The same holds for the set of parameters α^y, β^y and τ^y.

[3] The subscripts are ommitted, since the same holds for both sets of parameters.

a prior standard deviation of 0.31. Finally, for the variance parameter τ shown in (33), the hyperparameter $B_\tau = 1$ is used. With the estimates of the stochastic volatility and parameter estimates $\hat{\boldsymbol{\theta}}$, I am able to calculate the h-period ahead expected conditional volatility as derived in (20) and construct individual uncertainty estimates for each of the dependent variables.

Expected individual uncertainties for $h = 1$ are presented in Figures 8 and 9. First, Figure 8 reports the uncertainty estimates for the for commodity front-month prices for the 4 most relevant commodities in terms of their impact on electricity prices, namely Brent price for crude oil, API2 (CIF ARA) Rotterdam Coal Futures price, German NCG gas futures price and CO2 EU Allowances futures price. Electricity futures prices for different products are reported in Figure 9. The variables present the continuous futures contracts constructed by combining sequential contracts of products for the same delivery period (next month, next quarter, etc.).

Figure 8: 1-step ahead individual uncertainty estimates for energy commodities futures

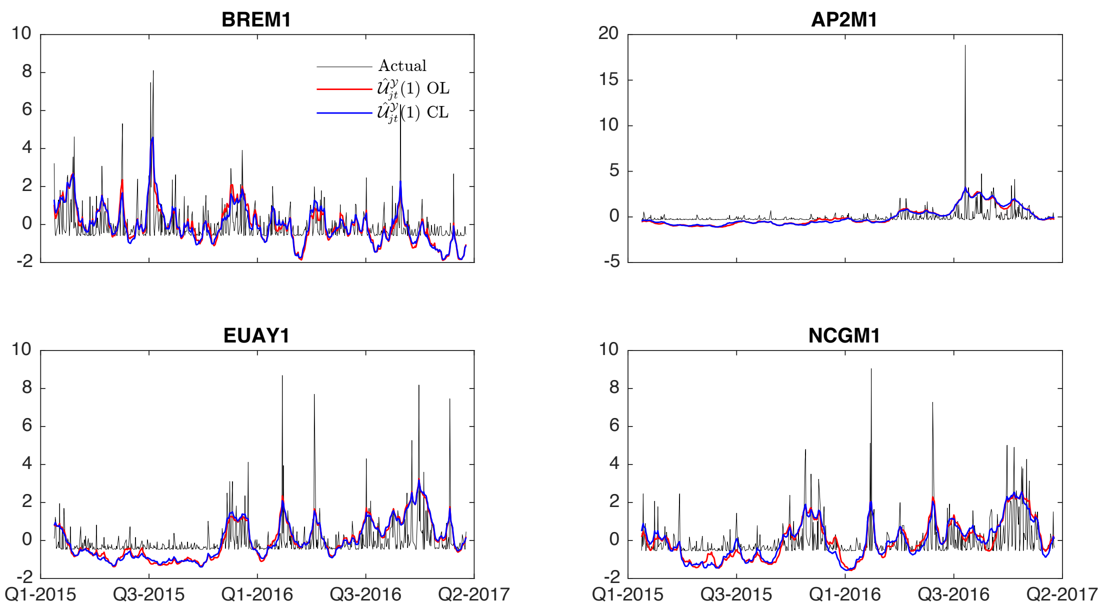

Source: Own work.

In both figures, three different series are plotted for each dependent variable. The black line represents a realized or actual volatility calculated as a squared difference of prices. The other two lines represent the estimated 1-step ahead individual uncertainty estimates using two different modelling approaches (OL models and CL models). All three series are also standardized, which could be thought of as a comparison of relative volatilities. With the red line I plot the uncertainty estimates based on the forecast errors using the Jurado, Ludvigson and Ng (2015) motivated methodology with open lag structure and a hard t-statistic threshold rule for predictors. The blue line on the other hand represents the uncertainty estimates based on the forecast errors obtained with BACE methodology and imposing a closed lag model structure.

Figure 9: 1-step ahead individual uncertainty estimates for electricity futures

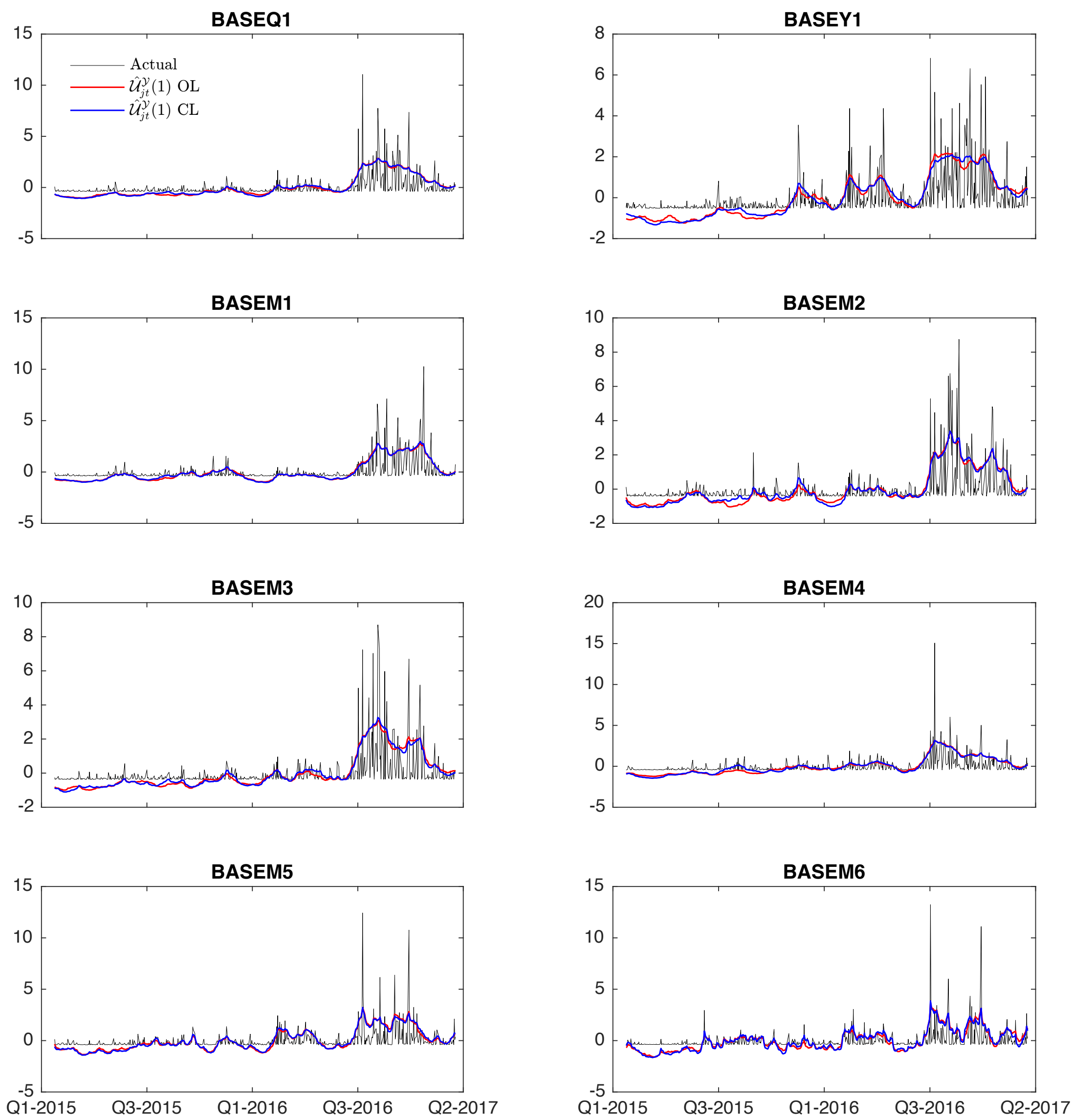

Source: Own work.

Observing Figures 8 and 9, the two methodologies seem to give similar estiamtes for $h = 1$, since the lines appear to be relatively well aligned. Moreover, one can observe that both methods produce similar predictions of volatility spikes present in the series, apart from a spike in coal price in Q3 2016, where CL models predicts significantly higher uncertainty than OL method.

Next, I compare the predicted uncertainties to the realised volatilities. Figure 8 shows that the a general trend of realised volatility is well described by the uncertainty estimated by the two modelling methodologies. Looking into the predictions of coal, gas and EUA realised volatility, it can be observed that the periods of higher volatility are relatively well fitted by both estimates of uncertainty. Moreover, one can also observe the alignment of the spikes in individual uncertainty estimates and the spikes in realised volatility, where the latter are on average significantly higher. Similar conclusions can be drawn by observing Figure 9. Additionally, the period of high realized volatility in the second half of 2016 for example appears to be well described by the uncertainty estimates.

Table 6: In-sample forecasting accuracy

	OL modelst			CL models		
Model	MAE	RMSE	RMSPE	MAE	RMSE	RMSPE
BREM1	0,693	0,923	18,751	0,690	0,923	21,266
AP2M1	0,656	1,081	14,687	0,556	1,115	11,105
NCGM1	0,710	0,988	10,251	0,717	0,997	10,500
EUAY1	0,717	0,984	101,040	0,712	0,966	114,810
BASEY1	0,615	0,973	18,585	0,620	0,972	18,000
BASEQ1	0,680	0,942	10,744	0,683	0,943	10,384
BASEM1	0,581	0,925	20,808	0,568	0,918	19,177
BASEM2	0,600	0,906	39,088	0,583	0,891	40,266
BASEM3	0,602	0,951	23,445	0,594	0,939	22,704
BASEM4	0,639	0,991	18,197	0,633	0,983	20,249
BASEM5	0,655	1,003	71,075	0,663	1,000	72,442
BASEM6	0,685	1,011	177,330	0,660	0,972	137,580
MEAN	0,653	0,973	43,667	**0,640**	**0,968**	**41,540**

Source: Own work.

In order to empirically analyze the in-sample forecast accuracy of the suggested modelling approaches the following measures of differences between realised and predicted values of volatility are calculated; Root Mean Squared Error (hereinafter: RMSE), the Mean Absolute Error (hereinafter: MAE) and the Root Mean Squared Percentage Error (hereinafter: RMSPE). The results for each model are presented in Table 6. It can be observed that the difference is not significant. However, the predictive accuracy of the estimates based on the CL modelling methodology in general outperform the CL based estimates. Moreover, on average (as reported in the final row) OL models exhibit a better in-sample fit for $h = 1$ predictions according to all three measures.

5.2 Electricity futures market uncertainty

In this section I present estimates of electricity futures market uncertainty for German market. The h period forecast is obtained by employing simple averaging across corresponding estimates of individual h period uncertainties denoted by

$$\overline{\mathscr{U}}_t^{\mathscr{Y}}(h) = \frac{1}{N_{\mathscr{Y}}} \sum_{j=1}^{N_{\mathscr{Y}}} \hat{\mathscr{U}}_{jt}^{\mathscr{Y}}(h). \tag{57}$$

Estimates of electricity futures market uncertainty for $h = 1,5$ and 10 are presented in Figure 10 where the results correspond to CL modelling methodology (with BACE).

Alongside with the electricity market uncertainty estimates for the three horizons, I also report the correlation coefficients with squared innovations in electricity price for yearly product. The coefficients are 0.562, 0.558 and 0.553 for $h = 1, 5$ and 10 respectively. This indicates decreasing but robust correlation of predictions across the forecasting horizon where correlation coefficient is slightly decreasing as the forecasting horizon extends from $h = 1$ to $h = 10$. Additionally, I also report the mean and standard deviation of the estimates for each of the horizons. It can be observed that uncertainty on average increases with h, while the variability of uncertainty decreases with h. This is because the forecast trends to the unconditional mean with h approaching infinity.

Figure 10: Aggregate uncertainty $\bar{\mathscr{U}}_t^{\mathscr{Y}}(h)$ for $h = 1, 5$ and 10

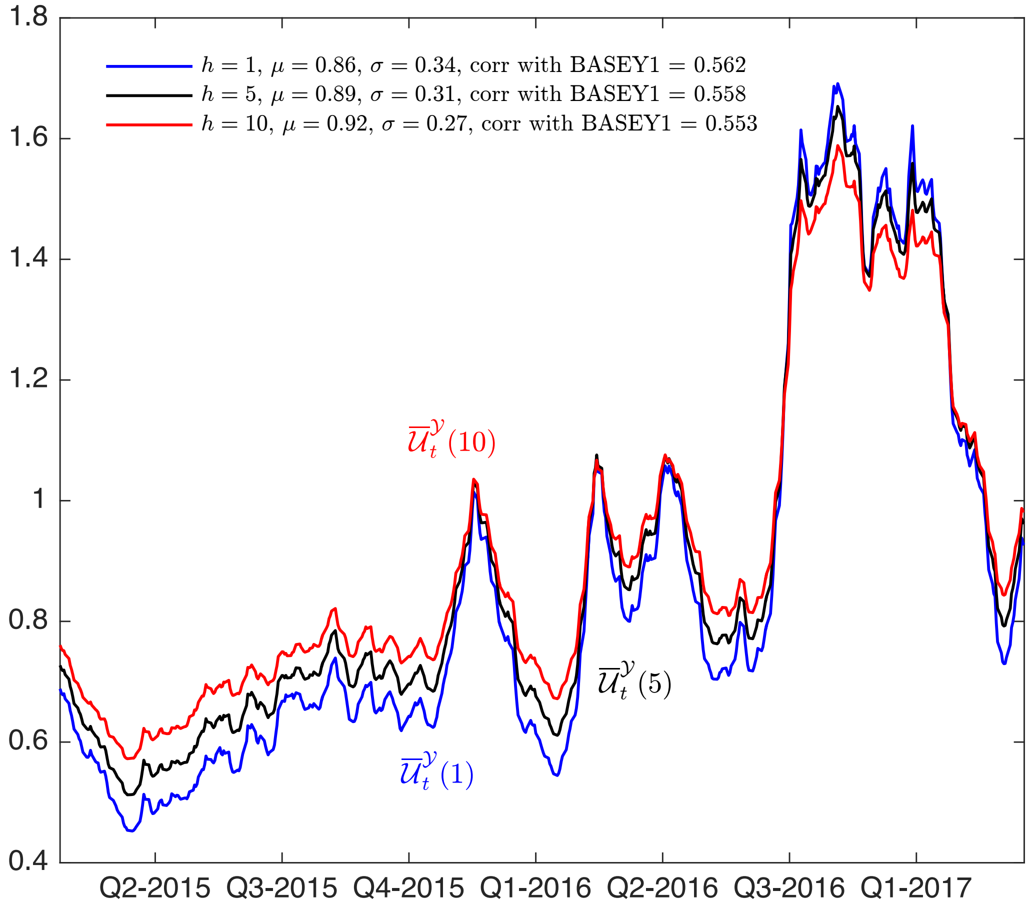

Source: Own work.

It is evident from Figure 10 that the second half of the year 2016 strikes out as the period with the highest uncertainty in German electricity market. This results are also in line with the analysis presented by EEX in their 2016 Annual Report. EEX stated that the main cause for high volatility and strong price fluctuations was the unscheduled production downtime of French nuclear power plants. As in 2015 the French Nuclear Safety Authority (ASN) announced the detection of an anomaly in a nuclear reactor under construction, the nuclear components came under increased scrutiny. Implications of this were broad based and observed across European power markets as the country is traditionally export oriented. Moreover, the magnitude of investigations that were ordered impacted 22 of the 58 nuclear reactors in the French nuclear fleet (ICIS, 2016). This resulted in price increases on the power derivatives markets. EEX also notes that causal relationship can be observed between high volatility and trading activity, since broad ranged price fluctuations in commodity prices boost the need for adjustments of hedging positions by market participants.

Following the definition in (1) individual uncertainty presents the volatility of unforecastable component of the series. However, this volatility can be impacted either by systemic market uncertainty shocks or by idiosyncratic uncertainty shocks. In order to estimate the relative impact of systemic market uncertainty in individual uncertainties and consequently in total uncertainty (summed over individual uncertainties), I compute for each of the 12 estimated individual uncertainties

$$R^2_{j\tau}(h) = \frac{\mathrm{var}_\tau\left(\hat{\varphi}_{j\tau}(h)\bar{\mathscr{U}}^y_t(h)\right)}{\mathrm{var}_\tau\left(\hat{\mathscr{U}}^y_{jt}(h)\right)}, \tag{58}$$

where $\hat{\varphi}_{j\tau}(h)$ represents the regression coefficient from regressing $\hat{\mathscr{U}}^y_{jt}(h)$ on $\bar{\mathscr{U}}^y_t(h)$ (and a constant). Moreover, $R^2_{j\tau}(h)$ represents the coefficient of determination explaining the share of variation in $\hat{\mathscr{U}}^y_{jt}(h)$ explained by market uncertainty $\bar{\mathscr{U}}^y_t(h)$ in subsample τ. This analysis is carried out for all $h = 1, ..., 20$ and for 3 different samples or subsamples. First the coefficients were estimated on the full sample. Additionally, the full sample was split in half where, as can be observed from Figure 10, the first half is intended to represent the period with low market uncertainty while the subsample with second half of observations represents the period with high market uncertainty. Finally, the larger as the $R^2_\tau(h) \equiv \frac{1}{N_y}\sum_{j=1}^{N_y} R^2_{j\tau}(h)$, the higher importance of market uncertainty shocks in explaining the total uncertainty.

Firstly, Table 7 represents the results of individual regressions. It can be observed that in general market level uncertainty is more important in explaining the individual uncertainties for electricity futures prices than prices of other energy commodity futures. This is an expected result, as electricity prices present larger portion in the sample used for estimation of market uncertainty. Additionally, in Table 7 I confirm the stylised fact about importance of coal prices for German electricity prices, as the German market uncertainty plays a relatively important role in coal price uncertainty compared to uncertainties in other commodity prices.[4] The series with highest $R^2_{j\tau}(h)$ across all h is BASEY1 which is the price of electricity for the front year. With an average and relatively constant $R^2_{j\tau}(h)$ of 0.96 it appears to be very strongly explained by market uncertainty. On the other hand, the series with the lowest $R^2_{j\tau}(h)$ is BREM1, which is front month price for Brent Crude oil. With the $R^2_{j\tau}(h)$ ranging from 0.06 to 0.09 it appears to be relatively unrelated to German electricity market uncertainty.

[4]Note that the causal relationship is likely to be reversed, but this is not analysed here.

Table 7: $R^2_{j\tau}(h)$ from regressions between uncertainties

h	BREM1	AP2M1	NCGM1	EUAY1	BASEY1	BASEQ1	BASEM1	BASEM2	BASEM3	BASEM4	BASEM5
1	0,06	0,82	0,59	0,34	0,89	0,96	0,75	0,83	0,84	0,83	0,86
2	0,06	0,82	0,59	0,34	0,90	0,96	0,75	0,84	0,84	0,84	0,86
3	0,07	0,82	0,59	0,34	0,90	0,96	0,76	0,84	0,85	0,84	0,87
4	0,07	0,82	0,59	0,34	0,90	0,96	0,76	0,85	0,85	0,84	0,87
5	0,07	0,83	0,59	0,34	0,90	0,96	0,76	0,85	0,86	0,85	0,87
6	0,07	0,83	0,59	0,35	0,90	0,96	0,76	0,86	0,86	0,85	0,87
7	0,08	0,83	0,59	0,35	0,91	0,96	0,77	0,86	0,86	0,85	0,87
8	0,08	0,83	0,59	0,35	0,91	0,96	0,77	0,87	0,87	0,86	0,87
9	0,08	0,83	0,59	0,35	0,91	0,96	0,77	0,87	0,87	0,86	0,87
10	0,08	0,84	0,58	0,35	0,91	0,96	0,77	0,88	0,87	0,86	0,87
11	0,08	0,84	0,58	0,34	0,91	0,96	0,78	0,88	0,88	0,87	0,87
12	0,08	0,84	0,58	0,34	0,92	0,96	0,78	0,88	0,88	0,87	0,87
13	0,08	0,84	0,58	0,34	0,92	0,96	0,78	0,89	0,88	0,87	0,87
14	0,09	0,84	0,58	0,34	0,92	0,96	0,78	0,89	0,89	0,87	0,87
15	0,09	0,84	0,58	0,34	0,92	0,96	0,78	0,89	0,89	0,88	0,87
16	0,09	0,84	0,57	0,34	0,92	0,96	0,78	0,90	0,89	0,88	0,86
17	0,09	0,84	0,57	0,34	0,93	0,96	0,79	0,90	0,89	0,88	0,86
18	0,09	0,84	0,57	0,34	0,93	0,96	0,79	0,90	0,90	0,88	0,86
19	0,09	0,84	0,57	0,34	0,93	0,96	0,79	0,90	0,90	0,88	0,86
20	0,09	0,85	0,57	0,34	0,93	0,96	0,79	0,90	0,90	0,89	0,86

Notes: $R^2_{j\tau}(h)$ values are from regressions of individual uncertainties $\hat{\mathscr{U}}^y_{jt}(h)$ on constructed market uncertainty $\bar{\mathscr{U}}^y_t(h)$ with a constant and for all forecasting horizons $h = 1, ..., 20$.

Source: Own work.

Next, Table 8 presents the results of $R^2_\tau(h)$ again for all $h = 1, ..., 20$. It can be observed that market uncertainty $\bar{\mathscr{U}}^y_t(h)$ on average explains 72 % of variation in total uncertainty considering full sample. It is also evident that the relative importance of market uncertainty in individual uncertainties $\hat{\mathscr{U}}^y_{jt}(h)$ increases with h. Specifically, the average share of individual uncertainties explained by market uncertainty increases from 70 % for $h = 1$ to 73 % for $h = 20$.

Table 8 also shows the $R^2_\tau(h)$ values for the two subsamples. The full sample was split into two equally large ($T/2$) subsamples, where the First Half subsample is intended to represent the period with lower uncertainty whereas the Second Half subsample represents the period with higher uncertainty. Specifically, the mean $\bar{\mathscr{U}}^y_t(1)$ of the second subsample is for 68 % higher then the mean of the first subsample. It is evident from Table 8 that individual uncertainties are better explained by market uncertainty in periods with higher uncertainty than in periods with lower uncertainty. Moreover, these results are showing that in periods of high uncertainty, significantly larger part of total uncertainty in the market is driven by a systemic market uncertainty shocks rather than idiosyncratic shocks.

5.2.1 Comparison with GARCH conditional volatility

In this section, I present an assessment and further evaluation of the market uncertainty estimates as formalized in (57). This was carried out by employing a comparison with results

Table 8: Averages of R^2

h	$R^2_{FullSample}$	$R^2_{FirstHalf}$	$R^2_{SecondHalf}$
1	0,70	0,49	0,66
2	0,71	0,49	0,67
3	0,71	0,50	0,67
4	0,71	0,50	0,67
5	0,71	0,50	0,68
6	0,71	0,50	0,68
7	0,72	0,50	0,68
8	0,72	0,50	0,68
9	0,72	0,50	0,69
10	0,72	0,50	0,69
11	0,72	0,50	0,69
12	0,72	0,50	0,69
13	0,72	0,50	0,69
14	0,72	0,50	0,69
15	0,72	0,50	0,69
16	0,72	0,50	0,70
17	0,72	0,50	0,70
18	0,73	0,50	0,70
19	0,73	0,50	0,70
20	0,73	0,50	0,70

Source: Own work.

from a different modelling approach. Specifically, conditional volatilities were estimated by employing a GARCH (p,q) model for each of the 12 series that constitute the market uncertainty. This was carried out in two steps for each of the series. In the first step, an AR (p) model was estimated, where up to 5 AR terms were considered and the optimal value for p was chosen based on AIC information criterion. Using the optimal lag structure, the AR model was estimated to obtain the innovations or disturbances which were then used in the conditional volatility model. GARCH (p,q) was employed in the second step for each of the obtained innovations. Analogously the lag structure was determined by considering all possible combinations with p and q ranging up to 4, and the optimal model was again chosen based on the AIC. The model structures for all 12 series are presented in Table 9. It can be observed that in general, using only 1 GARCH term was optimal, while ARCH and AR terms range from 1 to 4 and 5 respectively.

Obtaining the individual conditional volatility estimates by employing the models described in Table 9 allows me to analogously construct an estimate of market conditional volatility or uncertainty. Specifically, by doing a simple average of individual conditional volatility estimates I construct a benchmark or challenger market uncertainty estimate. This is similarly done for all $h = 1, ..., 20$.

Table 9: GARCH Model specifications

Model	AR	GARCH	ARCH
BREM1	1	1	1
AP2M1	5	1	1
EUAY1	5	1	4
NCGM1	3	1	2
BASEQ1	1	1	1
BASEY1	1	1	3
BASEM1	1	1	2
BASEM2	2	1	1
BASEM3	1	1	1
BASEM4	1	1	1
BASEM5	1	1	1
BASEM6	2	1	1

Notes: The numbers in each column represent AR order (number of time lags) p, The degree of GARCH polynomial P, which is composed of lagged conditional variances and the degree of ARCH polynomial Q, which is composed of lagged squared innovations respectively.

Source: Own work.

Key results are depicted in Figure 11, where I plot the estimated market uncertainty $\hat{\mathscr{U}}_{jt}^{y}(h)$ for $h = 1$ coloured blue against the red line, which is the benchmark market conditional volatility estimate again for $h = 1$. The latter is constructed as the average of individual conditional volatilities estimated with GARCH. Additionally, I also plot the actual or realized market volatility which is constructed as a simple average of the individual realized volatilities presented in section 5.1.3. Again, all series are standardized for a relative comparison.

It can be observed in Figure 11 that both estimates relatively similarly describe the realized innovations as they, in general, follow the same trend. Both estimates similarly follow the key increases in volatility with the largest one in H2 2016. However, it can be observed, that the GARCH estimates are more sensitive to spikes in actual innovations, which results in more volatile estimates of conditional volatility. Moreover, it can be observed in a few short periods in the first half of the sample for example, that small spikes in actual innovations result in spikes in GARCH estimates of conditional volatility, while the estimated market uncertainty remains relatively stable. This sheds some light on the impact of forecastability of these spikes as by definition the uncertainty estimate of this thesis is founded only on the unforecastable component. Similarly, there are a few relatively significant short drops in GARCH conditional volatility in the period of high uncertainty in the second half of 2016 while the uncertainty estimate $\hat{\mathscr{U}}^{y}_{jt}(h)$ remains relatively stable.

In order to empirically evaluate if the market uncertainty estimate $\hat{\mathscr{U}}^{y}_{jt}(h)$ differ from GARCH conditional volatility, the Diebold-Mariano (hereinafter: DM) test of predictive accuracy was employed. The null hypothesis of the test is that the predictive accuracy does not differ between the two competing forecasts (Diebold & Mariano, 1995). Harvey, Leybourne, and Newbold (1997) have later proposed an adjustment to the DM-statistic that improved small-sample properties. The test with adjusted DM statistic (HLN) was carried out for all values of $h = 1, \ldots, 20$, and the results are presented in Table 10. It is evident, that I can reject the null for $h = 1$, which means that the one-period ahead forecasts are significantly different. It can also be observed that these differences decrease with h as the forecasts tend towards unconditional means. However, this is only evident for $h = 18$ and higher. Prior to that, the differences between the accuracies of the two predictions appear to be statistically significant.

Figure 11: Aggregate uncertainty $\bar{\mathscr{U}}^{\mathscr{Y}}_{t}(1)$ vs Actual

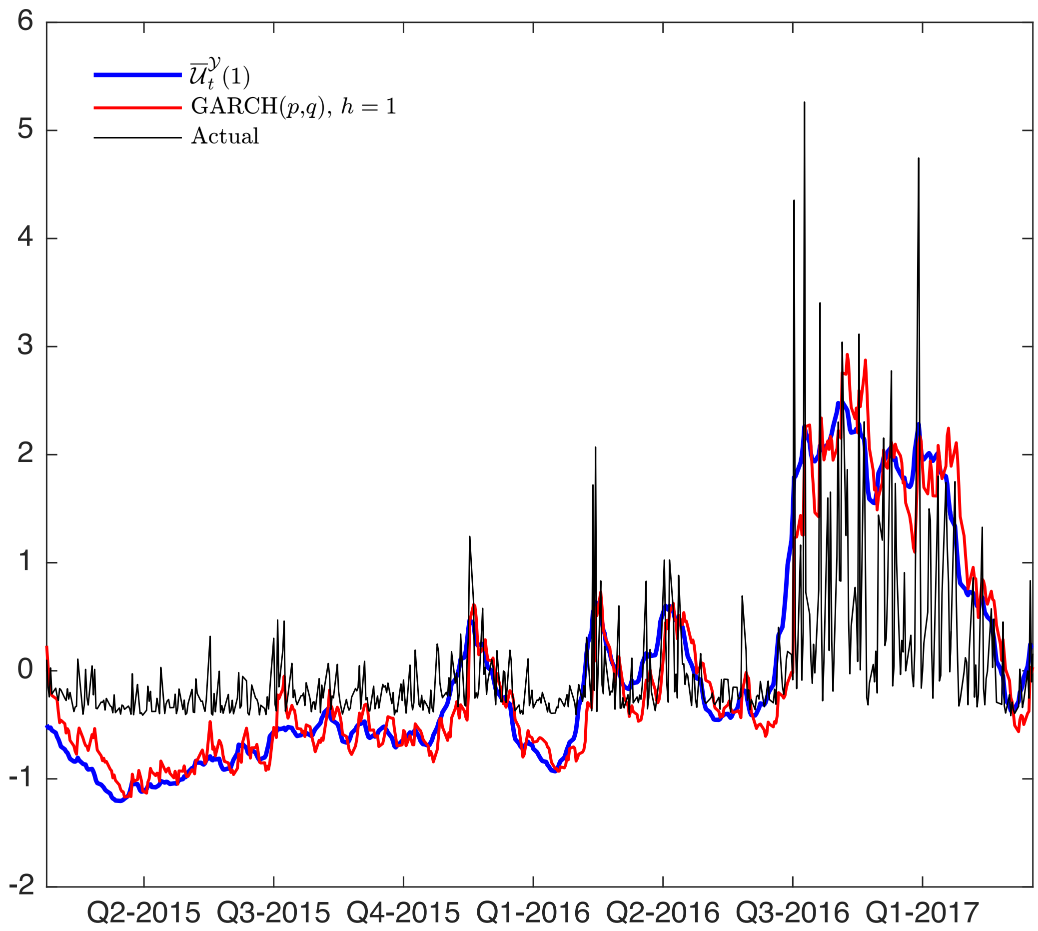

Source: Own work.

These results show that on average, the uncertainty estimate $\hat{\mathscr{U}}^{y}_{jt}(h)$ follows the same trend as the conditional volatility from GARCH models. However, the former appears to be more stable across the sample with smaller or no spikes in the low volatility period and with smaller or avoided drops in the period with higher volatility.

Table 10: Results of Diebold-Mariano test for predictive accuarcy

h	HLN	p-value
1	-3,685	0,000
2	-3,784	0,000
3	-3,331	0,001
4	-3,026	0,003
5	-3,019	0,003
6	-3,081	0,002
7	-2,606	0,009
8	-2,587	0,010
9	-2,274	0,023
10	-2,538	0,011
11	-2,625	0,009
12	-2,844	0,005
13	-2,967	0,003
14	-2,506	0,012
15	-2,424	0,016
16	-3,044	0,002
17	-2,409	0,016
18	-1,942	0,053
19	-1,829	0,068
20	-1,680	0,094

Source: Own work.

Next, the out-of-sample (hereinafter: OOS) forecasting accuracy of the two predictions was investigated. For this, I adopted the idea behind the Walk Forward Analysis (hereinafter: WFA) used in financial trading and trading strategy optimization (Pardo, 2011). The concept for the WFA is similarly based on using the in-sample and out-of-sample periods. However, instead of estimating the parameters on $T-h$ observations and using the last h observations of data for testing, the OOS testing is done across last k observations where $k >> h$. This is done by first estimating the model on $T-k$ subsample and forecasts are formed for the following h observations.[5] In the next step, the estimation subsample is extended with the actual data for these h observations and the model is re-estimated. With the new model parameters, the predictions are formed for the next h observations and the two sets of OOS predictions are combined into one longer ($2h$) OOS testing window. These steps are then repeated until all k OOS predictions are formed and combined into one OOS testing sample.

[5]From $T-k+1$ to $T-k+h$.

Figure 12: Aggregate uncertainty $\bar{\mathscr{U}}_t^{\mathscr{Y}}(h)$ vs Actual

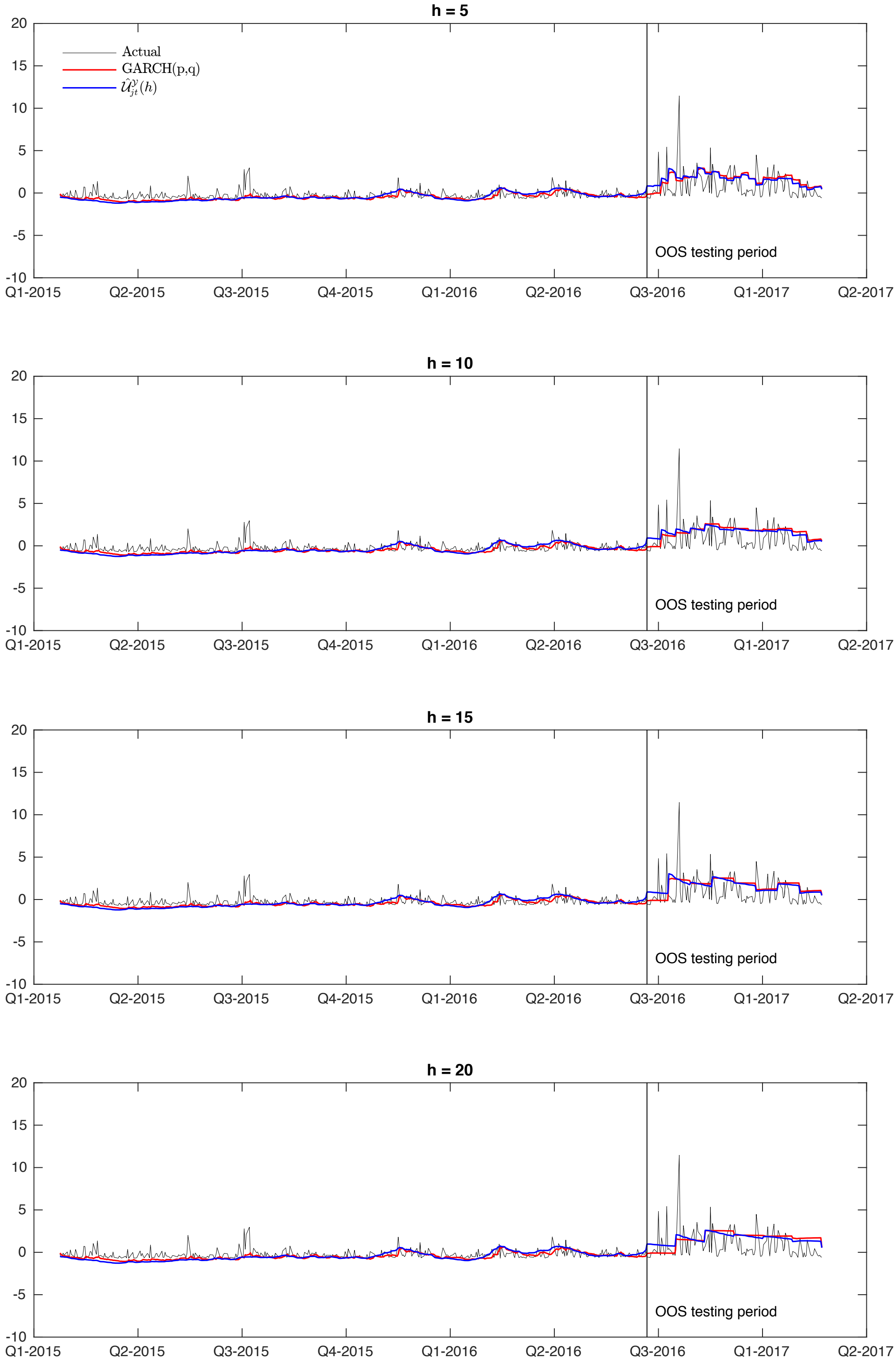

Source: Own work.

The OOS forecasting accuracy was tested in this analysis by setting $k = 140$, which means that the period after September 16, 2016 was analysed. The test was performed for all h

from 1 to 20. The results are presented in Figure 12, where I present the OOS testing results for $h = 5$, 10, 15 and 20. Again, the red line depicts the conditional volatility predictions obtained with GARCH models, while the blue line depicts the estimated market uncertainty $\hat{\mathscr{U}}_{jt}^{y}(h)$. Additionally, the black vertical line shows the start of the OOS analysis.

Table 11: Out-of-sample forecasting accuracy

	$\hat{\mathscr{U}}_{jt}^{y}(h)$			GARCH(p,q)			$\hat{\mathscr{U}}_{jt}^{y}(h)$/GARCH$(p,q)$		
h	MAE	RMSE	RMSPE	MAE	RMSE	RMSPE	MAE	RMSE	RMSPE
1	1,495	1,861	35,552	1,514	1,910	33,295	0,988	0,974	1,068
2	1,515	1,878	33,533	1,516	1,914	31,802	1,000	0,981	1,054
3	1,490	1,849	36,878	1,506	1,904	33,762	0,989	0,971	1,092
4	1,488	1,865	36,980	1,492	1,908	35,977	0,997	0,977	1,028
5	1,454	1,830	38,850	1,477	1,893	38,580	0,985	0,967	1,007
6	1,511	1,841	35,536	1,508	1,899	33,168	1,002	0,969	1,071
7	1,489	1,844	35,891	1,517	1,934	36,658	0,982	0,953	0,979
8	1,481	1,839	36,846	1,494	1,873	35,025	0,992	0,981	1,052
9	1,498	1,840	35,212	1,504	1,887	32,612	0,996	0,975	1,080
10	1,415	1,758	27,428	1,444	1,848	27,803	0,980	0,951	0,987
11	1,474	1,861	29,373	1,498	1,919	29,948	0,984	0,970	0,981
12	1,461	1,839	28,040	1,478	1,906	26,950	0,989	0,965	1,040
13	1,485	1,851	30,837	1,503	1,936	29,724	0,988	0,956	1,037
14	1,481	1,843	37,696	1,514	1,912	36,937	0,979	0,964	1,021
15	1,461	1,840	38,143	1,505	1,912	36,219	0,971	0,962	1,053
16	1,494	1,870	36,454	1,527	1,934	33,055	0,979	0,967	1,103
17	1,441	1,787	40,395	1,486	1,886	35,542	0,970	0,947	1,137
18	1,480	1,843	36,275	1,495	1,941	32,119	0,990	0,950	1,129
19	1,472	1,853	24,925	1,507	1,955	25,704	0,976	0,948	0,970
20	1,444	1,798	24,593	1,491	1,930	23,631	0,968	0,932	1,041
Mean	1,476	1,839	33,972	1,499	1,910	32,426	0,985	0,963	1,046

Source: Own work.

First, it can be observed that the results presented in Figure 12 align with the findings from Table 10. Specifically, the forecasts appear to differ the most at the beginning of the forecasting horizon, for $h = 1$. This could be the result of different models being employed to estimate the forecast errors, which are used for conditional volatility estimation. Next, it is also evident from Figure 12 that the dynamic of the predictions is different between the two models, where the predictions of conditional volatility using GARCH methodology appear to be relatively flat compared to more dynamic predictions of market uncertainty $\hat{\mathscr{U}}_{jt}^{y}(h)$. The predictive accuracy of the two approaches against squared innovations was additionally compared using the MAE, RMSE and RMPSE measures for which the results are presented in Table 11. According to MAE and RMSE, estimates of market uncertainty $\hat{\mathscr{U}}_{jt}^{y}(h)$ outperform GARCH (p,q) conditional volatility forecasts. It can also be observed, that the actual volatility measured by squared innovations is better described by $\hat{\mathscr{U}}^y_{jt}(h)$ compared to GARCH estimates as h increases.

5.2.2 Decomposition

It was shown that the uncertainty estimates presented in this thesis differ from GARCH conditional volatility estimates. In this section, I further investigate these differences. For the purpose of analyzing possible reasons, I turn back to the definition of market uncertainty estimate, where Jurado, Ludvigson and Ng (2015) emphasize the importance of removing the predictable variation in order to not assign these fluctuations to uncertainty.

Turning back to the DI forecasting model

$$y_{jt+1} = \alpha + \phi^y_1 y_{jt} + \cdots + \phi^y_{p_y} y_{jt-p_y} + \sum_{k=1}^{k_i} (\gamma^k_1 \hat{\mathbf{Z}}^k_t + \cdots + \gamma^k_q \hat{\mathbf{Z}}^k_{t-q}) + v^y_{jt+1}, \tag{59}$$

with $\mathbf{Z}_t = (\hat{\mathbf{F}}_t, \mathbf{W}_t)'$ the future values of predictors $\mathbf{F}$ and $\mathbf{W}$ are unknown. Additionally, each predictor's future value is described by an AR (5) process. As it was already explained, the time-varying volatility in forecast errors of each of the predictors also contributes to h-step ahead uncertainty for each dependent variable y_{jt+1} where $h > 1$.

Figure 13: The role of predictors: 1-step ahead individual uncertainties for energy commodities futures

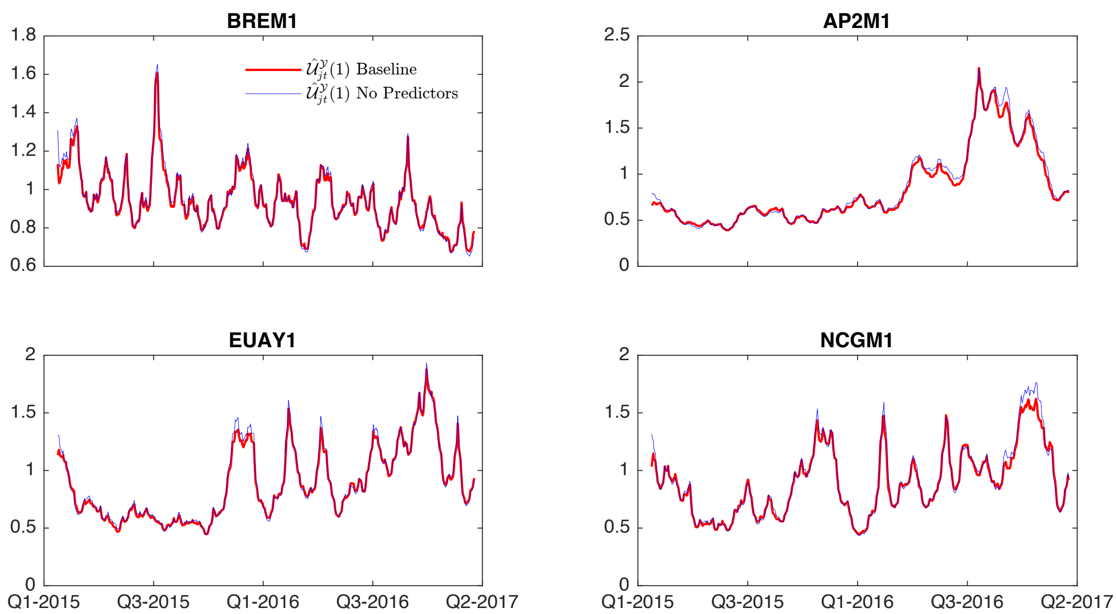

Source: Own work.

Another possible reason for the differences in addition to the stochastic volatility effect just described can also stem from the DI forecasting model itself. Moreover, the predictors directly translate into the level of the forecast. As noted by Jurado, Ludvigson, and Ng (2015) an important aspect of this approach is exploiting the data-rich environment which

Figure 14: The role of predictors: 1-step ahead individual uncertainties for electricity futures

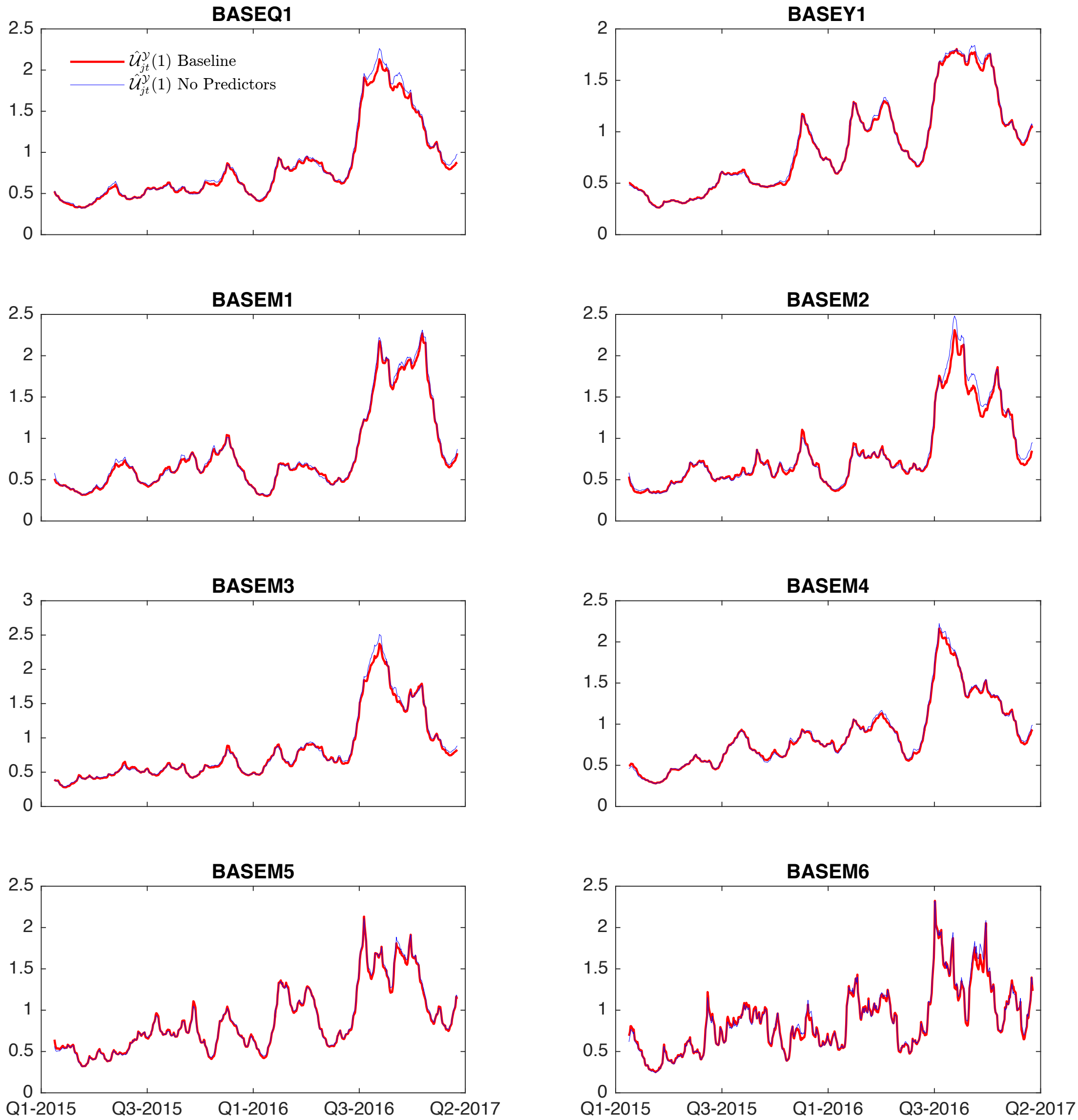

Source: Own work.

allows the possibility to control for any forecastable variation in the predictor set, which is a consequence not erroneously attributed to uncertainty estimates.

In order to investigate the role that this model specification with the full predictor set plays in my uncertainty estimates, I re-estimate the uncertainty for each of the dependent series. For this, I assume the following simple and potentially misspecified model

$$y_{jt+1} = \mu + \tilde{v}_{jt+1}, \tag{60}$$

where $\tilde{v}_{jt+1} = \tilde{\sigma}_{jt+1}\tilde{\varepsilon}_{jt+1}$, which is a simple model with constant conditional mean. Figures 13 and 14 plot the estimates for 1-step uncertainty using this model against my baseline uncertainty estimates using the full set of predictors for the 12 dependent variables that constitute the market uncertainty.

Figure 15: Decomposition of Aggregate uncertainty $\bar{\mathscr{U}}_t^{\mathscr{Y}}(1)$

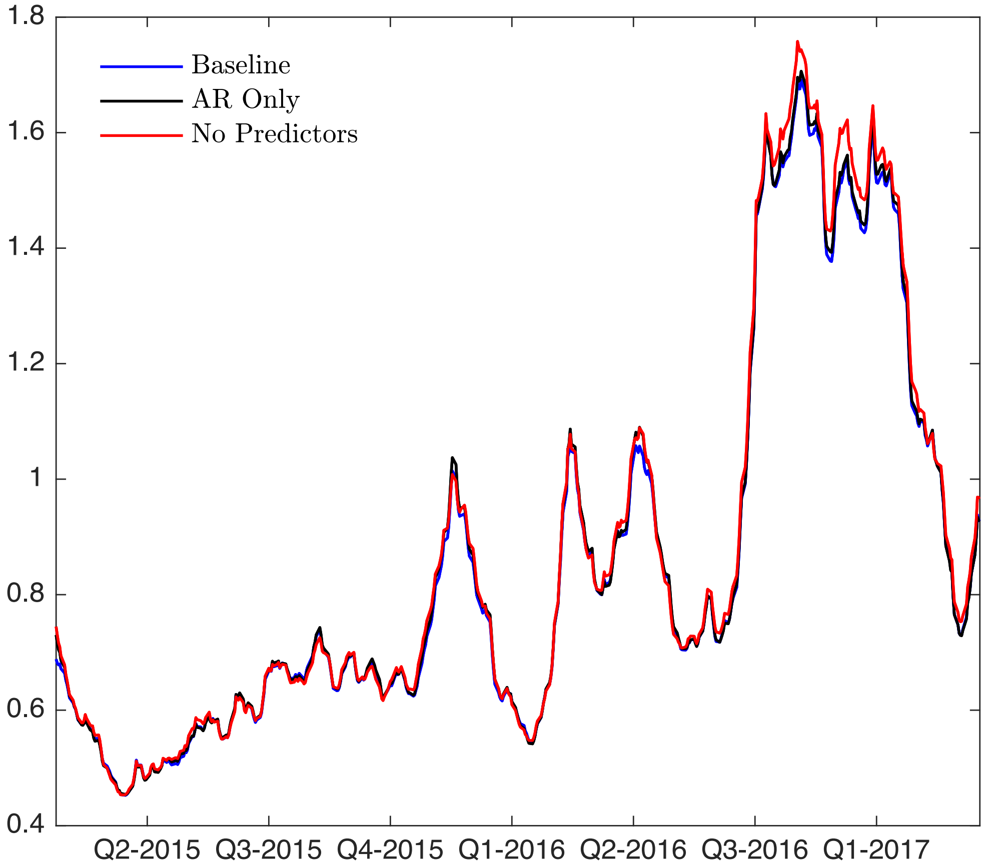

Source: Own work.

Both figures suggest that there is significant heterogeneity between the uncertainty estimates across the variables. This suggests that a significant part of the uncertainty is series-specific. On the other hand, these figures do not suggest a significant influence by the inclusion of predictor set into the model. This could mean that removing the forecastable component does not significantly influence the uncertainty estimates or that the forecastable component itself is negligible and possibly un-forecastable. However, there are slight indications that including a predictor set has an impact on the uncertainty estimates. This is evident in periods with high uncertainty, where the uncertainty is estimated to be lower with the predictive component removed. These results would suggest that larger part of the variation is predictable in these periods and should not be attributed to uncertainty.

In addition to the simple model described above, I have also tested for the contribution of the exogenous predictors alone. For this, I assumed additional model specification with autoregressive terms and a constant only as

$$y_{jt+1} = \tilde{\phi}_j(L) y_{jt} + \tilde{v}_{jt+1}, \tag{61}$$

with up to 5 AR terms in each of the series. Figure 15 plots the market uncertainty estimates using these two simple forecasting models and compares them to the baseline market uncertainty estimates.

It can be observed that when controlling for the autoregressive component, the difference between the estimates is even smaller. However, one can again see that the distinction increases in the periods of high uncertainty. Specifically, the uncertainty estimates using the model including only constant term are the highest, followed by the model with added the autoregressive component and when controlling for the predictive component, the uncertainty estimates are the lowest. These results also suggest, as a relatively small difference is explained either by variation in predictors or by controlling for the forecastable component, that employing the SV model for the conditional volatility of the innovations plays an important role when comparing the results to GARCH conditional volatility estimates.

CONCLUSION

A new phenomenon that was driven by liberalization and gained much attention in the electricity market is uncertainty. The importance of uncertainty in electricity markets grew very fast after liberalization process started. One of the main reasons for such development are new instruments and markets that were introduced. Another contribution to the growth of uncertainty in electricity markets came from structural changes brought by intensive financial support for investment in fluctuant renewable energy sources. So on one hand, regulated producer prices for electricity were replaced with volatile wholesale prices, and on the other hand, the carbon market establishment led to uncertain cost on the production side.

Additionally, volatile electricity generation from renewable sources also leads to uncertainty regarding the amount of power that has to be supplied by suppliers from conventional production sources like hard coal, lignite or gas, to serve the residual load (Keles, 2013). Since the number of uncertain parameters was limited to a specific range in the past, investment decisions and evaluations were predominantly carried out by using perfect foresight strategies and models together with sensitivity analyses. However, under newer market conditions, investment decisions have to be made in a significantly more uncertain environment. This makes perfect foresight strategies less appropriate. Moreover, with the consideration of very volatile parameters such as electricity prices and renewable power generation, new methodologies have to be developed to better understand and estimate them (Keles, 2013).

This thesis is centered around the analysis of electricity prices with a focus on their volatility and uncertainty. The volatility of electricity prices has been gaining attention ever since the trading on exchanges has been established. Moreover, it plays an important role in the valuation of standardized products on the derivatives market. It is the aim of this thesis to contribute to the research community, that is not yet as mature compared to the research done for financial markets, and on the other hand to provide new insights to market participants that operate with these products. Specifically, it was the main goal of this analysis to construct estimates of time-varying future volatility and uncertainty of electricity prices, where the approach of Jurado, Ludvingston and Ng (2015) and their econometric formalization of uncertainty was adopted. Moreover, an estimate of market level uncertainty was constructed to inform about possible price or volatility misalignments.

As it was suggested in the literature there are numerous possible sources of uncertainty from seasonality to unpredictable generation and governmental impacts. A data-rich environment was used in this analysis to best control for all possible drivers of uncertainty. A market level uncertainty estimate was then constructed by employing DI forecasting where conditional volatility of innovations were modelled with a stochastic volatility model. Forecasts were then created for 1 to 20 periods ahead, which were compared to the realized volatility and to conditional volatility predictions using a simpler GARCH methodology.

First, it was observed that the choice of model structure for DI forecasting impacts the uncertainty estimates. Forcing a closed lag structure and employing the Bayesian averaging appeared to slightly outperform the more restrictive model selection procedure used by Jurado, Ludvingston and Ng (2015). Analyzing the market uncertainty estimates also shows that the forecasts converge to unconditional mean as the forecasting horizon tends to infinity. Additionally, it was shown that a larger part of uncertainty in the German electricity market is driven by a systematic component rather than by idiosyncratic shock. The results also point to the importance of the coal market as one of the key drivers of electricity prices in Germany. Comparing these market-level uncertainty estimates to realized volatility defined as squared innovations shows that the general trend of historical volatility is well described by the model. Moreover, it implies that the second half of 2016 is a period with the highest uncertainty, which is also in line with the reports by the EEX.

Further analyzing these estimates and comparing them to market level conditional volatility estimates using a GARCH model, shows that the general trend is similarly described by both sets of results. However, focusing on 1-period ahead predictions shows greater sensitivity to spikes in innovations by the GARCH model. The differences were also tested for statistical significance by employing the Diebold-Mariano test for predictive accuracy. This showed that the differences between forecasts for $h = 1$ are statistically significant. However, these differences tend to zero as the forecasting horizon increases and both predictions converge towards unconditional means. Additionally, the OOS analysis shows that the out-of-sample performance is similar to my market uncertainty estimates slightly outperforming GARCH predictions according to MAE and RMSE measures. The differences were further investigated by decomposing the market uncertainty estimates where it was shown that controlling for the forecastable components results in slightly lower uncertainty estimates in periods with high overall uncertainty. These results point to a possible overestimation of volatility by employing simple GARCH models.

In general, reasons explaining possible differences in conditional volatility estimates may be split on two key parts. First, conditional variance may be impacted through the construction of forecast errors. This was already analysed and described above. However, the second and vital part is the methodology applied to model the second moment of the forecast error series. SV model was employed here which also appears to be the key determinant of the differences when comparing the conditional volatility estimates to results obtained by employing a GARCH modelling methodology. Simple SV model as already proposed by Kim, Shephard and Chib (1998) was employed here with baseline sampling configurations in terms of prior distributions and sampling algorithms as proposed by Kastner (2016). A thorough investigation of implications of these configurations with analysis of convergence to the stationary distribution of the chain would be a next logical step which is not the scope of this thesis. Additionally, possible modifications to the forecasting model could also be tested to ensure the robustness of forecasting errors.

REFERENCE LIST

1. Arismendi, J. C., Back, J., Prokopczuk, M., Paschke, R. & Rudolf, M. (2016). Seasonal stochastic volatility: Implications for the pricing of commodity options. *Journal of Banking & Finance, 66*, 53–65.
2. Bai, J. & Ng, S. (2002). Determining the number of factors in approximate factor models. *Econometrica, 70*(1), 191–221.
3. Barndorff-Nielsen, O. E., Benth, F. E. & Veraart, A. E. (2014). Modelling electricity futures by ambit fields. *Advances in Applied Probability, 46*(3), 719–745.
4. Bauwens, L., Hafner, C. M. & Pierret, D. (2013). Multivariate volatility modeling of electricity futures. *Journal of Applied Econometrics, 28*(5), 743–761.
5. Bencivenga, C., Sargenti, G. & D'Ecclesia, R. L. (2010). Energy markets: crucial relationship between prices. In *Mathematical and statistical methods for actuarial sciences and finance* (pp. 23–32). Milano: Springer.
6. Bessec, M., Fouquau, J. & Meritet, S. (2016). Forecasting electricity spot prices using time-series models with a double temporal segmentation. *Applied Economics, 48*(5), 361–378.
7. Biagini, F., Bregman, J. & Meyer-Brandis, T. (2015). Electricity futures price modeling with lévy term structure models. *International Journal of Theoretical and Applied Finance, 18*(01).

8. Bunn, D. W. (2000). Forecasting loads and prices in competitive power markets. *Proceedings of the IEEE, 88*(2), 163–169.
9. Carmona, R., Coulon, M. & Schwarz, D. (2013). Electricity price modeling and asset valuation: a multi-fuel structural approach. *Mathematics and Financial Economics, 7*(2), 167–202.
10. Carter, C. K. & Kohn, R. (1996). Markov chain monte carlo in conditionally gaussian state space models. *Biometrika, 83*(3), 589–601.
11. Chamberlain, G. & Rothschild, M. (1982). *Arbitrage, factor structure, and mean-variance analysis on large asset markets*. Cambridge: National Bureau of Economic Research.
12. Chib, S., Nardari, F. & Shephard, N. (2002). Markov chain Monte Carlo methods for stochastic volatility models. *Journal of Econometrics, 108*(2), 281–316.
13. Connor, G. & Korajczyk, R. A. (1993). A test for the number of factors in an approximate factor model. *The Journal of Finance, 48*(4), 1263–1291.
14. Deb, P. & Sefton, M. (1996). The distribution of a lagrange multiplier test of normality. *Economics Letters, 51*(2), 123–130.
15. deJong, C. & Huisman, R. (2002). Option formulas for mean-reverting power prices with spikes. *ERIM Report Series Research in Management*(ERS-2002-96-F&A).
16. Deng, S.-J. & Oren, S. S. (2006). Electricity derivatives and risk management. *Energy, 31*(6–7), 940–953.
17. Diebold, F. X. & Mariano, R. S. (1995, July). Comparing predictive accuracy. *Journal of Business & Economic Statistics, 13*(3), 253–263.
18. Diebold, F. X. & Mariano, R. S. (2002). Comparing predictive accuracy. *Journal of Business & economic statistics, 20*(1), 134–144.
19. Diebold, F. X. & Yilmaz, K. (2012). Better to give than to receive: Predictive directional measurement of volatility spillovers. *International Journal of Forecasting, 28*(1), 57–66.
20. Doppelhofer, G., Miller, R. I., Sala-i-Martin, X. (2004). Determinants of long-term growth: A Bayesian averaging of classical estimates (BACE) approach. *American economic review, 94*(4), 813–835.
21. Fanelli, V., Maddalena, L. & Musti, S. (2016). Modelling electricity futures prices using seasonal path-dependent volatility. *Applied energy, 173*, 92–102.
22. Frömmel, M., Han, X. & Kratochvil, S. (2014). Modeling the daily electricity price volatility with realized measures. *Energy Economics, 44*, 492–502.
23. Frühwirth-Schnatter, S. & Wagner, H. (2010). Stochastic model specification search for gaussian and partial non-gaussian state space models. *Journal of Econometrics, 154*(1), 85–100.
24. Frydenberg, S., Onochie, J. I., Westgaard, S., Midtsund, N. & Ueland, H. (2014). Long-term relationships between electricity and oil, gas and coal future prices—evidence from N ordic countries, C ontinental E urope and the U nited K ingdom. *OPEC Energy Review, 38*(2), 216–242.

25. Füss, R., Mahringer, S. & Prokopczuk, M. (2015). Electricity derivatives pricing with forward-looking information. *Journal of Economic Dynamics and Control, 58*, 34– 57.
26. García-Martos, C. & Conejo, A. J. (2001). Price forecasting techniques in power systems. *Wiley Encyclopedia of Electrical and Electronics Engineering*, 1–23.
27. Haldrup, N., Knapik, O. & Proietti, T. (2016). *Ageneralized exponential time series regression model for electricity prices*. *CREATES*, 1930.
28. Haldrup, N. & Nielsen, M. Ø. (2006). A regime switching long memory model for electricity prices. *Journal of econometrics, 135*(1–2), 349–376.
29. Harvey, A., Ruiz, E. & Shephard, N. (1994). Multivariate stochastic variance models. *The Review of Economic Studies, 61*(2), 247–264.
30. Harvey, A. C. & Peters, S. (1990). Estimation procedures for structural time series models. *Journal of Forecasting, 9*(2), 89–108.
31. Harvey, D., Leybourne, S. & Newbold, P. (1997). Testing the equality of prediction mean squared errors. *International Journal of Forecasting, 13*(2), 281–291.
32. Hautsch, N. & Ou, Y. (2008).Discrete-Time Stochastic Volatility Models and MCMC-Based Statistical Inference. Available at SSRN: https://ssrn.com/abstract=1292494 or http://dx.doi.org/10.2139/ssrn.1292494.
33. Hong, T. (2014). Energy forecasting: Past, present, and future. *Foresight: The International Journal of Applied Forecasting*(32), 43–48.
34. ICIS. (2016, December). *The french nuclear outages of 2016: the backstory*. Retrieved January 15, 2019, from https://www.icis.com/explore/resources/news/2016/12/29/10066294/the-french-nuclear-outages-of-2016-the-backstory.
35. Islyaev, S. & Date, P. (2015). Electricity futures price models: Calibration and forecasting. *European Journal of Operational Research, 247*(1), 144–154.
36. Jaeck, E. & Lautier, D. (2014). Samuelson hypothesis and electricity derivative markets. *In 31st international french finance association conference, affi 2014*, p. 24.
37. Jalles, J. T. (2009). Structural time series models and the kalman filter: a concise review. FEUNL Working Paper No. 541. Available at SSRN: https://ssrn.com/abstract=1496864 or http://dx.doi.org/10.2139/ssrn.1496864.
38. Jurado, K., Ludvigson, S. C. & Ng, S. (2015). Measuring uncertainty. *The American Economic Review, 105*(3), 1177–1216.
39. Kastner, G. (2016). Dealing with stochastic volatility in time series using the r package stochvol. *Journal of Statistical software, 69*(5), 1–30.
40. Kastner, G. & Frühwirth-Schnatter, S. (2014). Ancillarity-sufficiency interweaving strategy (asis) for boosting mcmc estimation of stochastic volatility models. *Computational Statistics & Data Analysis, 76*, 408–423.
41. Keles, D. (2013). *Uncertainties in energy markets and their consideration in energy storage evaluation* (Vol. 4). KIT Scientific Publishing.
42. Keles, D. (2014). *Uncertainties in energy markets and their consideration in energy storage evaluation* (Vol. 4). KIT Scientific Publishing.
43. Kim, S., Shephard, N. & Chib, S. (1998). Stochastic volatility: likelihood inference and comparison with arch models. *The review of economic studies, 65*(3), 361–393.

44. Madaleno, M., Moutinho, V. & Mota, J. (2015). Time relationships among electricity and fossil fuel prices: Industry and households in europe. *International Journal of Energy Economics and Policy, 5*(2), 525–533.
45. Mahringer, S. & Prokopczuk, M. (2015). An empirical model comparison for valuing crack spread options. *Energy Economics, 51*, 177–187.
46. McCausland, W. J., Miller, S. & Pelletier, D. (2011). Simulation smoothing for state–space models: A computational efficiency analysis. *Computational Statistics & Data Analysis, 55*(1), 199–212.
47. Misiorek, A., Trueck, S. & Weron, R. (2006). Point and interval forecasting of spot electricity prices: Linear vs. non-linear time series models. *Studies in Nonlinear Dynamics & Econometrics, 10*(3).
48. Möst, D. & Keles, D. (2010). A survey of stochastic modelling approaches for liberalised electricity markets. *European Journal of Operational Research, 207*(2), 543–556.
49. Newbery, D. M. (2002). Problems of liberalising the electricity industry. *European Economic Review, 46*(4), 919–927.
50. Newey, W. K. & West, K. D. (1986). *A simple, positive semi-definite, heteroskedasticity and autocorrelationconsistent covariance matrix*. National Bureau of Economic Research
51. Omori, Y., Chib, S., Shephard, N. & Nakajima, J. (2007). Stochastic volatility with leverage: Fast and efficient likelihood inference. *Journal of Econometrics, 140*(2), 425–449.
52. Pardo, R. (2011). *The evaluation and optimization of trading strategies* (Vol. 314). Hoboken, New Jersey: John Wiley & Sons.
53. Pruckner, M. & German, R. (2013). A simulation model to analyze the residual load during the extension of highly fluctuating renewables in bavaria, germany. *In Power engineering, energy and electrical drives (powereng), 2013 fourth international conference on* (pp. 540–545).
54. EEX Group. (2018, April). *EEX Group Annual Report 2017*. Retrieved August 12, 2018, from https://www.eex.com/en/about/eex/annual-report
55. European Network of Transmission System Operators for Electricity (ENTSOe). (2017, May). *Statistical factsheet 2016*. Retrieved September 12, 2018, from https://www.entsoe.eu/publications/
56. KU Leuven Energy Institute. (January, 2015). *Ei fact sheet: The current electricity market design in europe*. Retrieved Septemebr 12, 2018, from https://set.kuleuven.be/ei/factsheets
57. The European Parliament And The Council Of The European Union. (1996). *Directive 96/92/ec of the european parliament and of the council of 19 december 1996 concerning common rules for the internal market in electricity*. Retrieved August 27, 2018, from https://eur-lex.europa.eu/eli/dir/1996/92/oj
58. The European Parliament And The Council Of The European Union. (2003, June). *Directive 2003/54/ec of the european parliament and of the council of 26 june 2003*

concerning common rules for the internal market in electricity and repealing directive 96/92/ec - statements made with regard to decommissioning and waste management activities. Retrieved August 27, 2018, from https://eur-lex.europa.eu/eli/dir/2003/54/oj

59. The European Parliament And The Council Of The European Union. (2009, July). *Directive 2009/72/ec of the european parliament and of the council of 13 july 2009 concerning common rules for the internal market in electricity and repealing directive 2003/54/ec (text with eea relevance)*. Retrieved August 27, 2018, from https://eur-lex.europa.eu/eli/dir/2009/72/oj
60. Rue, H. (2001). Fast sampling of gaussian markov random fields. *Journal of the Royal Statistical Society: Series B (Statistical Methodology), 63*(2), 325–338.
61. Schill, W.-P. (2014). Residual load, renewable surplus generation and storage requirements in germany. *Energy Policy, 73*, 65–79.
62. Stock, J. H. & Watson, M. W. (1989). New indexes of coincident and leading economic indicators. *NBER macroeconomics annual, 4*, 351–394.
63. Stock, J. H. & Watson, M. W. (1998). *Diffusion indexes* (Tech. Rep.). National bureau of economic research.
64. Stock, J. H. & Watson, M. W. (2002a). Forecasting using principal components from a large number of predictors. *Journal of the American statistical association, 97*(460), 1167–1179.
65. Stock, J. H. & Watson, M. W. (2002b). Macroeconomic forecasting using diffusion indexes. *Journal of Business & Economic Statistics, 20*(2), 147–162.
66. Stock, J. H. & Watson, M. W. (2006). Forecasting with many predictors. *Handbook of economic forecasting, 1*, 515–554.
67. Taylor, S. J. (1982). Financial returns modelled by the product of two stochastic processes-a study of the daily sugar prices 1961–75. *Time series analysis: theory and practice, 1*, 203–226.
68. Ventosa, M., Baıllo, A., Ramos, A. & Rivier, M. (2005). Electricity market modeling trends. *Energy policy, 33*(7), 897–913.
69. Wei, C.-C. (2016). Modeling and analyzing the mean and volatility relationship between electricity price returns and fuel market returns. *International Journal of Economics and Finance, 8*(7), 55.
70. Weron, R. (2006). *Modeling and forecasting loads and prices in deregulated electricity markets*. Agencja Rynku Energii.
71. Weron, R. (2014). Electricity price forecasting: A review of the state-of-the-art with a look into the future. *International journal of forecasting, 30*(4), 1030–1081.
72. Yu, Y. & Meng, X.-L. (2011). To center or not to center: That is not the question— an ancillarity–sufficiency interweaving strategy (asis) for boosting mcmc efficiency. *Journal of Computational and Graphical Statistics, 20*(3), 531–570.

APPENDICES

Appendix A: Povzetek v slovenskem jeziku

OCENA IN NAPOVED VOLATILNOSTI CEN TERMINSKIH PRODUKTOV ELEKTRIČNE ENERGIJE

Trgom z električno energijo je bilo v zadnjih dvajsetih oziroma tridesetih letih posvečeno vse več pozornosti. Pozitivni učinki liberalizacije in deregulacije nekaterih drugih vertikalno integriranih trgov, kot so železnice in telekomunikacija, so vodili k začetkom podobne preobrazbe tudi na trgu električne energije. Do devetdesetih let je bila električna energija proizvedena, prodana in prenešena predvsem z vertikalno integriranimi podjetji v državni lasti, ki so delovala na monopolnih trgih. V devetdesetih letih pa je Evropski energetski trg doživel pomembno preobrazbo, kjer so vse članice EU liberalizirale svoje trge z električno energijo, z izjemo Malte in Bolgarije. Glavni cilji liberalizacije so bili nižje učinkovitost, cene in transparentnost trga, končni cilj pa je bil vzpostaviti enoten energetski trg na ravni EU. Da bi dosegli povezovanje trgov, je bilo treba odpraviti razlike med državami članicami. Za dosego tega cilja pa je bila potrebna vzpostavitev konkurenčnega trga dobave na evropski ravni, skupna pravila, transparentnost in uskladitev cen ter enotno okoljsko politiko. Za ta namen je EU sprejela več svežnjev zakonodaje, katerih glavni cilj je bila podpora liberalizacije in integracije trgov članic EU s ciljem spodbuditve in vzpostavitve konkurenčnega trga. Z liberalizacijo trga z električno energijo pa se je pojavila potreba po organizaciji trga na debelo. V ta namen so bile ustanovljene številne borze, ki so omogočale organizirano trgovanje z električno energijo.

Električna energija se kot tržno blago od preostalih dobrin razlikuje zaradi njenih posebnih lastnosti. Električne energije se namreč ne da učinkovito skladiščiti,[6] kar pomeni kontinuirano izenačitev porabe in proizvodnje, ob upoštevanju izgub na prenosnem omrežju. Poleg omejitev na strani ponudbe in povpraševanja pa h kompleksnosti trga doprinese še transport električne energije. Prenos energije poteka preko prenosnih vodov, pri katerih obstaja omejitev prenosa, oziroma njihove zmogljivosti, ki lahko privede do zamašitev in motenj prenosnih poti. Kot tretje, pa je za trg z električno energijo značilna tudi neelastičnost odjemalcev, saj ta dobrina nima učinkovitega substituta oziroma je nadomeščanje električne energije z nekonvencionalnimi viri drago in nefleksibilno.

Specifične lastnosti električne energije se odražajo tudi v gibanju cen. To gre opaziti predvsem v izredno nestanovitnih cenah na promptmem trgu z elektirčno energijo. Zaradi tega je trgovanje na organiziranih trgih postalo bistveno za vse tržne udeležence, kjer elektroenergetska podjetja poizkušajo ublažiti tveganja povzročena z negotovim gibanjem cen. Slednje je spodbudilo naračšanje povpraševanja po izvedenih finančnih produktih, ki se uporabljajo predvsem za obvladovanje cenovnih tveganj in varovanje pred nezaželjenimi izgubami. V ta namen je bilo na trgu uvedenih veliko različnih finančnih inštrumentov, kjer

[6]Izjema skladiščenja energije v večji meri so črpalne hidroelektrarne.

pa glavno vlogo igrajo terminske pogodbe na dobavo ali odjem električne energije za v naprej določeno obdobje v prihodnosti.

Nenadzorovana izpostavljenost tveganj povezanih z nepredvidljivimi premiki tržnih cen ima lahko drage posledice za udeležence na trgu v elektroenergetski industriji. Na podlagi zgodovine in izkušenj na finančnih trgih gre sklepati da je lahko pravilna uporaba in razumevanje izvedenih finančnih inštrumentov izredno dragoceno pri obvladovanju tržnih tveganj. Za učinkovito in ustrezno uporabo slednjih inštrumentov pa so udeleženci na trgu soočeni z vrednotenjem le teh, kjer pomembno vlogo igra tudi volatilnost. Volatilnost ozrioma nestanovitnost, ki je eden ključnih parametrov, meri stopnjo odstopanj cene od povprečja. Dve gavni vrsti volatilnosti sta dejanska (zgodovinska) in pa implicitna, ki je usmerjena v prihodnost in izhaja iz vrednotenj opcijskih cen. Z namenom boljšega razumevanja tega pojava se je širok spekter raziskovalcev in tržnih udeležencev posvetil ocenjevanju, modeliranju in napovedovanju volatilnosti, vendar predvsem na finančnih trgih.

Glavni cilj te analize je izdelati oceno negotovosti na trgu s treminskimi produkti električne energije. V ta namen sem implementiral pristop Jurada, Ludvigson in Ng (2015) ter njihovo ekonometrično formalizacijo negotovosti. Posamezne negotovosti so ocenjene za dnevne cene električne energije ter surovin ključnih za ta trg. Nadalje ocenim tudi mero oziroma indeks negotovosti na terminskem trgu z elektirčno energijo, ki je oblikovan z agregiranjem posamičnih ocen negotovosti. Tržno mero negotovosti kasneje primerjam z dejansko volatilnostjo cen na treminskih trgih, s pogojnimi volatilnostmi ocenjenimi z modelom GARCH (p,q) ter dodatno analiziram njene značilnosti.

Pri ocenjevanju celovite mere negotovosti na terminskem trgu z električno energijo, je moja hipoteza, da se te ocene razlikujejo od ocen pogojne volatilnosti ocenjene z modelom GARCH. Hkrati tudi analiziram napovedno natančnost obeh pristopov, pri čemer trdim, da bi morala ob upoštevanju široke palete eksternih dejavnikov moja ocena tržne negotovosti doseči boljšo napovedno sposobnost pri napovedovanju izven vzorca. Dodatno predvidevam, da dinamika pojasnjevalnih spremenljivk pomembno prispeva k ocenam negotovosti.

Negotovost cen na terminskem trgu električne energije je v tej analizi definirana kot pogojna volatilnost rezidualov napovednega modela. Natančneje so posamezne napovedi za h-opazovanj v prihodnost označene z $\mathcal{U}_{jt}^{y}(h)$ in predstavljajo pogojno volatilnost nenapovedljivega dela vrednosti, ki jo model napoveduje. To pomeni, da pogojna pričakovanja glede kvadratov napak v napovedih direktno vplivajo na nivo ocene posamezne negotovosti. Z agregiranjem teh posameznih ocen za vsako opazovanje t pa kasneje izračunam oceno oziroma indeks negotovosti na nivoju celotnega trga.

Pri tej analizi je v prvem koraku potrebno pridobiti osnovo za oceno posameznih vrednosti negotovosti – napovedne napake. Za napovedovanje sem uporabil širok nabor prediktorjev in z njimi poizkušal pojasniti vplive vseh možnih virov negotovosti. Stock & Watson

(2002b) sta predstavila metodo za napovedovanje z velikim številom pojasnjevalnih spremenljivk, kjer je celoten spekter spremenljivk opisan z majhnim številom faktorjev oziroma indeksov. Ta pristop sem uporabil tudi v tej analizi, kjer sem z uporabo metode glavnih komponent (Principal Component Analysis) zmanjšal dimenzijo matrike prediktorjev. V naslednjem koraku sem za 12 odvisnih spremenljivk y_t generiral napovedi z uporabo napovednega modela s faktorji, kar mi omogoča izračun napovednih napak.

Za oceno napovedi sem implementiral in primerjal dva različna pristopa. V prvem pristopu je po vzoru Jurada, Ludvingson in Ng (2015) niz končnih pojasnjevalnih spremenljivk v vsakem modelu določen z konzervativnim pragom za določanje statistične značilnosti. Natančneje je vsak model sprva ocenjen z vsemi možnimi prediktorji, kjer so v naslednjem koraku vse spremenljikve katerih regresijki koeficient ni statistično značilno različen od 0 izpuščene. Pri tem se kot že omenjeno upošteva prag, ki je določen pri t statistiki 1.96. Na koncu so modeli ponovno ocenjeni z uporabo končnega niza prediktorjev.

V drugem pristopu pa implementiram Bayesiansko povprečenje cenilk regresijskih koeficientov (Byesian Averaging of Clasical Estimates), ki mi omogoča boljši zajem širokega spektra pojasnjevalnih spremenljivk (Sala- i-Martin et al., 2004). V prvem koraku je tu najprej potrebna konstrukcija in ocena vseh možnih kombinacij modelov kjer je vsakemu modelu dodeljena utež glede na njegovo napovedno natančnost in pri upoštevanju modelske kompleksnosti. Z uporabo teh uteži (posterior weights) so izračunane aposteriorna povprečja regresijskih koeficientov, ki so v vsakem od modelov ocenjeni z metodo najmanjših kvadratov (OLS). Dodatno je pomembna razilka med pristopoma tudi ta, da imajo v slednjem modeli vsiljeno zaprto obliko odlogov, torej da vmesni odlogi pojansjevalnih spremenjivk niso izpuščeni.

Ker je predpostavljena avtoregresijka dinamika faktorjev, je končen model predstavljen v obliki vektorsko avtoregresijskega modela razširjenega s faktorji (FAVAR), kjer so pridobljene napovedne napake za napovedno obdobje $h = 1, ..., 20$. V zadnjem koraku pa sledi modeliranje variance napak napovednega modela z uporabo modela stohastične volatilnosti (stockastic volatility model). Jurado, Ludvigson & Ng (2015) kot enega glavnih razlogov za uporabo te metode predstavijo neodvisnost med reziduali v y_t in šoki v varianci, v čemer se metodologija razlikuje od uporabe modelov tipa GARCH. Jurado, Ludvigson & Ng (2015) hkrati tudi pokažejo, kako volatilnost v prediktorjih vpliva na končno oceno negotovosti odvisne spremenljivke za napovedi kjer je $h > 1$.

Za namen te analize je bil pripravljen širok nabor 312 spremenljivk relevantnih za nemški elektroenergetski trgi, ki so bile po natančnem pregledu združene v matriko $\mathbf{X}$ z 550 dnevnimi opazovanji, ki rangirajo od Februarja 2015 do Aprila 2017. Poleg pregleda za manjkajočimi in pretirano odstopajočimi vrednostmi, so bile vse spremenljivke pretvorjene v stacionarno obliko z uporabo temeljnih transformacij in testirane za nestacionarnost. Zaradi specifičnih karakteristik cen električne energije, so bile razvite in implementirane tudi dodatne transformacije, za zagotovitev nepristranskosti analize.

Z uporabo obeh pristopov napovedovanja najprej pridobim dva različna niza napak napovednih vrednosti za vseh 12 odvisnih spremenljikv. Pri primerjavi rezultatov prvega pristopa povzetega po Jurado, Ludvigson & Ng (2015), ki dovoli odprto strukturo odlogov (OL), ter pristopa z vsiljeno zaprto strukturo odlogov in Bayesianskim povprečenjem OLS cenilk regresijskih koeficientov lahko opazimo, da se oblika modelov bistveno razlikuje. Natančneje gre opaziti, da modeli z OL vsebujejo precej manjše število spremenljik kot modeli z CL pristopom. Dodatno je potrebno poudariti, da so aposteriorne verjetnosti modelov pri CL pristopu relativno enakovredne, s čimer se izognem prevladi majhnega števila faktorjev. Dodatna analiza in primerjava standardiziranih napovedi posameznih negotovosti obeh pristopov pokaže, da so rezultati primerljivi za $h = 1$, kjer dodatno obe oceni relativno dosledno napovesta večje skoke v zgodovinski volatilnosti. Pri primerjavi napovedne natančnosti z uporabo standardnih mer kot so povprečna absolutna napaka (MAE), kvadratni koren povprečne kavdratne napake (RMSE) in pa kvadratni koren povprečne kavdratne odstotne napake (RMPSE) pa lahko opazimo, da CL pristop v povprečju daje bolj natančne napovedi kot OL pristop.

Nadalje z agregiranjem posamenznih ocen negotovosti izračunam indeks negotovosti za terminski trg električne energije, kjer se osredotočam na nemški trg. Ocene tržne negotovosti pokažejo na veliko porast negotovosti v drugi polovici leta 2016, kar sovpada z ugotovitvami EEX iz njihovega letnega poročila za isto leto. Analzia pokaže tudi na konvergenco ocen negotovosti k brezpogojni sredini s povečevanjem napovednega horizonta, saj se z večjim h sredina vzorca povečuje ob padajoči varianci. Po definiciji negotovosti v tej analizi le ta predstavlja pogojno volatilnost nenapovedljive komponente v napovedih odivsnih časovnih serj. Dodatno pa Jurado, Ludvigson & Ng (2015) opozarjajo, da lahko na ocene negotovosti vpliva sistematična tržna negotovost ali pa šoki idiosinkratične negotovosti posameznih serij. V ta namen sem ocenil vplv sistematične tržne negotovosti na posamezne negotovosti, kjer za vsako od 12 odvisnih serij ocenim determinacijski koeficient (R^2) pri linearni regresiji tržne negotovosti na posamezno negotovost vsake serije. V povprečju gre opaziti, da igra tržna negotovost večjo vlogo kot idiosinkratični šoki pozameznih serij. Dodatno je iz rezultatov razvidno, da je gibanje cen premoga izredno pomembno pri negotovosti na nemškem trgu električne energije, kar sovpada z nemško proizvodnjo strukturo, kjer je bilo v 2016 več kot 46 % električne energije proizvedene v premogovnih termo elektrarnah. Z izračnom povprečnih vrednosti R^2 za vsak h dodatno pokažem, da tržna negotovost v povrpečju pojasni 72 % variance v celotni negotovosti izračunani kot vsota vseh posameznih ocen. Razvidno je tudi, da se ta delež povečuje s h. Hkrati pa z oceno R^2 na dveh različnih podvzorcih pokažem tudi, da igra sistematična tržna negotovost pomembnejšo vlogo v obdobjih z višjo negotovostjo.

V zadnjem delu analize izvedem tudi primerjavo ocen negotovosti na trgu električne energije z ocenami pogojne volatilnosti z uporabo GARCH metode. V ta namen ocenim AR-GARCH model za vsako od 12 odvisnih časocnih serij, kjer je optimalna struktura odlogov določena z statistiko Akaike (AIC). Rezulati te primerjave pokažejo na večjo odvisnost GARCH metode od manjših konic v osnovni seriji, kar rezultira v bolj volatilnih ocenah. Za empirično oceno razlik med napovedmi obeh metod sem uporabil Diebold-Mariano test napovedne natančnosti, ki pokaže, da se napovedi za $h = 1$ statistično značilno razlikujejo. Hkrati pa test pokaže tudi, da se ta razlika z h zmanjšuje, kajti obe oceni tendirata k brezpogojni sredini. Za dodatno primerjavo metod sem izvedel tudi analizo napovedne natančnosti izven vzorca (out-of-sample). Ta analiza je bila razvita in prirejena po vzoru "Walk Forward" analize (WFA), kjer z združitvijo večih ocen izven vzorca primerjam napovedno natančnost. Analiza pokaže, da je napovedna natančnost izven vzorca na podalgi MAE in RMSE statistik boljša z uporabo tržne ocene negotovosti. Obratno pa pokaže statistika RMPSE, kjer je napovedna natančnost rahlo boljša z uporabo GARCH metode.

Razlike so bile dodatno analizirane z dekompozicijo ocen tržne negotovosti kjer se je pokazalo, da so ob kontroli za prediktabilno kmponento nekoliko nižje ocene negotovosti v obdobjih z visoko splošno negotovostjo. Ti rezultati kažejo na možno precenjevanje volatilnosti z uporabo enostavnih GARCH modelov. Vendar pa ti rezultati kažejo tudi, da je ključna determinanta razlike med obema metodologijama uporaba SV modela za oceno pogojne volatilnosti inovacij pri napakah v napovedih v primerjavi s pogojno volatilnostjo GARCH modela.

Appendix B: Data Description

Table 12: Electricity prices

No	Id	Name	Type	Source	Vartype
1	BREM1	BRENT Price M+1	Futures contract	ICE	1
2	AP2M1	API2 Price M+1	Futures contract	ICE	1
3	EUAY1	EUA Y+1	Futures contract	ICE	1
4	NCGM1	NCG Price M+1	Futures contract	POWERNEXT	1
5	BASEQ1	Baseload price DE Q+1	Futures contract	EEX	1
6	BASEY1	Baseload price DE Y+1	Futures contract	EEX	1
7	BASEM1	Baseload price DE M+1	Futures contract	EEX	1
8	BASEM2	Baseload price DE M+2	Futures contract	EEX	1
9	BASEM3	Baseload price DE M+3	Futures contract	EEX	1
10	BASEM4	Baseload price DE M+4	Futures contract	EEX	1
11	BASEM5	Baseload price DE M+5	Futures contract	EEX	1
12	BASEM6	Baseload price DE M+6	Futures contract	EEX	1
13	DE_S0	Day-ahead price DE	Day-ahead price	EPEX	2
14	FR_S0	Day-ahead price FR	Day-ahead price	EPEX	2
15	NRDPL_S0	Day-ahead price NORDPOOL	Day-ahead price	NORDPOOL	2
16	AT_S0	Day-ahead price AT	Day-ahead price	EPEX	2
17	CH_S0	Day-ahead price CH	Day-ahead price	EPEX	2
18	PUN_S0	Day-ahead price PUN	Day-ahead price	TERNA	2
19	UK_S0	Day-ahead price UK	Day-ahead price	APX	2
20	CZ_S0	Day-ahead price CZ	Day-ahead price	EEX	2
21	PL_S0	Day-ahead price PL	Day-ahead price	EEX	2

Source: Own work.

Table 13: Spot exchange rates

No	Id	Name	Type	Source	Vartype
22	EURUSD	EUR/USD	Exchange rate	YahooFinance	3
23	EURGBP	EUR/GBP	Exchange rate	YahooFinance	3
24	EURPLN	EUR/PLN	Exchange rate	YahooFinance	3

Source: Own work.

Table 14: Temperature

No	Id	Name	Type	Source	Vartype
25	TEMP_DE	Temperature DE	Temperature	Ogimet	4

Source: Own work.

Table 15: Electricity consumption, production and commercial exchange

No	Id	Name	Type	Source	Vartype
26	LOAD_DE	Total Load DE	Consumption	ENTSO-e	5
27	LOAD_FR	Total Load FR	Consumption	ENTSO-e	5
28	LOAD_AT	Total Load AT	Consumption	ENTSO-e	5
29	LOAD_NO	Total Load NO	Consumption	ENTSO-e	5
30	LOAD_PL	Total Load PL	Consumption	ENTSO-e	5
31	LOAD_CH	Total Load CH	Consumption	ENTSO-e	5
32	LOAD_CZ	Total Load CZ	Consumption	ENTSO-e	5
33	LOAD_DK	Total Load DK	Consumption	ENTSO-e	5
34	SCHPROD_FR	Day Ahead Scheduled Generation FR	Scheduled Generation	ENTSO-e	6
35	SCHPROD_AT	Day Ahead Scheduled Generation AT	Scheduled Generation	ENTSO-e	6
36	SCHPROD_NO	Day Ahead Scheduled Generation NO	Scheduled Generation	ENTSO-e	6
37	SCHPROD_PL	Day Ahead Scheduled Generation PL	Scheduled Generation	ENTSO-e	6
38	SCHPROD_CZ	Day Ahead Scheduled Generation CZ	Scheduled Generation	ENTSO-e	6
39	SCHPROD_DK	Day Ahead Scheduled Generation DK	Scheduled Generation	ENTSO-e	6
40	WINDFOR_DE	Daf-ahead wind generation forecast DE	Daf-ahead generation forecast	ENTSO-e	6
41	HYD_DE	Realised hydro generation DE	Realised generation per type	ENTSO-e	6
42	HYD_FR	Realised hydro generation FR	Realised generation per type	ENTSO-e	6
43	HYD_AT	Realised hydro generation AT	Realised generation per type	ENTSO-e	6
44	HYD_CZ	Realised hydro generation CZ	Realised generation per type	ENTSO-e	6
45	HYD_PL	Realised hydro generation PL	Realised generation per type	ENTSO-e	6
46	NUC_FR	Realised nuclear generation FR	Realised generation per type	ENTSO-e	6
47	WIND_DE	Realised wind generation DE	Realised generation per type	ENTSO-e	6
48	SOL_DE	Realised solar generation DE	Realised generation per type	ENTSO-e	6
49	WIND_DK	Realised wind generation DK	Realised generation per type	ENTSO-e	6
50	WIND_UK	Realised wind generation UK	Realised generation per type	ENTSO-e	6
51	SOLAR_UK	Realised solar generation UK	Realised generation per type	ENTSO-e	6
52	WIND_FR	Realised wind generation FR	Realised generation per type	ENTSO-e	6
53	SOLAR_FR	Realised solar generation FR	Realised generation per type	ENTSO-e	6
54	TERMO_PL	Realised termo generation PL	Realised generation per type	ENTSO-e	6
55	NETCOMLFW_DE_AT	Net scheduled Commercial exchange DE>AT	Scheduled Commercial exchange	ENTSO-e	7
56	NETCOMLFW_DE_CZ	Net scheduled Commercial exchange DE>CZ	Scheduled Commercial exchange	ENTSO-e	7
57	NETCOMLFW_DE_DK	Net scheduled Commercial exchange DE>DK	Scheduled Commercial exchange	ENTSO-e	7
58	NETCOMLFW_DE_FR	Net scheduled Commercial exchange DE>FR	Scheduled Commercial exchange	ENTSO-e	7
59	NETCOMLFW_DE_LUX	Net scheduled Commercial exchange DE>LUX	Scheduled Commercial exchange	ENTSO-e	7
60	NETCOMLFW_DE_NL	Net scheduled Commercial exchange DE>NL	Scheduled Commercial exchange	ENTSO-e	7
61	NETCOMLFW_DE_PL	Net scheduled Commercial exchange DE>PL	Scheduled Commercial exchange	ENTSO-e	7
62	NETCOMLFW_DE_CH	Net scheduled Commercial exchange DE>CH	Scheduled Commercial exchange	ENTSO-e	7

Source: Own work.

Table 16: Financial market

No	Id	Name	Type	Source	Vartype
63	LIN	Linde	Stock price	YahooFinance	8
64	VOW3	Volkswagen Group	Stock price	YahooFinance	8
65	FME	Fresenius Medical Care	Stock price	YahooFinance	8
66	DBK	Deutsche Bank	Stock price	YahooFinance	8
67	DAI	Daimler	Stock price	YahooFinance	8
68	CBK	Commerzbank	Stock price	YahooFinance	8
69	DTE	Deutsche Telekom	Stock price	YahooFinance	8
70	SAP	SAP	Stock price	YahooFinance	8
71	IFX	Infineon Technologies	Stock price	YahooFinance	8
72	DB1	Deutsche Börse	Stock price	YahooFinance	8
73	ADS	Adidas	Stock price	YahooFinance	8
74	FRE	Fresenius	Stock price	YahooFinance	8

Table continues on next page

Table 16: Financial market (cont.)

No	Id	Name	Type	Source	Vartype
75	MRK	Merck	Stock price	YahooFinance	8
76	ALV	Allianz	Stock price	YahooFinance	8
77	RWE	RWE	Stock price	YahooFinance	8
78	TKA	ThyssenKrupp	Stock price	YahooFinance	8
79	LHA	Deutsche Lufthansa	Stock price	YahooFinance	8
80	BMW	BMW	Stock price	YahooFinance	8
81	MUV2	Munich Re	Stock price	YahooFinance	8
82	PSM	ProSiebenSat.1 Media	Stock price	YahooFinance	8
83	BAYN	Bayer	Stock price	YahooFinance	8
84	HEN3	Henkel	Stock price	YahooFinance	8
85	EOAN	E.ON	Stock price	YahooFinance	8
86	GDAXI	DAX Index	Stock price	YahooFinance	8
87	DPW	Deutsche Post	Stock price	YahooFinance	8
88	BEI	Beiersdorf	Stock price	YahooFinance	8
89	HEI	HeidelbergCement	Stock price	YahooFinance	8
90	SIE	Siemens	Stock price	YahooFinance	8
91	Agric	Agriculture	49 Industry Portfolios - Returns	Kenneth R. French Data Library	9
92	Food	Food Products	49 Industry Portfolios - Returns	Kenneth R. French Data Library	9
93	Soda	Candy & Soda	49 Industry Portfolios - Returns	Kenneth R. French Data Library	9
94	Beer	Beer & Liquor	49 Industry Portfolios - Returns	Kenneth R. French Data Library	9
95	Smoke	Tobacco Products	49 Industry Portfolios - Returns	Kenneth R. French Data Library	9
96	Toys	Recreation	49 Industry Portfolios - Returns	Kenneth R. French Data Library	9
97	Fun	Entertainment	49 Industry Portfolios - Returns	Kenneth R. French Data Library	9
98	Books	Printing and Publishing	49 Industry Portfolios - Returns	Kenneth R. French Data Library	9
99	Hshld	Consumer Goods	49 Industry Portfolios - Returns	Kenneth R. French Data Library	9
100	Clths	Apparel	49 Industry Portfolios - Returns	Kenneth R. French Data Library	9
101	Hlth	Healthcare	49 Industry Portfolios - Returns	Kenneth R. French Data Library	9
102	MedEq	Medical Equipment	49 Industry Portfolios - Returns	Kenneth R. French Data Library	9
103	Drugs	Pharmaceutical Products	49 Industry Portfolios - Returns	Kenneth R. French Data Library	9
104	Chems	Chemicals	49 Industry Portfolios - Returns	Kenneth R. French Data Library	9
105	Rubbr	Rubber and Plastic Products	49 Industry Portfolios - Returns	Kenneth R. French Data Library	9
106	Txtls	Textiles	49 Industry Portfolios - Returns	Kenneth R. French Data Library	9
107	BldMt	Construction Materials	49 Industry Portfolios - Returns	Kenneth R. French Data Library	9
108	Cnstr	Construction	49 Industry Portfolios - Returns	Kenneth R. French Data Library	9
109	Steel	Steel Works Etc	49 Industry Portfolios - Returns	Kenneth R. French Data Library	9
110	FabPr	Fabricated Products	49 Industry Portfolios - Returns	Kenneth R. French Data Library	9
111	Mach	Machinery	49 Industry Portfolios - Returns	Kenneth R. French Data Library	9
112	ElcEq	Electrical Equipment	49 Industry Portfolios - Returns	Kenneth R. French Data Library	9
113	Autos	Automobiles and Trucks	49 Industry Portfolios - Returns	Kenneth R. French Data Library	9
114	Aero	Aircraft	49 Industry Portfolios - Returns	Kenneth R. French Data Library	9
115	Ships	Shipbuilding, Railroad Equipment	49 Industry Portfolios - Returns	Kenneth R. French Data Library	9
116	Guns	Defense	49 Industry Portfolios - Returns	Kenneth R. French Data Library	9
117	Gold	Precious Metals	49 Industry Portfolios - Returns	Kenneth R. French Data Library	9
118	Mines	Non-Metallic and Industrial Metal Mining	49 Industry Portfolios - Returns	Kenneth R. French Data Library	9
119	Coal	Coal	49 Industry Portfolios - Returns	Kenneth R. French Data Library	9
120	OilNg	Petroleum and Natural Gas	49 Industry Portfolios - Returns	Kenneth R. French Data Library	9
121	Util	Utilities	49 Industry Portfolios - Returns	Kenneth R. French Data Library	9
122	Telcm	Communication	49 Industry Portfolios - Returns	Kenneth R. French Data Library	9
123	PerSv	Personal Services	49 Industry Portfolios - Returns	Kenneth R. French Data Library	9
124	BusSv	Business Services	49 Industry Portfolios - Returns	Kenneth R. French Data Library	9
125	Hardw	Computers	49 Industry Portfolios - Returns	Kenneth R. French Data Library	9
126	Softw	Computer Software	49 Industry Portfolios - Returns	Kenneth R. French Data Library	9
127	Chips	Electronical Equipmet	49 Industry Portfolios - Returns	Kenneth R. French Data Library	9
128	LabEq	Measuring and Control Equipment	49 Industry Portfolios - Returns	Kenneth R. French Data Library	9
129	Paper	Business Supplies	49 Industry Portfolios - Returns	Kenneth R. French Data Library	9
130	Boxes	Shipping Containers	49 Industry Portfolios - Returns	Kenneth R. French Data Library	9
131	Trans	Transportation	49 Industry Portfolios - Returns	Kenneth R. French Data Library	9
132	Whlsl	Wholesale	49 Industry Portfolios - Returns	Kenneth R. French Data Library	9
133	Rtail	Retail	49 Industry Portfolios - Returns	Kenneth R. French Data Library	9
134	Meals	Restaurants, Hotels, Motels	49 Industry Portfolios - Returns	Kenneth R. French Data Library	9
135	Banks	Banking	49 Industry Portfolios - Returns	Kenneth R. French Data Library	9
136	Insur	Insurance	49 Industry Portfolios - Returns	Kenneth R. French Data Library	9
137	RlEst	Real Estate	49 Industry Portfolios - Returns	Kenneth R. French Data Library	9
138	Fin	Trading	49 Industry Portfolios - Returns	Kenneth R. French Data Library	9
139	Other	Almost Nothing	49 Industry Portfolios - Returns	Kenneth R. French Data Library	9

Source: Own work.

Table 17: Energy market ETFs

No	Id	Name	Type	Source	Vartype
140	XOP	SPDR S&P Oil & Gas Exploration & Production ETF	ETF Price - Energy	YahooFinance	10
141	CANE	Teucrium Sugar Fund	ETF Price - Commodities	YahooFinance	10
142	UNG	United States Natural Gas Fund LP	ETF Price - Oil & Gas	YahooFinance	10
143	USAG	United States Agriculture Index Fund	ETF Price - Commodities	YahooFinance	10
144	PALL	ETFS Physical Palladium Shares	ETF Price - Commodities	YahooFinance	10
145	GRU	Elements MLCX Grains Index-Total Return ETN	ETF Price - Commodities	YahooFinance	10
146	DBGR	Deutsche X-trackers MSCI Germany Hedged Equity ETF	ETF Price - Germany Total Market	YahooFinance	10
147	SLVO	Credit Suisse X-Links Silver Shares Covered Call ETN	ETF Price - Commodities	YahooFinance	10
148	DBA	PowerShares DB Agriculture Fund	ETF Price - Commodities	YahooFinance	10
149	JJE	iPath Bloomberg Energy Subindex Total Return ETN	ETF Price - Commodities	YahooFinance	10
150	GLTR	ETFS Physical Precious Metals Basket Shares	ETF Price - Commodities	YahooFinance	10
151	GASL	Direxion Daily Natural Gas Related Bull 3X Shares	ETF Price - Energy	YahooFinance	10
152	UAG	ETRACS UBS Bloomberg CMCI Agriculture Total Return ETN	ETF Price - Commodities	YahooFinance	10
153	DBO	PowerShares DB Oil Fund	ETF Price - Commodities	YahooFinance	10
154	PXJ	PowerShares Dynamic Oil & Gas Services Portfolio	ETF Price - Energy	YahooFinance	10
155	PXE	PowerShares Dynamic Energy Exploration & Production Portfolio	ETF Price - Energy	YahooFinance	10
156	EWGS	iShares MSCI Germany Small Cap ETF	ETF Price - Germany Total Market	YahooFinance	10
157	OLO	DB Crude Oil Long ETN	ETF Price - Commodities	YahooFinance	10
158	GYEN	AdvisorShares Gartman Gold/Yen ETF	ETF Price - Commodities	YahooFinance	10
159	HEVY	iPath Pure Beta Industrial Metals ETN	ETF Price - Commodities	YahooFinance	10
160	GCC	WisdomTree Continuous Commodity Index Fund	ETF Price - Commodities	YahooFinance	10
161	FOIL	iPath Pure Beta Aluminum ETN	ETF Price - Commodities	YahooFinance	10
162	ICLN	iShares Global Clean Energy ETF	ETF Price - Alternative Energy	YahooFinance	10
163	QDEU	SPDR MSCI Germany StrategicFactors ETF	ETF Price - Germany Total Market	YahooFinance	10
164	GSG	iShares S&P GSCI Commodity Indexed Trust	ETF Price - Commodities	YahooFinance	10
165	USO	United States Oil Fund LP	ETF Price - Commodities	YahooFinance	10
166	RYE	Guggenheim S&P 500 Equal Weight Energy ETF	ETF Price - Energy	YahooFinance	10
167	PBD	PowerShares Global Clean Energy Portfolio ETF	ETF Price - Alternative Energy	YahooFinance	10
168	MLPY	Morgan Stanley Cushing MLP High Income Index ETN	ETF Price - Energy	YahooFinance	10
169	MLPJ	Global X Junior MLP ETF	ETF Price - Energy	YahooFinance	10
170	OUNZ	VanEck Merk Gold	ETF Price - Commodities	YahooFinance	10
171	UGA	United States Gasoline Fund LP	ETF Price - Commodities	YahooFinance	10
172	NIB	iPath Bloomberg Cocoa Subindex Total Return ETN	ETF Price - Commodities	YahooFinance	10
173	BLNG	iPath Pure Beta Precious Metals ETN	ETF Price - Commodities	YahooFinance	10
174	IAU	iShares Gold Trust	ETF Price - Commodities	YahooFinance	10
175	OIH	VanEck Vectors Oil Services ETF	ETF Price - Energy	YahooFinance	10
176	IYE	iShares U.S. Energy ETF	ETF Price - Energy	YahooFinance	10
177	YMLI	VanEck Vectors High Income Infrastructure MLP ETF	ETF Price - Energy	YahooFinance	10
178	PSCE	PowerShares S&P SmallCap Energy Portfolio	ETF Price - Energy	YahooFinance	10
179	LIT	Global X Lithium & Battery Tech ETF	ETF Price - Europe	YahooFinance	10
180	MLPS	ETRACS 1XMonthly Short Alerian MLP Infrastructure TR ETN	ETF Price - Energy	YahooFinance	10
181	SBV	iPath Pure Beta S&P GSCI-Weighted ETN	ETF Price - Commodities	YahooFinance	10
182	HEDJ	WisdomTree Europe Hedged Equity Fund	ETF Price - Europe	YahooFinance	10
183	CMDT	iShares Commodity Optimized Trust	ETF Price - Commodities	YahooFinance	10
184	GSC	GS Connect S&P GSCI Enhanced Commodity TR Strategy ETN	ETF Price - Commodities	YahooFinance	10
185	WEET	iPath Pure Beta Grains ETN	ETF Price - Commodities	YahooFinance	10
186	JJC	iPath Bloomberg Copper Subindex Total Return ETN	ETF Price - Commodities	YahooFinance	10
187	KOL	VanEck Vectors Coal ETF	ETF Price - Energy	YahooFinance	10
188	GLDI	Credit Suisse X-Links Gold Shares Covered Call ETN	ETF Price - Commodities	YahooFinance	10
189	FTGC	First Trust Global Tactical Commodity Strategy Fund	ETF Price - Commodities	YahooFinance	10
190	PUW	PowerShares WilderHill Progressive Energy Portfolio	ETF Price - Energy	YahooFinance	10
191	RJZ	Elements Rogers Int.Commodity Index-Metals Total Return ETN	ETF Price - Commodities	YahooFinance	10
192	HEWG	iShares Currency Hedged MSCI Germany ETF	ETF Price - Germany Total Market	YahooFinance	10
193	IXC	iShares Global Energy ETF	ETF Price - Energy	YahooFinance	10
194	ENY	Guggenheim Canadian Energy Income ETF	ETF Price - Energy	YahooFinance	10
195	BOIL	ProShares Ultra Bloomberg Natural Gas	ETF Price - Oil & Gas	YahooFinance	10
196	GAZ	iPath Bloomberg Natural Gas Subindex Total Return ETN	ETF Price - Oil & Gas	YahooFinance	10
197	MLPG	ETRACS Alerian Natural Gas MLP ETN	ETF Price - Energy	YahooFinance	10
198	GEX	VanEck Vectors Global Alternative Energy ETF	ETF Price - Alternative Energy	YahooFinance	10
199	BAL	iPath Bloomberg Cotton Subindex Total Return ETN	ETF Price - Commodities	YahooFinance	10
200	MLPO	Credit Suisse S&P MLP Index ETN	ETF Price - Energy	YahooFinance	10
201	BNO	United States Brent Oil Fund LP	ETF Price - Commodities	YahooFinance	10
202	EMLP	First Trust North American Energy Infrastructure Fund	ETF Price - Energy	YahooFinance	10

Table continues on next page

Table 17: Energy market ETFs (cont.)

No	Id	Name	Type	Source	Vartype
203	UGAZ	VelocityShares 3X Long Natural Gas ETN	ETF Price - Oil & Gas	YahooFinance	10
204	NINI	iPath Pure Beta Nickel ETN	ETF Price - Commodities	YahooFinance	10
205	RJI	Elements Rogers International Commodity Index-Total Return ETN	ETF Price - Commodities	YahooFinance	10
206	COPX	Global X Copper Miners ETF	ETF Price - Europe	YahooFinance	10
207	PXI	PowerShares DWA Energy Momentum Portfolio	ETF Price - Energy	YahooFinance	10
208	FUD	ETRACS UBS Bloomberg CMCI Food Total Return ETN	ETF Price - Commodities	YahooFinance	10
209	KOLD	ProShares UltraShort Bloomberg Natural Gas	ETF Price - Oil & Gas	YahooFinance	10
210	MLPI	ETRACS Alerian MLP Infrastructure Index ETN	ETF Price - Energy	YahooFinance	10
211	USCI	United States Commodity Index Fund	ETF Price - Commodities	YahooFinance	10
212	DDG	ProShares Short Oil & Gas	ETF Price - Energy	YahooFinance	10
213	CHOC	iPath Pure Beta Cocoa ETN	ETF Price - Commodities	YahooFinance	10
214	FCG	First Trust Natural Gas ETF	ETF Price - Energy	YahooFinance	10
215	SOYB	Teucrium Soybean Fund	ETF Price - Commodities	YahooFinance	10
216	MLPX	Global X MLP & Energy Infrastructure ETF	ETF Price - Energy	YahooFinance	10
217	GLD	SPDR Gold Trust	ETF Price - Commodities	YahooFinance	10
218	PICK	iShares MSCI Global Metals & Mining Producers ETF	ETF Price - Europe	YahooFinance	10
219	TAN	Guggenheim Solar ETF	ETF Price - Alternative Energy	YahooFinance	10
220	CUPM	iPath Pure Beta Copper ETN	ETF Price - Commodities	YahooFinance	10
221	DJP	iPath Bloomberg Commodity Index Total Return ETN	ETF Price - Commodities	YahooFinance	10
222	PPLT	ETFS Physical Platinum Shares	ETF Price - Commodities	YahooFinance	10
223	ONG	iPath Pure Beta Energy ETN	ETF Price - Commodities	YahooFinance	10
224	AMZA	InfraCap MLP ETF	ETF Price - Energy	YahooFinance	10
225	COW	iPath Bloomberg Livestock Subindex Total Return ETN	ETF Price - Commodities	YahooFinance	10
226	OLEM	iPath Pure Beta Crude Oil ETN	ETF Price - Commodities	YahooFinance	10
227	JJU	iPath Bloomberg Aluminum Subindex Total Return ETN	ETF Price - Commodities	YahooFinance	10
228	SLV	iShares Silver Trust	ETF Price - Commodities	YahooFinance	10
229	IPW	SPDR S&P International Energy Sector ETF	ETF Price - Energy	YahooFinance	10
230	DBC	PowerShares DB Commodity Index Tracking Fund	ETF Price - Commodities	YahooFinance	10
231	GEUR	AdvisorShares Gartman Gold/EURO ETF	ETF Price - Commodities	YahooFinance	10
232	URA	Global X Uranium ETF	ETF Price - Oil & Gas	YahooFinance	10
233	YMLP	VanEck Vectors High Income MLP ETF	ETF Price - Energy	YahooFinance	10
234	UCI	ETRACS UBS Bloomberg Con.Maturity Commodity Index TR ETN	ETF Price - Commodities	YahooFinance	10
235	UBC	ETRACS UBS Bloomberg CMCI Livestock Total Return ETN	ETF Price - Commodities	YahooFinance	10
236	XLE	Energy Select Sector SPDR Fund	ETF Price - Energy	YahooFinance	10
237	DGAZ	VelocityShares 3X Inverse Natural Gas ETN	ETF Price - Oil & Gas	YahooFinance	10
238	PTM	ETRACS UBS Bloomberg CMCI Platinum Total Return ETN	ETF Price - Commodities	YahooFinance	10
239	CAFE	iPath Pure Beta Coffee ETN	ETF Price - Commodities	YahooFinance	10
240	MLPC	C-Tracks Miller/Howard MLP Fundamental ETN	ETF Price - Energy	YahooFinance	10
241	JJS	iPath Bloomberg Softs Subindex Total Return ETN	ETF Price - Commodities	YahooFinance	10
242	QCLN	First Trust NASDAQ Clean Edge Green Energy Index Fund	ETF Price - Alternative Energy	YahooFinance	10
243	WEAT	Teucrium Wheat Fund	ETF Price - Commodities	YahooFinance	10
244	VDE	Vanguard Energy ETF	ETF Price - Energy	YahooFinance	10
245	DIG	ProShares Ultra Oil & Gas	ETF Price - Energy	YahooFinance	10
246	SIVR	ETFS Physical Silver Shares	ETF Price - Commodities	YahooFinance	10
247	VGK	Vanguard FTSE Europe ETF	ETF Price - Europe	YahooFinance	10
248	SGAR	iPath Pure Beta Sugar ETN	ETF Price - Commodities	YahooFinance	10
249	AMU	ETRACS Alerian MLP Index ETN	ETF Price - Energy	YahooFinance	10
250	FILL	iShares MSCI Global Energy Producers ETF	ETF Price - Energy	YahooFinance	10
251	GSP	iPath S&P GSCI Total Return Index ETN	ETF Price - Commodities	YahooFinance	10
252	CPER	United States Copper Index Fund	ETF Price - Commodities	YahooFinance	10
253	DBP	PowerShares DB Precious Metals Fund	ETF Price - Commodities	YahooFinance	10
254	FAN	First Trust ISE Global Wind Energy Index Fund	ETF Price - Alternative Energy	YahooFinance	10
255	LSTK	iPath Pure Beta Livestock ETN	ETF Price - Commodities	YahooFinance	10
256	EWG	iShares MSCI Germany ETF	ETF Price - Germany Total Market	YahooFinance	10
257	CHIE	Global X China Energy ETF	ETF Price - Energy	YahooFinance	10
258	UNL	United States 12 Month Natural Gas Fund LP	ETF Price - Oil & Gas	YahooFinance	10
259	DBS	PowerShares DB Silver Fund	ETF Price - Commodities	YahooFinance	10
260	SGOL	ETFS Physical Swiss Gold Shares	ETF Price - Commodities	YahooFinance	10
261	SGG	iPath Bloomberg Sugar Subindex Total Return ETN	ETF Price - Commodities	YahooFinance	10
262	USL	United States 12 Month Oil Fund LP	ETF Price - Commodities	YahooFinance	10
263	OIL	iPath S&P GSCI Crude Oil Total Return ETN	ETF Price - Commodities	YahooFinance	10
264	REMX	VanEck Vectors Rare Earth/Strategic Metals ETF	ETF Price - Europe	YahooFinance	10
265	FEZ	SPDR Euro STOXX 50 ETF	ETF Price - Europe	YahooFinance	10
266	DXGE	WisdomTree Germany Hedged Equity Fund	ETF Price - Germany Total Market	YahooFinance	10
267	GRN	iPath Global Carbon ETN	ETF Price - Commodities	YahooFinance	10
268	JJG	iPath Bloomberg Grains Subindex Total Return ETN	ETF Price - Commodities	YahooFinance	10
269	FXN	First Trust Energy AlphaDEX Fund	ETF Price - Energy	YahooFinance	10

Table continues on next page

Table 17: Energy market ETFs (cont.)

No	Id	Name	Type	Source	Vartype
270	ERY	Direxion Daily Energy Bear 3X Shares	ETF Price - Energy	YahooFinance	10
271	IMLP	iPath S&P MLP ETN	ETF Price - Energy	YahooFinance	10
272	DAX	Horizons DAX Germany ETF	ETF Price - Germany Total Market	YahooFinance	10
273	IEV	iShares Europe ETF	ETF Price - Europe	YahooFinance	10
274	UBM	ETRACS UBS Bloomberg CMCI Industrial Metals Total Return ETN	ETF Price - Commodities	YahooFinance	10
275	JO	iPath Bloomberg Coffee Subindex Total Return ETN	ETF Price - Commodities	YahooFinance	10
276	DBB	PowerShares DB Base Metals Fund	ETF Price - Commodities	YahooFinance	10
277	LEDD	iPath Pure Beta Lead ETN	ETF Price - Commodities	YahooFinance	10
278	RJA	Elements Rogers International Commodity Index-Agriculture TR ETN	ETF Price - Commodities	YahooFinance	10
279	ENFR	Alerian Energy Infrastructure ETF	ETF Price - Energy	YahooFinance	10
280	JJA	iPath Bloomberg Agriculture Subindex Total Return ETN	ETF Price - Commodities	YahooFinance	10
281	DGL	PowerShares DB Gold Fund	ETF Price - Commodities	YahooFinance	10
282	AMLP	Alerian MLP ETF	ETF Price - Energy	YahooFinance	10
283	USV	ETRACS UBS Bloomberg CMCI Silver Total Return ETN	ETF Price - Commodities	YahooFinance	10
284	MLPA	Global X MLP ETF	ETF Price - Energy	YahooFinance	10
285	AMJ	J.P. Morgan Alerian MLP Index ETN	ETF Price - Energy	YahooFinance	10
286	IEO	iShares U.S. Oil & Gas Exploration & Production ETF	ETF Price - Energy	YahooFinance	10
287	NLR	VanEck Vectors Uranium+Nuclear Energy ETF	ETF Price - Oil & Gas	YahooFinance	10
288	UBG	ETRACS UBS Bloomberg CMCI Gold Total Return ETN	ETF Price - Commodities	YahooFinance	10
289	FENY	Fidelity MSCI Energy Index ETF	ETF Price - Energy	YahooFinance	10
290	DBE	PowerShares DB Energy Fund	ETF Price - Commodities	YahooFinance	10
291	CTNN	iPath Pure Beta Cotton ETN	ETF Price - Commodities	YahooFinance	10
292	DUG	ProShares UltraShort Oil & Gas	ETF Price - Energy	YahooFinance	10
293	PZD	PowerShares Cleantech Portfolio ETF	ETF Price - Alternative Energy	YahooFinance	10
294	DBEU	Deutsche X-trackers MSCI Europe Hedged Equity ETF	ETF Price - Europe	YahooFinance	10
295	CORN	Teucrium Corn Fund	ETF Price - Commodities	YahooFinance	10
296	JJM	iPath Bloomberg Industrial Metals Subindex Total Return ETN	ETF Price - Commodities	YahooFinance	10
297	BCM	iPath Pure Beta Broad Commodity ETN	ETF Price - Commodities	YahooFinance	10
298	XME	SPDR S&P Metals & Mining ETF	ETF Price - Europe	YahooFinance	10
299	IEZ	iShares U.S. Oil Equipment & Services ETF	ETF Price - Energy	YahooFinance	10
300	RJN	Elements Rogers International Commodity Index-Energy TR ETN	ETF Price - Commodities	YahooFinance	10
301	GRWN	iPath Pure Beta Softs ETN	ETF Price - Commodities	YahooFinance	10
302	EZU	iShares MSCI Eurozone ETF	ETF Price - Europe	YahooFinance	10
303	DIRT	iPath Pure Beta Agriculture ETN	ETF Price - Commodities	YahooFinance	10
304	ERX	Direxion Daily Energy Bull 3x Shares	ETF Price - Energy	YahooFinance	10
305	XES	SPDR S&P Oil & Gas Equipment & Services ETF	ETF Price - Energy	YahooFinance	10
306	IOIL	IQ Global Oil Small Cap ETF	ETF Price - Oil & Gas	YahooFinance	10
307	PBW	PowerShares WilderHill Clean Energy Portfolio ETF	ETF Price - Alternative Energy	YahooFinance	10
308	JJP	iPath Bloomberg Precious Metals Subindex Total Return ETN	ETF Price - Commodities	YahooFinance	10
309	ATMP	Barclays ETN+ Select MLP ETN	ETF Price - Energy	YahooFinance	10
310	UHN	United States Diesel-Heating Oil Fund LP	ETF Price - Commodities	YahooFinance	10
311	UBN	ETRACS UBS Bloomberg CMCI Energy Total Return ETN	ETF Price - Commodities	YahooFinance	10
312	JJN	iPath Bloomberg Nickel Subindex Total Return ETN	ETF Price - Commodities	YahooFinance	10

Source: Own work.

Appendix C: Graphical Analysis of the Dependent Series

Figure 16: Electricity - Prices and historical volatilities

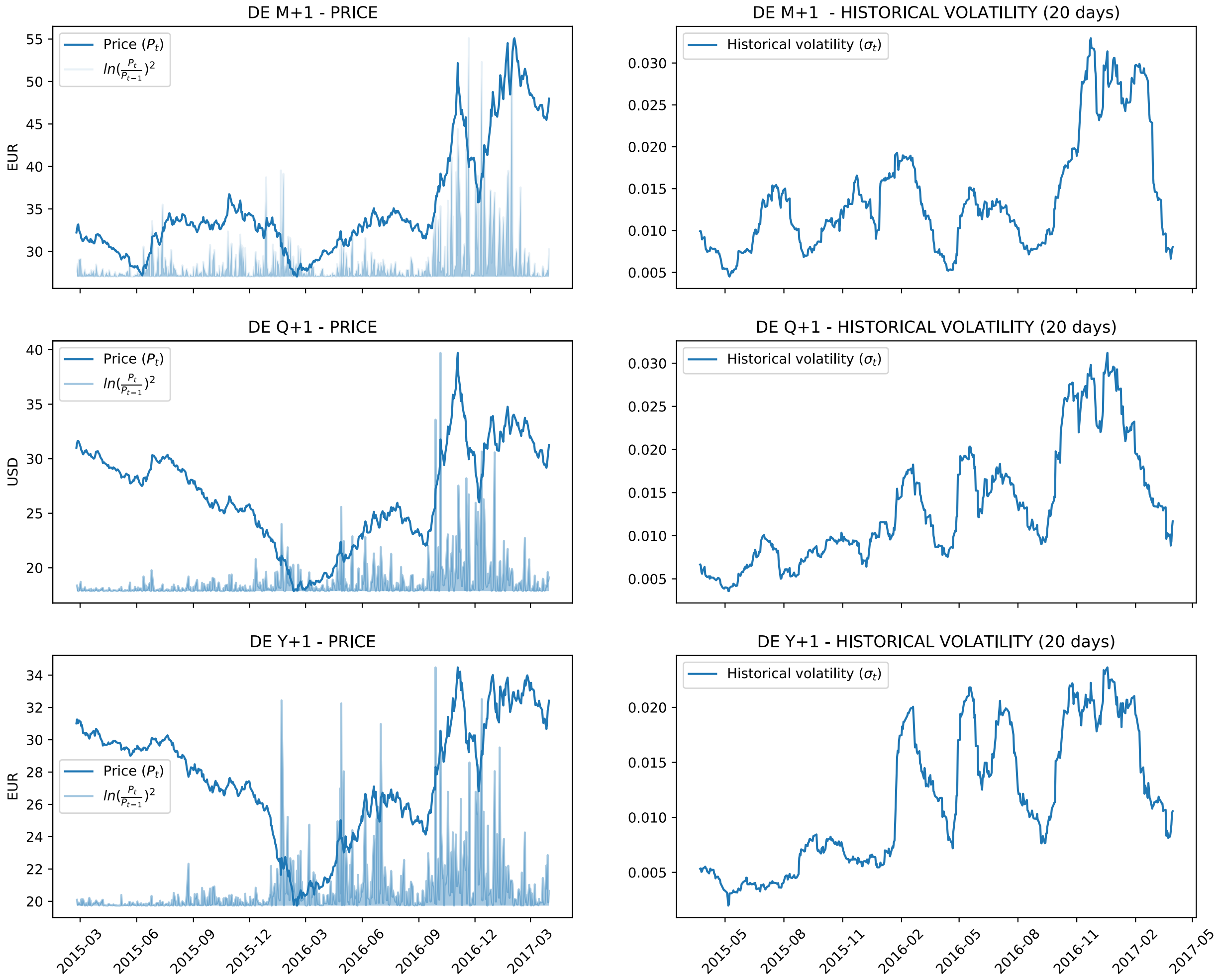

Source: Own work.

Figure 17: Electricity - Prices and historical volatilities

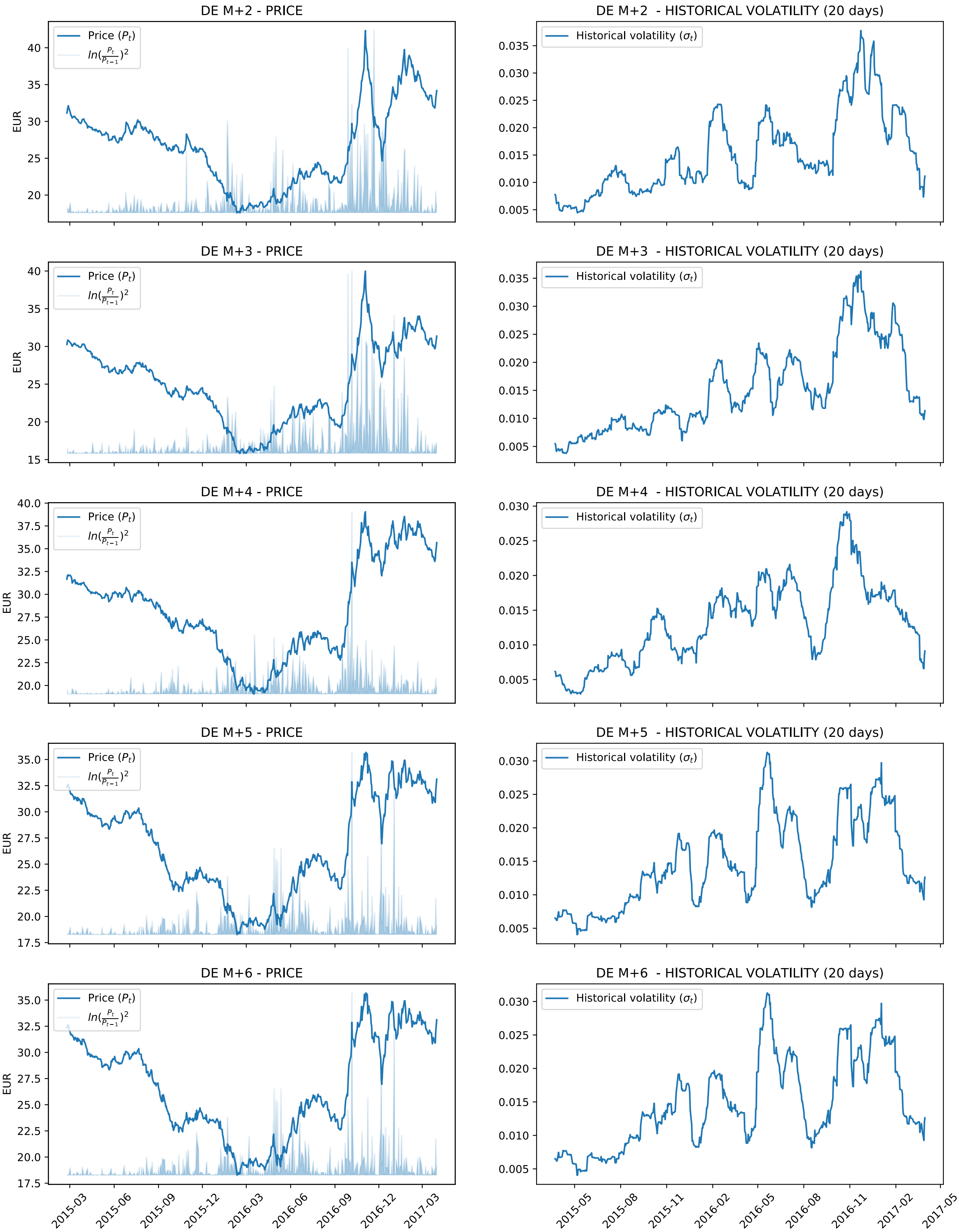

Source: Own work.

Figure 18: Commodities - Prices and historical volatilities

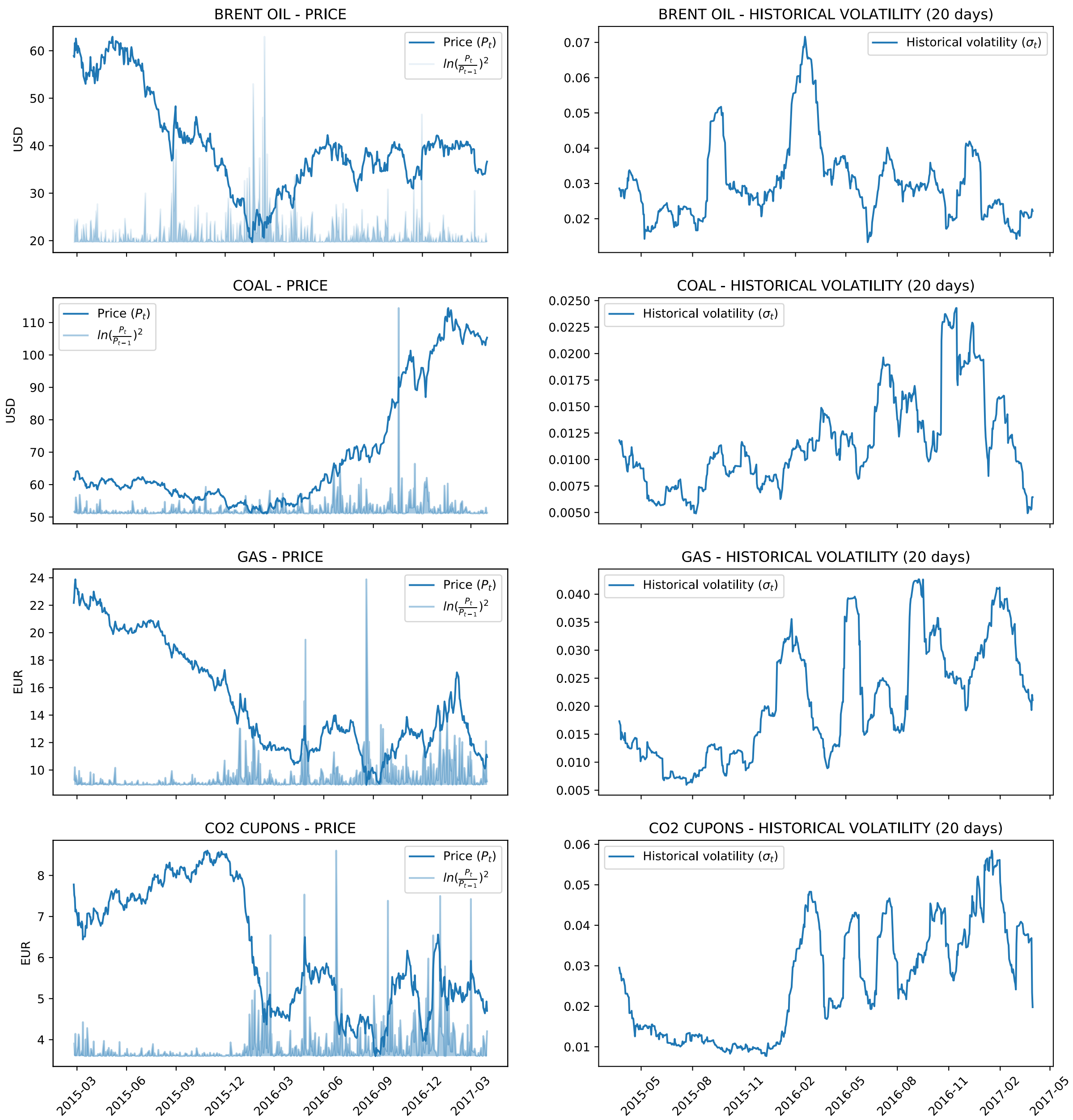

Source: Own work.

Figure 19: Dependent variables - empirical distributions

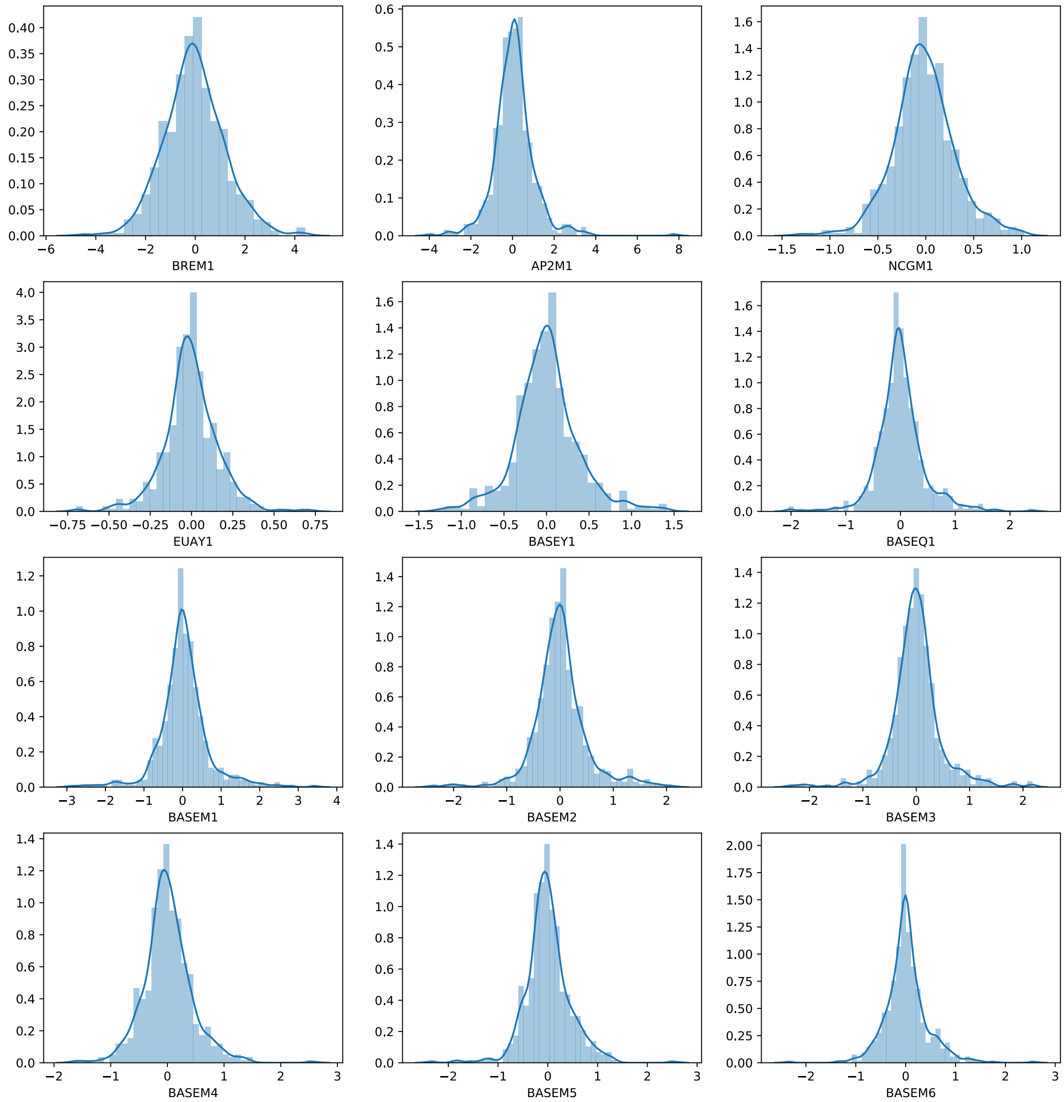

Source: Own work.

Appendix D: Factor Structure

Table 18: Common factors $\hat{F}_t$ of 312 series of $\boldsymbol{X}$

Factor	Share of explained variance	No	Vartype	Id	Marginal R_2
1	27,6%	193	10	IXC	0,84
		304	10	ERX	0,79
		245	10	DIG	0,79
		236	10	XLE	0,78
		244	10	VDE	0,78
		176	10	IYE	0,78
		289	10	FENY	0,78
		270	10	ERY	0,78
		292	10	DUG	0,78
		111	9	Mach	0,76
2	8,2%	260	10	SGOL	0,36
		217	10	GLD	0,35
		174	10	IAU	0,35
		253	10	DBP	0,35
		281	10	DGL	0,35
		170	10	OUNZ	0,34
		150	10	GLTR	0,33
		86	8	GDAXI	0,31
		221	10	DJP	0,31
		230	10	DBC	0,30
3	4,5%	150	10	GLTR	0,50
		246	10	SIVR	0,50
		228	10	SLV	0,49
		253	10	DBP	0,48
		174	10	IAU	0,42
		170	10	OUNZ	0,42
		217	10	GLD	0,42
		260	10	SGOL	0,42
		281	10	DGL	0,41
		259	10	DBS	0,39
4	3,4%	86	8	GDAXI	0,15
		280	10	JJA	0,13
		278	10	RJA	0,13
		69	8	DTE	0,13
		67	8	DAI	0,12
		63	8	LIN	0,12
		268	10	JJG	0,12
		83	8	BAYN	0,11
		121	9	Util	0,11
		76	8	ALV	0,11
5	2,6%	16	2	AT_S0	0,43
		13	2	DE_S0	0,40
		20	2	CZ_S0	0,28
		59	7	NETCOMLFW_DE_LUX	0,27
		54	6	TERMO_PL	0,25
		17	2	CH_S0	0,24
		27	5	LOAD_FR	0,22
		15	2	NRDPL_S0	0,22
		38	6	SCHPROD_CZ	0,20
		57	7	NETCOMLFW_DE_DK	0,19
6	2,3%	5	1	BASEQ1	0,35
		8	1	BASEM2	0,31
		9	1	BASEM3	0,31
		6	1	BASEY1	0,30
		10	1	BASEM4	0,28
		7	1	BASEM1	0,25
		11	1	BASEM5	0,21
		20	2	CZ_S0	0,16
		13	2	DE_S0	0,16
		12	1	BASEM6	0,16

Table continues on next page

Table 18: *Common factors $\hat{\boldsymbol{F}}_t$ of 312 series of $\boldsymbol{X}$ (cont.)*

Factor	Share of explained variance	No	Vartype	Id	Marginal R_2
7	2,0%	5	1	BASEQ1	0,31
		7	1	BASEM1	0,28
		8	1	BASEM2	0,27
		6	1	BASEY1	0,27
		9	1	BASEM3	0,25
		10	1	BASEM4	0,24
		11	1	BASEM5	0,21
		12	1	BASEM6	0,21
		2	1	AP2M1	0,10
		4	1	NCGM1	0,08
8	1,9%	148	10	DBA	0,20
		282	10	AMLP	0,18
		197	10	MLPG	0,16
		210	10	MLPI	0,15
		284	10	MLPA	0,15
		278	10	RJA	0,15
		249	10	AMU	0,15
		285	10	AMJ	0,14
		271	10	IMLP	0,14
		177	10	YMLI	0,14
9	1,8%	195	10	BOIL	0,69
		203	10	UGAZ	0,69
		237	10	DGAZ	0,69
		142	10	UNG	0,68
		258	10	UNL	0,63
		209	10	KOLD	0,41
		196	10	GAZ	0,30
		295	10	CORN	0,08
		268	10	JJG	0,07
		145	10	GRU	0,06
10	1,6%	26	5	LOAD_DE	0,33
		49	6	WIND_DK	0,29
		47	6	WIND_DE	0,28
		40	6	WINDFOR_DE	0,28
		55	7	NETCOMLFW_DE_AT	0,24
		30	5	LOAD_PL	0,23
		39	6	SCHPROD_DK	0,18
		56	7	NETCOMLFW_DE_CZ	0,17
		28	5	LOAD_AT	0,15
		27	5	LOAD_FR	0,13
11	1,4%	186	10	JJC	0,21
		276	10	DBB	0,19
		296	10	JJM	0,16
		252	10	CPER	0,14
		95	9	Smoke	0,13
		121	9	Util	0,12
		94	9	Beer	0,12
		47	6	WIND_DE	0,10
		40	6	WINDFOR_DE	0,10
		93	9	Soda	0,10

Source: Own work.